

601991

AN ELECTRICAL RESISTIVITY SURVEY OF THE
COLADO HOT SPRINGS PROSPECT,
PERSHING COUNTY, NEVADA

VOLUME II

Survey Method Description;
Data Acquisition, Reduction,
and Analysis Description;
Apparent Resistivity Values;
and Interpreted Depth Sounding Curves

SUBMITTED TO

GETTY OIL COMPANY

BY

ELECTRODYNE SURVEYS

SPARKS, NEVADA

APRIL, 1978

VOLUME II

TABLE OF CONTENTS

APPENDIX		PAGE
I	Glossary of Terms	1
II	Scalar AMT-MT Soundings	9
III	Vector Telluric Soundings	23
IV	Telluric Profile Measurements	27
V	Galvanic (dc) Electrical Resistivity Profiles	52
VI	Parallel (dc) Electrical Resistivity Soundings	77
VII	Time Domain Electromagnetic Soundings E_p (parallel) & H_z (vertical) Components	84

APPENDIX I

Glossary of Terms

Glossary of Terms

Apparent Depth of Penetration, D_a : The apparent depth of penetration is normally defined as the depth of penetration into the earth (which is not completely uniform), that would be computed based upon considerations of the electrical resistivity method used, the geometry of the source-receiver array and the assumption that the earth is a homogeneous half-space.

Apparent Resistivity, ρ_a : The apparent resistivity is normally defined as the resistivity of the earth, which is not completely uniform, that would be computed based upon considerations of the electrical resistivity method used, the geometry of the array and the assumption that the earth resistivity is homogeneous to the depth of penetration achieved. (MKS: ohm-meters) The apparent resistivity parameter may be viewed as the weighted average of the true resistivities from the surface to the depth of penetration.

Array: Any geometric combination of a source-receiver pair used in making electrical resistivity measurements.

Audio-Magnetotelluric Soundings, AMT: Vertical resistivity soundings of the earth utilizing the plane-wave response of naturally and culturally induced electromagnetic fields for the frequency band, 2.0 Hz to 1,000 Hz.

Coefficient of Anisotropy, λ : The coefficient of anisotropy is defined as the square root of the ratio of the resistivities measured in the two principal directions, that is, resistivity across the bedding planes, ρ_t , and the resistivity along the

bedding plane, ρ_1 , (non-dimensional). $\lambda = \rho_t / \rho_1$

Conductance, S: The measure of the ratio of the thickness of a conductive material between two insulating plates to the resistivity of the conductive material. An earth crust example is the conducting sedimentary section between the free-air half-space and electrical basement (generally granitic and/or Pre-Cambrian rocks).

Conductivity, σ : The relative ability of materials to conduct electricity when a voltage is applied across the material (MKS: mhos/meter). Conductivity is the reciprocal of resistivity.

Early Time: The portion of the transient response in a TDEM sounding related to the plane-wave (farfield) response of an FDEM sounding.

Effective Apparent Resistivity, ρ_{aE} : The logarithmic average of the apparent resistivities of orthogonal components of a vector apparent resistivity. $\rho_{aE} = (\rho_{ax} \cdot \rho_{ay})^{\frac{1}{2}}$

Effective Apparent Separation, r_E : The array separation that is calculated for source-receiver bipole arrays to equate the array to a source-receiver dipole array. The only bipole array where r_E is correctly calculated as a dipole array separation, r , is an equatorial bipole array.

Electrical Basement: Any thick sequence of rocks or thick layer at depth such as crystalline rocks, which presents a resistivity contrast of 10:1 or greater to the rock sequences or layers above it. Usually the total resistance, T , (a multiplication of resistivity times the sequence thickness) of the electrical basement is so large that it screens out any resolution of conductive rock sequences or layers below it.

Electro Sonde Log, ESL: A pseudo-electrical log of resistivity as a function of depth as determined from data obtained by a five-component surface-based electromagnetic receiver of both naturally induced and a surface-based controlled source(s) induced electromagnetic fields. The five-component receiver measures two orthogonal horizontal components of the electric field and three orthogonal components of the magnetic field. The total ESL system will perform measurements of the frequency spectrum from 0.001 Hz to 1,000 Hz. The frequency range measurements are sub-divided by sources as 0.001 Hz to 0.1 Hz, MT sources; 0.08 Hz to 20 Hz, controlled source; and 8.0 Hz to 1,000 Hz, AMT sources.

Electro Sonde Profiles, ESP: Measurements similar to ESL measurements are made along a continuous profile. One horizontal electric field component, inline with the profile, and a horizontal magnetic field component, perpendicular to the profile, and a vertical magnetic field component are measured at the receiver. The controlled source is a grounded bipole source aligned parallel to the profile with the source-receiver array separation at least twice the depth of penetration in the controlled source minimum frequency. The source field and frequency bands are identical to those for the ESL measurements.

Far Field: See Plane-Wave Field.

Formation Factor of Rocks: The ratio of the resistivity of a rock to the resistivity of the water filling the pore space for a given porosity.

Frequency Domain Electromagnetic Soundings, FDEM: Controlled source electromagnetic soundings generated by a frequency sweep source.

Galvanic Resistivity Sounding, VES: Nomenclature interchangeable with dc Electrical Resistivity sounding in the literature. Vertical electrical resistivity sounding of resistivity as a function of depth. A grounded electrical source generating a static electric field and grounded electrical receivers measuring potential drop between electrodes are utilized. Increase in the depth of penetration is effected by increasing the source-receiver separation of the array.

Geoelectric Section: The geoelectric section differs from the geologic section in that the boundaries between layers or features of contrast change at boundaries determined by resistivity contrasts rather than by the combination of factors used by the geologists in establishing these boundaries. The electrical resistivity of most rocks is determined primarily by the rock porosity, water content and water temperature. The boundaries in a geoelectric section coincide with the boundaries in a geologic section most often when there is a pronounced change in one of the above parameters.

Geometric Factor, K: The geometric factor accounts for the source-type and configuration, the receiver type and configuration, and the separation between the source and receiver geometry in the determination of apparent resistivity.

J-Factor: The ratio of apparent conductance at two locations determined from telluric current measurements at a specified frequency. For end-on-end or in-line telluric profiles, J is the ratio of the simultaneous potential drops measured at two locations. For vector telluric measurements, J is the ratio of the average ellipse areas simultaneously scribed by the two component telluric measurements at two locations.

Late Time: The portion of the transient response in a TDEM sounding between the early time response and the static field response.

The late time response for TDEM is directly related by the Fourier Transform to the quasistatic response of FDEM.

Longitudinal Conductance, S_1 : The conductance from the ratio of the total thickness to the parallel or bedding layers of an anisotropic geoelectric unit. $S_1 = H/\rho_1$

Longitudinal Resistivity, ρ_e : The resistivity determined by the parallel summation of resistivity values of parallel or bedding layers of an anisotropic geoelectric unit.

Magnetotelluric Sounding, MT: Vertical resistivity sounding of the earth utilizing the plane-wave response of naturally induced electromagnetic fields for the frequency band, 0.001 Hz to 1.0 Hz.

Near Field: Electromagnetic fields for frequencies such that the electromagnetic components are not orthogonal in the propagating source wave. The near field response includes both the quasistatic response and static response portions of FDEM soundings.

P_c Frequency Band: Frequency band from 0.001 Hz to 0.1 Hz.

Plane-Wave Response: The frequency domain response where the electric field and magnetic fields are orthogonal to one another in electromagnetic propagation frequency spectrum.

Quasistatic Response: The frequency domain response between the plane-wave response and static response of an electromagnetic propagation frequency spectrum.

Residual Conductance, S_R : The difference between the total dc electrical resistivity conductance and the total TDEM resistivity conductance. $S_R = S_{dc} - S_{EM}$.

Resistivity, ρ : Specific resistance offered by a material to current flow when a voltage is applied across the material (MKS: ohm-meters). Resistivity is the reciprocal of conductivity.

Scalar MT Analysis: Resistivity values are determined from data reduction and interpretation of ratio of the power spectrum of an electric field component to the power spectrum of an magnetic field component orthogonal to the electric field component.

Schumann Band Frequencies: The frequencies in the frequency range, 8 Hz to 44 Hz, caused by electromagnetic fields generated by lightning strokes that propagate in the earth-ionosphere wave guide.

Sonde: Equivalent to sounding.

Static Response: Frequency Domain EM response near zero frequency. The static electric field response is used to calculate the apparent dc electrical resistivity value. The static magnetic field response is independent of the resistivity parameter; therefore, it has no interpretation value in the determination of the geoelectric section.

Telluric Currents: Currents caused to flow in the earth by natural electromagnetic source wave induction.

Tensor MT Analysis: A highly sophisticated analysis of magnetotelluric data which attempts to analyze only assured plane-wave energy fields (based upon coherence tests) and can give two and three-dimensional interpretation capability.

Thickness, H : The thickness of any rock sequence that appears macroscopically homogeneous in resistivity to the interpretation of a particular electrical method (MKS: meters).

Tipper Analysis: Analysis leading to data for interpretation of lateral resistivity variation about an MT recording site. The data reflects the wave-tilt from vertical propagation of the electromagnetic wave propagating in the earth.

Total-field Apparent Conductance, ST: The conductance of the nonuniform overburden and sedimentary column that rests upon an electrical insulator at a finite depth, which is not completely uniform, and which is underlain at finite depth by an electrical insulator, which is based upon the assumption of cylindrical current spreading from each source electrode in a completely uniform earth (MKS: mhos).

Total-field Apparent Resistivity, RT: The observed resistivity of the earth, which is not completely uniform, that would be computed based upon the geometric factor due to a finite length source with spherical current spreading from each source-electrode in a completely uniform earth (MKS: ohm-meters).

Transmittance (Transverse Resistance), T: The product of the thickness and the series summation of the resistivity values of parallel or bedding layers of an anisotropic geoelectric unit.

Transverse Resistivity, ρ_t : The resistivity determined by the series summation of resistivity values of parallel or bedding layers of an anisotropic geoelectric unit.

Type A Geoelectric Section: Resistivity distribution of a three layer sequence. $\rho_1 < \rho_2 < \rho_3$

Type H Geoelectric Section: Resistivity distribution of a three layer sequence. $\rho_1 > \rho_2 < \rho_3$

Type K Geoelectric Section: Resistivity distribution of a three layer sequence. $\rho_1 < \rho_2 > \rho_3$

Type Q Geoelectric Section: Resistivity distribution of a three layer sequence. $\rho_1 > \rho_2 > \rho_3$

APPENDIX II

SCALAR AMT-MT SOUNDINGS

Contents:

General Description of AMT-MT Sources and Wave Propagation.
Magnetotelluric Receiver and Data Acquisition Requirements.
Electrodyne's Scalar AMT-MT Data Acquisition.
Electrodyne's Scalar AMT-MT Data Reduction.
Interpretation Considerations.
Table of Scalar AMT-MT Apparent Resistivity Values.

General Description of AMT-MT Sources and Wave Propagation

In the magnetotelluric (MT) sounding method and the telluric current methods, naturally occurring electromagnetic fields are used as source fields. Electromagnetic waves impinging on the earth's surface are generally refracted vertically into the earth medium below. This happens because of the resistivity contrast at the free air - earth interface. The incoming electromagnetic wave (in free space) essentially has only one component, a magnetic field component, because the free space has a nearly infinite resistivity value, therefore current will not flow. Once the electromagnetic wave has been refracted into the relatively conductive earth space, the magnetic field induces an electric field component.

There are two criteria for the electromagnetic wave propagation that must be met before the "state of the art" MT interpretation can be performed. These criteria are:

1. The electromagnetic waves must propagate vertically into the earth at the free space-earth interface. (An example of where the criteria is not met is on Greenland and its ice cap).
2. The electromagnetic wave must be a plane-wave, that is, the magnetic field component and its induced electric field component must be orthogonal to one another. If one assumes a point source, such as a lightning stroke (spheric), the source location must be at least one free-space wave-length away from the point of measurement.

Criteria 1 above is met adequately over most of the surface of the earth, excluding the polar regions where there is an ice cover.

Criteria 2 above is met by much of the energy classified as P_c frequencies (1.0×10^{-5} Hz to 2.0 Hz) and the Audio MT frequencies (2.0 Hz to 1000 Hz) energy. See Figure 1 below.

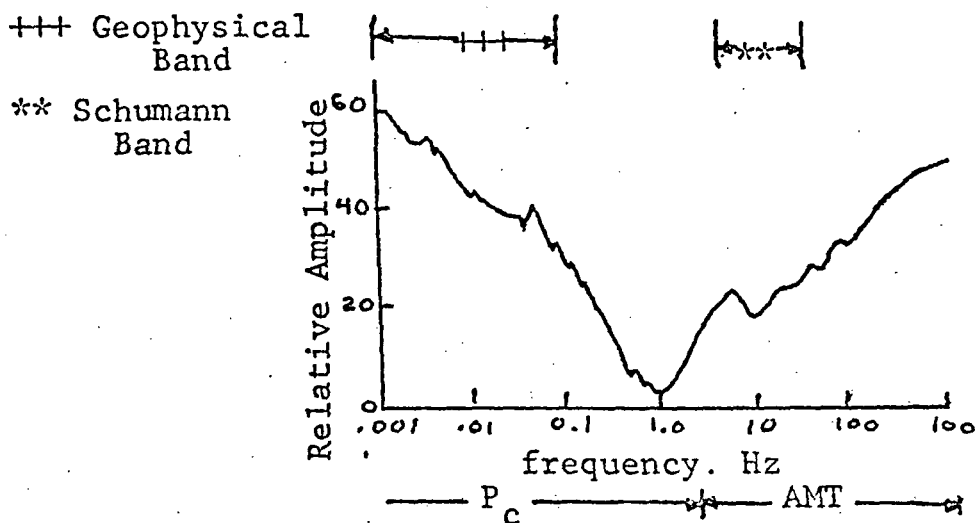


Figure 1. Typical distribution of electromagnetic change vs. freq.

In the 2.0 Hz to 1000 Hz (AMT) spectrum, the electromagnetic waves propagate in the earth-ionosphere wave-guide and/or along the earth's surface. The major source type found in this spectrum is the spheric source which generates frequencies in the Schumann Band (8.0 Hz to 44.0 Hz). Spheric source energy from the three major storm cell areas of the earth (Central Africa, Brazil, and Pacific Ocean storm areas) provide plane-wave energy over most of the earth. One cannot use this energy if a measuring site is within 1000 kilometers of the edges of any one of the storm cells. Further, local thunder storms are usually too close to provide plane-wave energy (far field energy).

In the 1.0×10^{-5} Hz (approximate diurnal variation frequency) to the 2.0 Hz spectrum, pseudo-electromagnetic waves are generated by large ring currents and standing waves established by the interaction of the solar winds and the earth's magnetic field and its ionosphere. The effective very large pseudo-wave fronts generate plane-wave electromagnetic waves in the earth. These wave-fronts impinge nearly vertical on the earth.

Geophysicists generally limit their use of these waves to the to the 0.001 Hz to the 2.0 Hz frequency band.

Magnetotelluric Receivers & Data Acquisition Requirements

Magnetotelluric receivers, thereby the type of interpretation one wishes to make; qualitative or quantitative. This interpretation criteria specifies the data reduction technique to be used. The data reduction techniques all face the decision as to what signals in a given time window are plane-wave in character and propagating in a vertical sense just below the earth-free space interface and as to what signals are not. The later signals are noise to be overcome.

The above decision, for qualitative interpretation, is generally made on the basis of repeatability of power spectra ratios, J-Factor ratios or individual signal signature ratios which give statistical repeatability of the intrinsic impedance, \bar{Z} ,

$$\bar{Z}(k)_{f_i} = \frac{\bar{E}(k)}{\bar{H}(k)} f_i$$

where $\bar{E}(k)$ is the electric field for a sampling of k units, $\bar{H}(k)$ is the magnetic field for a sampling of k units, at some frequency, f_i . (Impedance is used in the calculation of apparent resistivity because it eliminates the need to know the source strength as would be necessary for apparent resistivity calculations from either the electric field or magnetic field components alone). Repeatable intrinsic impedance, no matter how derived, is what is termed Scalar MT Analysis.

There are two specific frequency ranges where the qualitative data reduction provides a high degree of precision or correctness of the determination of apparent resistivity. These ranges are the 0.01 Hz to 0.1 Hz range and the 8.0 Hz to 36 Hz range (within the Schumann Band. Figure 1 above of the natural field spectrum shows

that these ranges have a relative high energy level and shows high energy peaks at discrete frequencies within each of the ranges.

The qualitative data reduction approach is not reliable in the 0.1 Hz to 5.0 Hz frequency range (the frequency range showing minimum energy, Figure 1). Therefore, scalar data reduction doesn't provide a continuous spectrum for interpreting soundings.

If one wishes to determine an MT sounding utilizing the full MT-AMT spectrum, one must resort to tensor analysis for data reduction. This approach which provides data for quantitative interpretation, and goes beyond the the reduction for qualitative interpretation by the use of various schemes of the autopower spectrum and cross power spectrum analysis of the electromagnetic components on a number of selected time windows of the MT signal.

Electrodyne does not perform tensor MT soundings. Pritchard and others at the Colorado School of Mines and the USGS reached the conclusion, during the IGY and ISQY Programs, 1957 thru 1965, along with many others on a world wide basis, that there are some basic drawbacks to deriving adequate interpretation of the electrical resistivity distribution of the earth crust by MT soundings alone. The above group of investigators have found that an approach of supplementing the 0.1 Hz to 5.0 Hz spectrum "hole" by controlled source electromagnetic measurements is a wiser course of action to achieve reliable data for interpretation. This "hole" frequency band is the the frequency band that most often gives interpretation--quantitative interpretation at the depth of maximum interest in the geologic section. Therefore, this band for interpretation has to be retrieved with as much accuracy as possible. *(reference)*

Pritchard and many other investigators have found that scalar data acquisition and reduction of data in the two high energy frequency bands mentioned above provide a useful and cost effective

for reconnaissance surveys. These reconnaissance surveys help to locate areas with zones of high contrast in the resistivity parameter (both shallow and at depth) in the geologic section. Also, these measurements will often locate the major and/or regional structural trends in Basin and Range type geoelectric sections.

Electrodyne Scalar AMT-MT Data Acquisition

Scalar AMT-MT data in the Schumann Band frequencies (8 Hz to 32 Hz) and the P_c band frequencies (0.02 Hz to 0.06 Hz) are obtained by simultaneous recording of orthogonal horizontal components of the naturally occurring telluric and magnetic fields. The telluric field is generally measured using delta potential dipoles 190 meters in length and the magnetic field is measured by a two-axis fluxgate magnetometer with a 0.5 gamma sensitivity. For most Basin and Range Province surveys, the Y-telluric component is oriented along an azimuth of N20E, if possible, and the X-telluric component is orthogonal to the Y-component or oriented along an azimuth of N110E (see Plate I of the text). The typical scalar AMT-MT site used is shown in Figure 2.

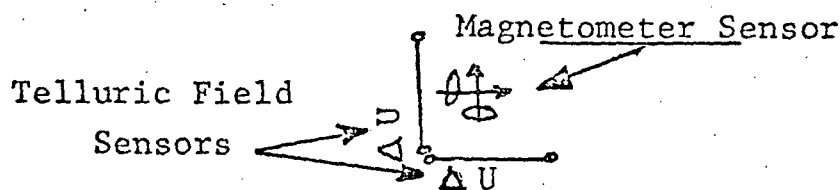


Figure 2. Scalar Magnetotelluric Site Layout.

The data or incoming signal is passed through a signal conditioner (filters and amplifiers) and recorded on a 4-channel analog tape. The peak amplitude resolution of these tape recordings is 45 db. In addition to the tape recordings, graphic recordings of the incoming signal are made for quality control of the tape recordings and as a back up measurement in case of failure of the tape recorders.

The fluxgate magnetometer mentioned above, with a 0.5 gamma sensitivity used in 1977 by Electrodyne, did not always give

adequate signal recovery of the magnetic field in the Schumann Band frequencies. For this reason, normalized scalar apparent resistivity values were determined for these frequencies by considering the telluric signal strength alone. how?

It was discovered during the IGY and IQSY programs, and possibly before, that the telluric field strength of spheric source signals from the world storm centers only vary by ± 50 percent in amplitude on any given day. This was found to be true by Pritchard among others, and Electrodyne has retested this variation criteria on numerous occasions during 1977 and found that the criteria still holds. The most recent reference to this criteria was made by Telford, 1977, where he states the variation is only ± 30 percent in his findings. There are numerous references to this variation in the Journal of Geophysical Research (AGU) during the period of 1957 to 1966.

Because of this important criteria, one can make use of the Schumann Band frequencies for qualitative investigations, even in the event that the signal is too small to be measured by a magnetometer at any given time. Investigators in their surveys use the qualitative reconnaissance tellurics and AMT-MT measurements to discover areas that show gross anomalous change in resistivity over an area. The gross changes in resistivity looked for are of the order of 2 to 10 or even greater. The corresponding changes in amplitude are from 200 to 1,000 percent or even greater. 2 to 10 So it is seen that the small percent change over any given day of recording is small and insignificant in light of the spatial variations looked for in reconnaissance surveys.

Electrodyne has upgraded its scalar magnetic field detection capability by incorporating an active fluxcollector, fluxgate mag-

Telford, W. M., 1977, Characteristics of audio and sub-audio telluric signals, Geophysical Prospecting, v. 25, 321-333.

netometer whose internal noise level (peak to peak) is about 20 milligammas. Presently, Electrodyne is continuing support of the R. & D effort on the magnetometer to reduce the internal noise level to a 5 milligamma threshold in the Schumann Band frequencies.

Electrodyne Scalar AMT-MT Data Reduction

Electrodyne normally performs scalar AMT-MT data reduction by amplitude spectral analysis of visually inspected windows of recording time. The analysis procedure stacks, thereby averages, a number of spectral amplitude versus frequency curves to get a good statistical average of a data segment. The stacking of the amplitude spectra for various wide band frequency recordings is as follows:

1. stacking of spectrums from 4 to 8 time-windows in the P_c range, and
2. stacking of spectrums from 16 to 64 time-windows in the Schumann Band range. More than one data segment is analysed for each frequency range and the best statistical average of the component impedances, i. e.,

$$Z_{xy} = \frac{E_x}{H_y} \quad \text{and} \quad Z_{yx} = \frac{E_y}{H_x}$$

are used to derive the component scalar apparent resistivities.

Scalar AMT-MT Apparent Resistivity Calculation / Spectrum Frequency

$$\rho_a = 0.2 (1/f) \left| \frac{E}{H} \right|^2$$

where

- ρ_a is the scalar apparent resistivity (ohm-meters),
- f is the cyclic frequency of the amplitude spectra (Hz),
- E is the amplitude of the telluric field component (mv/km),
- H is the amplitude of the magnetic field component (gammas).

The resulting apparent resistivity components are:

$$\rho_{a_{xy}} = 0.2 (1/f) \left| \frac{E_x}{H_y} \right|^2$$

and

$$\rho_{a_{yx}} = 0.2 (1/f) \left| \frac{E_y}{H_x} \right|^2$$

An Effective scalar apparent resistivity is derived from the above component resistivities for final interpretation.

Effective Apparent Resistivity

$$\rho_{a_E} = \left| \rho_{a_{xy}} \times \rho_{a_{yx}} \right|^{\frac{1}{2}} \quad (\text{logarithmic average})$$

The spectral analysis approach is used in the scalar data reduction to give the investigator a qualitative judgement as to the degree that the measurements are affected by two and/or three dimensional variations. Figure 3 presents an example of Electrodyne's spectral analysis for Z_{xy} for a set of time windows over the various frequency ranges of interest.

Interpretation Considerations

The Schumann Band AMT frequencies, which more often than not, are limited in depth of penetration to no greater than 1,000 feet in most Basin and Range Province surveys. The general interpretation feature of this frequency band is the apparent resistivity contrasts alone in the near-surface geoelectric section. The apparent depth of penetration over the prospect varies approximately as the square root of the increase or decrease of this apparent resistivity.

For the low frequency P_c frequency band, deep penetration into the geologic section is caused, probably the penetration is well into the electrical basement section at most of the measuring sites. Therefore, one should not expect apparent resistivity values in this band to give as low a resistivity value nor an accurate depth estimate to conductive sections above electrical basement. But, the location of the areal location of conductive zones above electrical basement should be indicated very well by these measurements when large contrasts in resistivity are found in the survey coverage. Relatively low apparent resistivity values may indicate areas having fault-like features (two and three dimensional effects). Large areas showing relatively low apparent resistivity values may be thought to be caused by decreases in the section resistivity, ect. These considerations are true for apparent resistivity contour maps of scalar AMT-MT measurements. Because one has such a multitude of choices in interpretation to choose from, Electrodyne performs a high spatial density of measurement locations over the prospect area to provide a logical interpretation picture.

TABLE II-1
SCALAR MT-AMT APPARENT RESISTIVITY VALUES

STATION NUMBER	APPARENT RESISTIVITY (ohm-meter)	FREQUENCY (hz)	$\frac{A}{S}$ (km)	APPARENT RESISTIVITY {NORMALIZED}	FREQUENCY (hz)	S_m
1	28	0.045	12.5	0.57	14	101
2	19	0.04	1	2.8	14	225
3	180	0.04	33.7	3.8	14	262
4	160	0.04		3.2	14	
5	10	0.04	7.9	5.1	14	
6	500	0.04	56	3.7	14	
7	150	0.04		9.2	14	
8	1.2	0.04		1.8	14	
9	35	0.04		4.3	14	
10	12	0.04		1.5	14	
11	0.25	0.04		2.1	14	155
12	1.6	0.04		1.7	14	
13	56	0.035		HIGHLY SKEWED	—	7
14	0.36	0.04		2.3	14	
15	4.1	0.035		0.46	14	
16	14	0.035		1.6	14	
17	16	0.03		1.8	14	
18	5.5	0.03		4.0	14	
19	3.1	0.035		1.4	14	
20	7.2	0.03		3.9	14	
21	4.5	0.035		3.2	14	
22	9	0.04		5.4	14	
23	5	0.04		4.4	14	
24	97	0.035		2.4	14	
25	71	0.03		9.8	14	
26	N.V.	—		N.V.	—	
27	34	0.04		5.9	14	
28	7.9	0.04		3.9	14	
29	9.9	0.04		6.1	14	
30	5.3	0.05		2.3	14	
31	3.4	0.03		1.1	14	

Discussion

The vector telluric method criteria for wave-propagation, data acquisition, and reduction, and interpretation are the same as the criteria discussed for scalar AMT-MT soundings, Appendix II.

When making vector telluric measurements, one records the potential differences, on grounded dipoles for vectorial measurements, at a telluric vector base station and one or more roving vector telluric stations. See the Figure below.

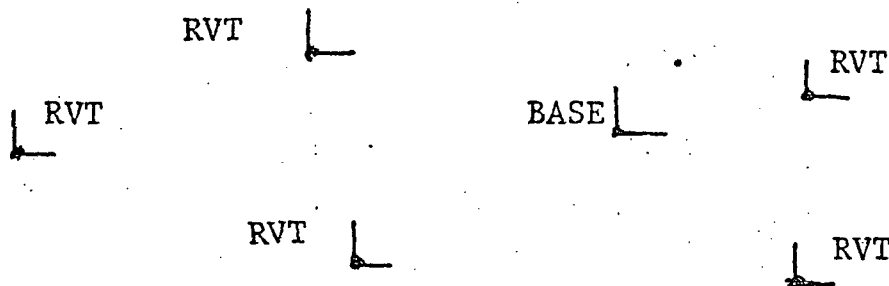


Figure 1. Typical Vector Telluric Survey Layout

The vector telluric measurements, like the telluric profile measurements discussed in Appendix IV, give normalized apparent resistivity values when taken in ratio for two or more stations. The parameters derived from the measurements are:

Normalized Apparent Resistivity Components

$$P_{ax} = Q \frac{E_x \text{ (RVT site)}}{E_x \text{ (Base)}}$$

$$\rho_{a_y} = Q \frac{E_y \text{ (RVT site)}}{E_y \text{ BASE}}$$

where

ρ_a is the normalized apparent resistivity,

E is the amplitude of the telluric field component,

and

Q is the apparent resistivity determined for the BASE Site by some other electromagnetic method, such as scalar AMT-MT measurements or controlled source measurements.

Effective Apparent Resistivity

$$\rho_{a_E} = \left| \rho_{a_x} \times \rho_{a_y} \right|^{\frac{1}{2}}$$

The vector telluric measurements were performed in this prospect for several reasons:

1. Electrodyne has been studying the cost effectiveness of several reconnaissance techniques. The results of the vector measurements study indicate that such measurements can only be cost effective for surveys of very large areas or on a long term contract basis for a vector telluric reconnaissance crew.
2. Electrodyne's study indicates that one can set-up closer to cultural noise features and on days of high wind than one can in making any AMT-MT measurements. This certainly a cost effective plus for this type of measurement.
3. 1977 was an extremely quiet (low amplitude) year for magnetotellurix signals; therefore telluric measurements of low amplitude are much more reliable than low amplitude magnetic field measurements. Certainly an MT base with cryogenic magnetometer and satellite tellurin vector telluric stations are a cost effective means of obtaining multiple MT soundings.

APPENDIX IV

Telluric Profile Measurements
In-line (End-On-End) Telluric Profiles

Contents:

Description and Discussion

Tables of Telluric Profile Apparent Resistivity Values

Description and Discussion

The telluric profile method criteria for natural field electromagnetic waves, wave-propagation, data acquisition and data reduction are similar to those for scalar AMT-MT soundings, Appendix II.

The telluric profiling method layout is two or more receiver dipoles, which are contiguous to one another and are oriented in-line along the profile, that are used to make simultaneous measurements of the natural electric field (telluric field) signals in the earth. This profiling method is known as the in-line or end-on-end telluric method.

By taking the ratio of the amplitudes of correlated telluric field signatures, on the different dipoles that have been recorded simultaneously, one determines the gradient of the electric field along the survey profile.

By Ohm's Law,

$$\vec{E} = \rho \vec{J}$$

where

\vec{E} is the electric field vector,

\vec{J} is the current density vector,

and

ρ is the resistivity of the medium of current flow, the gradient provides a measure of the apparent change in resistivity along the profile. This apparent change reflects both changes of resistivity as a function of depth and changes of resistivity laterally along the profile.

Figure 1 below shows a typical in-line telluric profile.

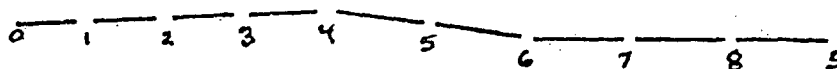


Figure 1.

Obviously, the apparent resistivity values determined from telluric profile measurements are normalized values rather than true values. The normalized values are adjusted to true apparent resistivity values by incorporation of results from scalar AMT-MT soundings, vector telluric soundings, or electromagnetic controlled source soundings performed at one or more locations along the profile.

Electrodyne does not use crossing telluric profile lines to provide the intertie of telluric profiles because the cross over points may be controlled by a feature in the subsurface that skews telluric signals in the vicinity of the cross over points. Further, Electrodyne tries to keep its telluric profiles oriented within a solid angle of ± 45 degrees of magnetic east and west to take optimum advantage of the predominant telluric current flow direction. Telluric profile measurements along profiles oriented along lines not within the solid angle tend to cause misinterpretation of the geoelectric section because nonplane wave signal information is analysed more frequently than not. Fortunately, the Basin and Range Province regional structural trends occur in a solid angle which is generally perpendicular to the maximum current flow solid angle. Generally, the value of telluric profile interpretation is optimized when the profiles cross the predominant structural control at or near an angle of 90 degrees.

Electrodyne uses a four electric dipole receiver scheme in its in its standard field operation. The four dipoles of information are recorded on analog tape for spectral analysis similar to that

used in the scalar AMT-MT analysis. The Hewlett-packard tape recorders used by Electrodyne require all dipole receivers to have a common reference. This is achieved by the layout scheme shown in Figure 2. Location 2 in the figure is the common reference mentioned above.

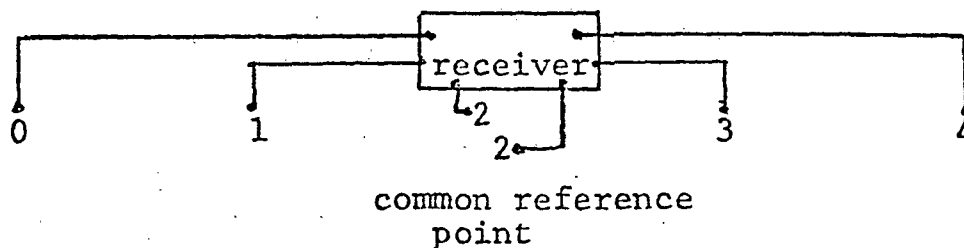


Figure 2. Electrodyne four dipole receiver layout.

The Electrodyne set-up normally uses a dipole resistivity density of 4 to 5 dipole receivers per mile.

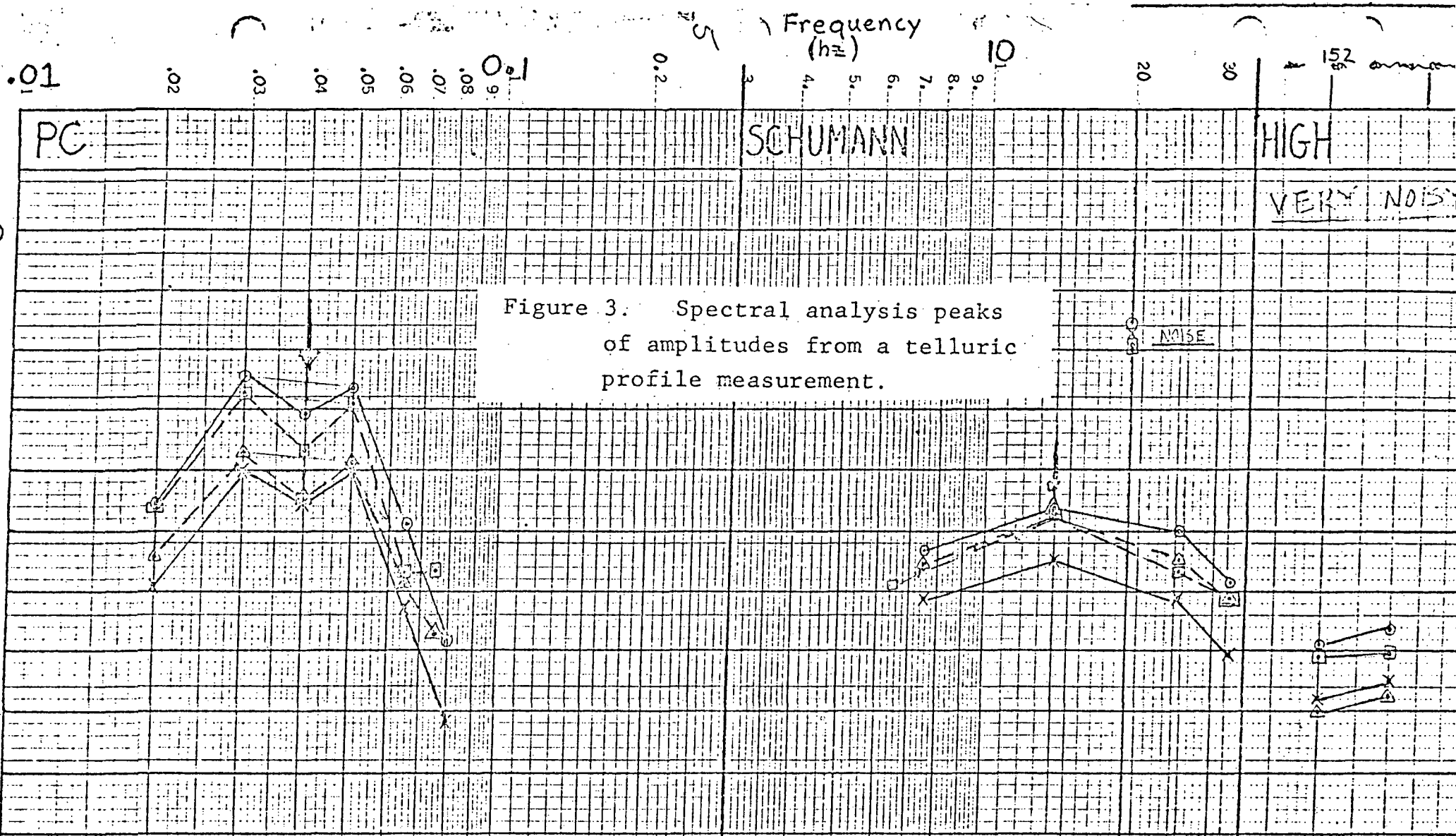
The desired dipole potential difference measurements for data analysis are:

$$\Delta U_{0-2}; \Delta U_{1-2}; \Delta U_{3-2}; \text{ and } \Delta U_{4-3}$$

The dipole potential difference measurements that are actually measured are:

$$\Delta U_{0-2}; \Delta U_{1-2}; \Delta U_{3-2}; \text{ and } \Delta U_{4-2}$$

The desired potential difference measurements are derived after the spectral analysis of visually selected time windows of proper data. Figure 3 gives an example of the spectral analysis results of a group of time windows. Note that the amplitude spectra of arrays ΔU_{0-2} and ΔU_{4-2} are approximately 6 db larger than the normalized spectra for ΔU_{1-2} and ΔU_{3-2} . The desired normalized values for ΔU_{0-1} and ΔU_{3-2} are determined by the amplitude spectra differences as follows:



	ARRAY	REC. GAIN	P.B. ATT.	RMS	COMMENT	REC. GAIN	P.B. ATT.	RMS	COMMENT	REC. GAIN	P.B. ATT.	R
1	O (0-2)	200 X 100	-30	-54.5	GOOD correlation & PKing	100 X 100	-30	-24	NOISY like TIS	100 X 10	-30	-4
2	X (1-2)	200 X 100	-30	-55.5		100 X 100	-30	-23.5	NOISY like TIS	100 X 10	-30	-4
3	Δ (2-3)	200 X 100	-30	-55.2		100 X 100	-30	-25.4	NOISY cut Sawtooth pic	100 X 10	-30	-4
4	□ (2-4)	200 X 100	-30	-49.1	Gd correlation	100 X 100	-30	-25.4	Ech FKS improving	100 X 10	-30	31-41

$$|\Delta U_{0-1}| = |\Delta U_{0-2}| - |\Delta U_{1-2}|$$

and

$$|\Delta U_{4-3}| = |\Delta U_{4-2}| - |\Delta U_{3-2}|$$

The spectral analysis approach is cost effective in data reduction (time saving) as compared to the hand picking of data from graphic records for amplitude ratio determinations. The approach is cost effective in field operation of data acquisition time because three dipoles of new data information per set-up are acquired as compared to one new dipole of information per set-up as in the standard layout approach. The wide-band recording with spectral analysis gives one considerably more confidence in the data reduction and gives a definite clue to dipole measurements that are affected by two and/or three dimensional lateral resistivity variations such as are caused by structural features, etc. See Figure 3.

TABLE IV-1

PROFILE 1

Telluric Profile Apparent Resistivity Values

STATION NUMBER	APPARENT RESISTIVITY (ohm-meter)	FREQUENCY (Hz)	APPARENT RESISTIVITY	FREQUENCY (Hz)	BASE NUMBER TIE
1	1.4	0.045	0.2	14	VTB-4
2	2.3	↓	0.86	↓	
3	2.3	↓	3.3	↓	
4	1.0	↓	2.1	↓	
5					
6					
7					
8					
9					
10					
11					
12					
13					
14					
15					
16					
17					
18					
19					
20					
21					
22					
23					
24					
25					
26					
27					
28					
29					
30					

TABLE IV-2

PROFILE 2

Telluric Profile Apparent Resistivity Values

STATION NUMBER	APPARENT RESISTIVITY (ohm-meter)	FREQUENCY (Hz)	APPARENT RESISTIVITY	FREQUENCY (Hz)	BASE NUMBER TIE
1	4.3	0.045	1.4	14	
2	3.1	↓	1.1	↓	
3	4.4		1.2		
4	1.9		1.3		
5	2.5		1.2		
6	1.8		1.0		
7	2.1		0.86		VT-14
8	1.6		0.60		
9					
10					
11					
12					
13					
14					
15					
16					
17					
18					
19					
20					
21					
22					
23					
24					
25					
26					
27					
28					
29					
30					

TABLE IV-3

PROFILE 3

Telluric Profile Apparent Resistivity Values

STATION NUMBER	APPARENT RESISTIVITY (ohm-meter)	FREQUENCY (Hz)	APPARENT RESISTIVITY	FREQUENCY (Hz)	BASE NUMBER TIE
1	3.4	0.045	0.91	14	
2	3.8		1.1		
3	4.4		1.5		
4	5.0		1.9		VT-13
5	5.7		2.9		
6	7.0		3.0		
7	5.8		7.7		
8	7.1		10		
9					
10					
11					
12					
13					
14					
15					
16					
17					
18					
19					
20					
21					
22					
23					
24					
25					
26					
27					
28					
29					
30					

TABLE IV-4

PROFILE 4

Telluric Profile Apparent Resistivity Values

STATION NUMBER	APPARENT RESISTIVITY (ohm-meter)	FREQUENCY (Hz)	APPARENT RESISTIVITY	FREQUENCY (Hz)	BASE NUMBER TIE
1	4.3	0.045	4.5	14	
2	3.5		4.7		
3	11.		5.8		
4	9.0		6.1		
5	9.9		6.1		VT-12
6	9.0		6.1		
7	10.		6.6		
8	11		7.1		
9	12		7.7		
10					
11					
12					
13					
14					
15					
16					
17					
18					
19					
20					
21					
22					
23					
24					
25					
26					
27					
28					
29					
30					

TABLE IV- 5

PROFILE 5

Telluric Profile Apparent Resistivity Values

STATION NUMBER	APPARENT RESISTIVITY (ohm-meter)	FREQUENCY (Hz)	APPARENT RESISTIVITY	FREQUENCY (Hz)	BASE NUMBER TIE
1	8.8	0.045	5.8	14	
2	9.4		6.7		
3	10		7.6		
4	11		8.7		
5	7.9		3.9		VTB-1
6	5.9		1.8		
7	1.7		2.2		
8					
9					
10					
11					
12					
13					
14					
15					
16					
17					
18					
19					
20					
21					
22					
23					
24					
25					
26					
27					
28					
29					
30					

TABLE IV-6

PROFILE 6

Telluric Profile Apparent Resistivity Values

STATION NUMBER	APPARENT RESISTIVITY (ohm-meter)	FREQUENCY (Hz)	APPARENT RESISTIVITY	FREQUENCY (Hz)	BASE NUMBER TIE
1	40	0.045	11	14	VTB-2
2	40		11		
3	36		10		
4	55		9.4		
5	39		13		VT-15
6	36		6.7		
7	21		6.3		
8	21		6.3		
9	12		0.57		
10	22		1.2		
11	38		2.0		
12	54		2.0		
13					
14					
15					
16					
17					
18					
19					
20					
21					
22					
23					
24					
25					
26					
27					
28					
29					
30					

TABLE IV-7

PROFILE 7

Telluric Profile Apparent Resistivity Values

STATION NUMBER	APPARENT RESISTIVITY (ohm-meter)	FREQUENCY (Hz)	APPARENT RESISTIVITY	FREQUENCY (Hz)	BASE NUMBER TIE
1	9.6	0.045	1.1	14	
2	8.9		2.1		
3	8.2		2.1		VT -16
4	14		2.1		
5	9.6		2.0		
6	5.5		2.7		
7	3.1		1.5		
8	1.8	↓	2.0	↓	
9					
10					
11					
12					
13					
14					
15					
16					
17					
18					
19					
20					
21					
22					
23					
24					
25					
26					
27					
28					
29					
30					

TABLE IV- 8

PROFILE 8

Telluric Profile Apparent Resistivity Values

STATION NUMBER	APPARENT RESISTIVITY (ohm-meter)	FREQUENCY (Hz)	APPARENT RESISTIVITY	FREQUENCY (Hz)	BASE NUMBER TIE
1	<0.1	0.045	.24	14	
2	.12		.58		
3	.12		.26		
4	.25		.62		
5	.34		1.7		
6	.32		1.1		
7	.5	↓	3.1	↓	VTB-3
8					
9					
10					
11					
12					
13					
14					
15					
16					
17					
18					
19					
20					
21					
22					
23					
24					
25					
26					
27					
28					
29					
30					

TABLE IV-9

PROFILE 9

Telluric Profile Apparent Resistivity Values

STATION NUMBER	APPARENT RESISTIVITY (ohm-meter)	FREQUENCY (Hz)	APPARENT RESISTIVITY	FREQUENCY (Hz)	BASE NUMBER TIE
1	43	0.045	17	14	VT-6
2	43		17		
3	43		17		
4	53		18		
5	41		19		
6	49		20		
7	54		23		
8	59		25		
9	66		28.		
10	63		63		
11	58		66		
12	29		150		
13					
14					
15					
16					
17					
18					
19					
20					
21					
22					
23					
24					
25					
26					
27					
28					
29					
30					

TABLE IV-10

PROFILE 10

Telluric Profile Apparent Resistivity Values

STATION NUMBER	APPARENT RESISTIVITY (ohm-meter)	FREQUENCY (Hz)	APPARENT RESISTIVITY	FREQUENCY (Hz)	BASE NUMBER TIE
1	17	0.045	120	14	
2	17		120		
3	28		110		
4	28		110		
5	34		91		
6	41		78		
7	49		68		
8	39		52		
9	39		52		
10	31		39		
11	11		41		
12	?		44		
13	3.9		39		
14	3.0		31		
15	2.4		31		
16	1.8		26		
17	0.41		26		
18	<0.1		6.9		
19.	<0.1		1.8		
20	0.23		0.49		
21	3.2		1.4		VT-8
22	1.5		3.1		
23	2.2		7.5		
24	2.2		10		
25	2.3		3.9		VTB-4
26					
27					
28					
29					
30					

APPENDIX III

Vector Telluric Measurements

Contents:

Discussion

Table of Vector Telluric Apparent Resistivity Values.

TABLE IV-11

PROFILE 11

Telluric Profile Apparent Resistivity Values

STATION NUMBER	APPARENT RESISTIVITY (ohm-meter)	FREQUENCY (Hz)	APPARENT RESISTIVITY	FREQUENCY (Hz)	BASE NUMBER TIE
1	1.4	0.045	1.6	14	
2	5.1		1.0		
3	5.1		4.6		
4	10		3.9		MT-20
5	14		4.8		
6	20		5.8		
7	16		3.5		
8	13		3.5		
9	10		2.1		
10					
11					
12					
13					
14					
15					
16					
17					
18					
19					
20					
21					
22					
23					
24					
25					
26					
27					
28					
29					
30					

TABLE IV-12

PROFILE 12

Telluric Profile Apparent Resistivity Values

STATION NUMBER	APPARENT RESISTIVITY (ohm-meter)	FREQUENCY (Hz)	APPARENT RESISTIVITY	FREQUENCY (Hz)	BASE NUMBER TIE
1	52	0.045	26	14	
2	22		26		
3	22		26		VT-7
4	22		26		
5	62		29		
6	49		25		
7	27		13		
8	15		7.2		
9	8.3		3.8		
10					
11					
12					
13					
14					
15					
16					
17					
18					
19					
20					
21					
22					
23					
24					
25					
26					
27					
28					
29					
30					

TABLE IV-13

PROFILE 13

Telluric Profile Apparent Resistivity Values

STATION NUMBER	APPARENT RESISTIVITY (ohm-meter)	FREQUENCY (Hz)	APPARENT RESISTIVITY	FREQUENCY (Hz)	BASE NUMBER TIE
1	6.6	0.045	120	14	
2	5.9		18		
3	1.3		12		
4	1.7		10		
5	1.4		9.9		
6	1.1		9.9		
7	1.1		7.5		
8	0.76		12.		
9	2.1		15		VT-9
10	1.4		40		
11	9.0	↓	37	↓	
12					
13					
14					
15					
16					
17					
18					
19					
20					
21					
22					
23					
24					
25					
26					
27					
28					
29					
30					

TABLE IV-14

PROFILE 14

Telluric Profile Apparent Resistivity Values

STATION NUMBER	APPARENT RESISTIVITY (ohm-meter)	FREQUENCY (Hz)	APPARENT RESISTIVITY	FREQUENCY (Hz)	BASE NUMBER TIE
1	4.7	0.045	26	14	
2	3.6		20		
3	0.46		0.2		
4	3.9		8.9		VT-6
5	5.5		7.8		
6	3.6		7.8		
7	3.8		10		
8	5.3	∇	6.0	∇	MT-10
9					
10					
11					
12					
13					
14					
15					
16					
17					
18					
19					
20					
21					
22					
23					
24					
25					
26					
27					
28					
29					
30					

TABLE IV-15

PROFILE 15

Telluric Profile Apparent Resistivity Values

STATION NUMBER	APPARENT RESISTIVITY (ohm-meter)	FREQUENCY (Hz)	APPARENT RESISTIVITY	FREQUENCY (Hz)	BASE NUMBER TIE
1	5.0	0.045	9.3	14	
2	4.8		8.8		VT-8
3	3.1		8.0		
4	2.4		6.3		
5	1.7		5.3		
6	1.1		3.2		
7	1.4		2.4		
8	0.17		3.9		
9	0.14		1.3		
10	0.1		1.4		
11	<0.1		4.5		
12	0.3		12		
13	5.3		3.9		
14	4.3		8.5		
15	5.3		6.0		
16	5.0		6.0		
17	5.5		1.9		
18	3.9		1.8		
19	7.4	↓	1.1	↓	MT-20
20					
21					
22					
23					
24					
25					
26					
27					
28					
29					
30					

TABLE IV-16

PROFILE 16

Telluric Profile Apparent Resistivity Values

STATION NUMBER	APPARENT RESISTIVITY (ohm-meter)	FREQUENCY (Hz)	APPARENT RESISTIVITY	FREQUENCY (Hz)	BASE NUMBER TIE
1	3.6	0.045	8.5	14	
2	?		7.5		
3	3.2		3.1		
4	3.4		16		
5	2.2		0.8		
6	2.3		1.9		
7	2.2		1.5		
8	2.2		0.81		
9	2.0		1.6		
10	2.0		2.1		
11	1.9		2.1		
12	2.7		5.6		
13	1.9		6.5		
14	3.0		3.6		
15	0.73		?		VT-10
16	2.1		13		
17	4.9		8.5		
18	5.7		8.5		
19	4.6		8.5		
20	4.6		8.5		
21	4.6		15		
22	9.2		13		
23	5.1		12		
24	?		4.6		
25					
26					
27					
28					
29					
30					

TABLE IV-17

PROFILE 17

Telluric Profile Apparent Resistivity Values

STATION NUMBER	APPARENT RESISTIVITY	FREQUENCY (Hz)	APPARENT RESISTIVITY	FREQUENCY (Hz)	BASE NUMBER TIE
1	71	0.045	2.6	14	
2	69		2.5		
3	54		2.3		
4	14		1.8		
5	16		1.8		
6	12		0.83		
7	12		0.9		
8	13		1.0		
9	12		0.85		
10	11		0.85		
11	11		0.85		VT-11
12	11		0.93		
13	11		0.72		
14	12		1.3		
15	13		2.1		
16	14		3.1		
17					
18					
19					
20					
21					
22					
23					
24					
25					
26					
27					
28					
29					
30					

TABLE IV-18
 PROFILE 15, 16

Telluric Profile Apparent Resistivity Values

STATION NUMBER	APPARENT RESISTIVITY (ohm-meter)	FREQUENCY (Hz)	APPARENT RESISTIVITY	FREQUENCY (Hz)	BASE NUMBER TIE
16 1 W	3.6	0.045			
1 E	3.1				
5 W	2.3				
5 E	2.4				
10 W	2.0				
10 E	1.7				
13 W	1.9				
13 E	2.7				
15 W	0.73				
15 E	40.1				
16 W	2.1				
16 E	76.4				
19 W	4.6				
19 E	723				
24 W	N.R.				
16 24 E	N.R.				
15 1 W	N.R.				
1 E	N.R.				
4 W	2.4				
4 E	2.7				
7 W	1.4				
7 E	1.8				
10 W	0.1				
10 E	0.09				
13 W	5.3				
13 E	6.6				
16 W	5.0				
15 16 E	4.8				

TABLE IV- 19

PROFILE 17

Telluric Profile Apparent Resistivity Values

STATION NUMBER	APPARENT RESISTIVITY (ohm-meter)	FREQUENCY (Hz)	APPARENT RESISTIVITY	FREQUENCY (Hz)	BASE NUMBER TIE
17 1 W	170	0.035			
1 1 E	71				
4 W	19				
4 E	14				
7 W	10				
7 E	12				
10 W	11				
10 E	17				
13 W	10				
17 13 E	11				
16					
17					
18					
19					
20					
21					
22					
23					
24					
25					
26					
27					
28					
29					
30					

APPENDIX V

Galvanic (dc) Electrical
Resistivity Soundings

Contents:

Description of Methods

Qualitative interpretative Concepts

Survey Sounding Curves

Description of the Galvanic dc Resistivity

Sounding and Profiling Methods

The galvanic dc resistivity sounding methods and profiling methods are:

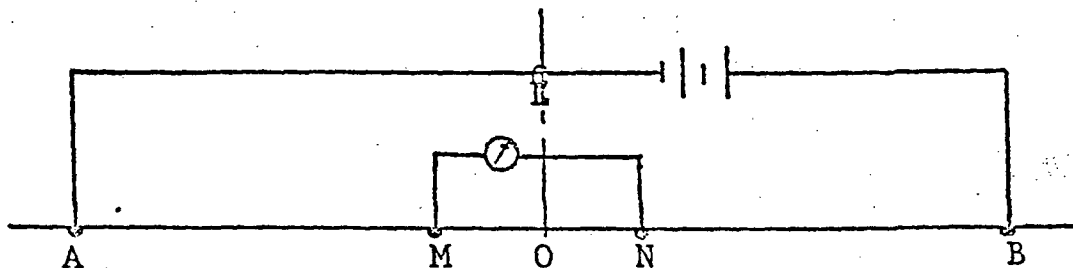
1. Schlumberger method.
2. Monopole method,
3. Various dipole methods,
4. Modified Schlumberger method
5. Modified Polar Dipole-Bipole method,
6. Dipole-dipole method.

The choice of which method to use depends on the following:

1. Best possible sounding data with a minimum of interference from lateral resistivity variations (geologic noise).
2. Economic considerations: Monopole-shallow, Schlumberger- intermediate, and Equitorial method- deep penetration soundings.
3. Profiling methods:
 - a. Modified sounding methods, Modified Schlumberger method and Modified Polar Dipole-Bipole methods for unknown depths of interest.
 - b. Dipole-dipole method for known range of depths of interest.

Schlumberger Method

The Schlumberger array orientation is shown in the figure below. The two electrode pairs are in line and symmetric about the point O, with the distance AB between the source electrode



Schlumberger Array Configuration

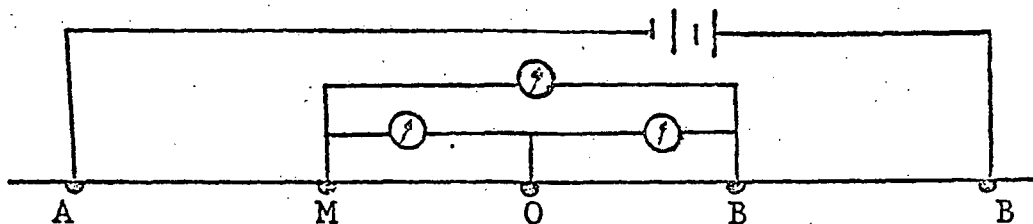
pair being very large compared to the distance \overline{MN} between the the measurement pair.

The depth of penetration is increased by increasing $\overline{AB}/2$. However, as $\overline{AB}/2$ is increased, the signal between M and N becomes too small to be detected reliably. When this occurs, the receiver separation is increased and the measurements and $\overline{AB}/2$ expansion continues.

The apparent probing depth of the Schlumberger array in a homogeneous earth is equivalent to $\overline{AB}/2$. The location of each measurement in the geoelectric section is below the center of the array at the effective depth of penetration.

The gradient of the potential is measured between M and N because the measuring electrode pair separation is maintained small compared to the source electrode pair separation, \overline{AB} .

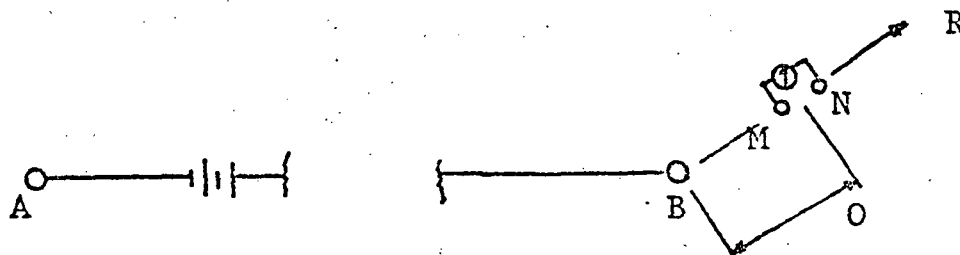
The Schlumberger array is less sensitive to lateral effects than any of the other sounding and profiling arrays, because only the source pair of electrodes is moved. These electrodes are at relatively great distances from the receiver pair, thus geologic noise in the vicinity of the source electrodes does not appreciably affect the gradient measurement. If geologic noise at the source electrodes is a factor in the measurements, the use of the Lee array configuration, as shown in the figure below, makes it possible to determine the lateral discontinuity effects. This is accomplished by making separate half-potential measurements, \overline{MO} and \overline{ON} , on each side of the center of the array.



Lee Array Configuration

Monopole Method

The Monopole array is shown in the figure below. The



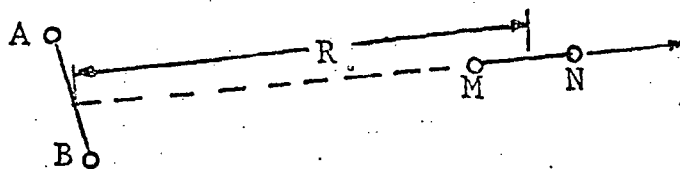
Monopole Array Configuration

distance AB is very large (assumed to be infinite) compared to the distance MN. Similarly, the distance AB is very large (assumed to be infinite) compared to the distance OB. The apparent depth of penetration in a homogeneous earth is increased directly as OB is increased. The separation MN is increased as the requirement for detectable signal dictates.

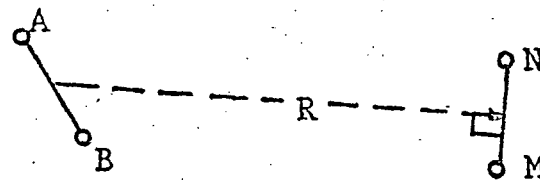
Dipole Arrays

The dipole arrays utilize an effective source dipole, \overline{AB} , and an effective receiver dipole, \overline{MN} . The dipole approximations are maintained by keeping \overline{AB} and \overline{MN} small compared to the source-receiver separation, R. See the figures below. Because two dipoles are used, the gradient of the E field is measured at \overline{MN} . The depth of penetration, DP, varies with each array used. The dipole arrays normally used are as follows:

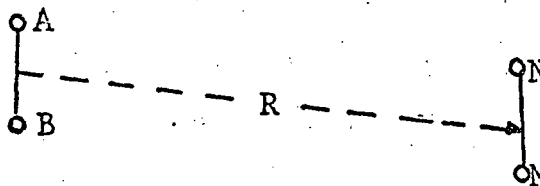
Radial Dipole Array
 $0.5R \leq DP \leq 0.67R$



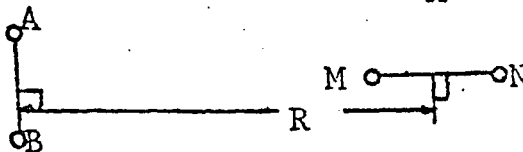
Tangential Dipole Array
 $0.67R \leq DP \leq R$



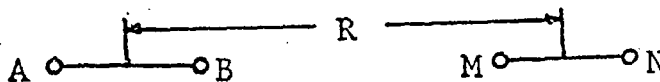
Parallel Dipole Array
 $0.5R \leq DP \leq R$



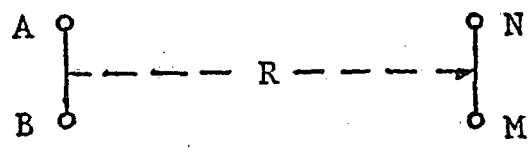
Perpendicular Dipole Array
 $DP = 0.67 R$



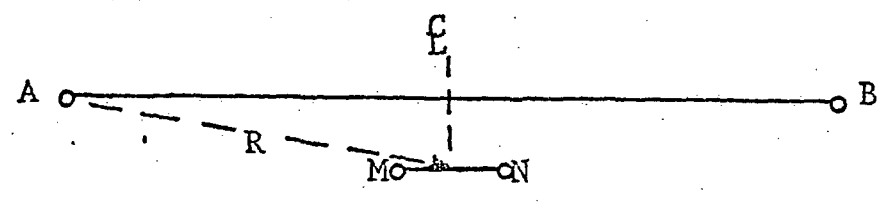
Polar Dipole Array
 $DP = 0.5R$



Equatorial Dipole Array
DP=R

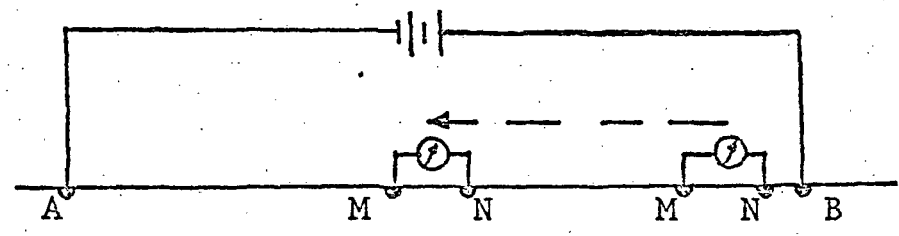


Equatorial Bipole-Dipole Array
(equivalent to Equatorial Dipole Array)
DP=R



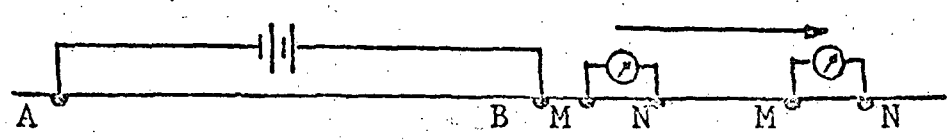
Modified Schlumberger Array

The Modified Schlumberger array is an expansion array of the receiver dipole, MN, away from one of the source electrodes (monopole approximation) to the mid-point AB/2. See the figure below.



Modified Polar Dipole-Bipole Array

The Modified Polar Dipole-Bipole array is an expansion array of the receiver dipole, MN, away from one of the source electrodes (monopole approximation) outside and inline with the source bipole, AB. Depth of effective penetration changes from the monopole depth of penetration toward the polar dipole depth of penetration as the array is expanded. See figure below.



Some Considerations in the Interpretation
of Resistivity Data

A permanent problem which must be routinely tackled in the interpretation of resistivity data is that of separating vertical effects from lateral effects. More correctly stated, one wants to discover both the lateral and depth distribution of resistivity in a geoelectric section.

A probable solution to the above ambiguities may be achieved by carrying out depth soundings at a high station density. However, such a solution is more often than not economically unacceptable.

One alternative to the costly high-density depth sounding approach is the use of combined modified Schlumberger soundings, monopole soundings, and equatorial soundings about a very long bipole source. This approach is very effective if the soundings are made about a crossed bipole source set-up as shown in Figure 1, although this approach is twice as costly as the single bipole source approach. The extra cost is offset by the following very positive interpretation features:

1. If an interpretation is totally correct from the sounding curves of one source, the interpretation for sounding from the other source will duplicate the interpretation found for the first source soundings. This seldom happens.
2. The multiple soundings from the two sources which provide depth of penetration to specific depths at different locations about the bipole source cross over point give one a very good interpretative handle on the lateral variation about the source location. For examples of this, see Figures 2 - 6, as

to the interpretation capability.

It should be apparent that the use of galvanic (dc) soundings about crossed long bipole sources is a very effective way of obtaining at least a qualitative description of the electrical resistivity distribution to depth and laterally within an area of interest in difficult interpretative sections such as are found in the Basin and Range Province. This sounding approach is relatively costly if done on a random basis. Therefore, Electrodyne performs reconnaissance surveys using the less expensive telluric profiling and scalar AMT-MT sounding methods to locate areas of interest for detailing soundings such as the crossed bipole dc soundings and EM soundings.

As with the electromagnetic sounding detailing (which prevents one from overlooking important conductors below resistive screening layers, layers that prevent detection of the conductors by the dc sounding methods); dc soundings should be made to prevent one from interpreting layers having large vertical anisotropy and/or overlooking screening layers by the EM soundings. The EM sounding interpretations will forecast depths to conductive sections that are underestimated for both of the above. Simply stated, one has to make both dc soundings and EM soundings in detailing surveys, if they wish to obtain a good interpretation of the geoelectric section in areas such as the Basin and Range Province.

There are two considerations in dc soundings when their results are compared to EM sounding results. These are:

1. The dc sounding interpretation will lead one to conclude that an anomalous conductive zone at depth will have a much larger areal extent than the EM interpretations will indicate.
2. The dc sounding interpretations of layer resistivity and layer thickness will always be equal to or greater than those interpreted from EM soundings for a layered earth interpretation.

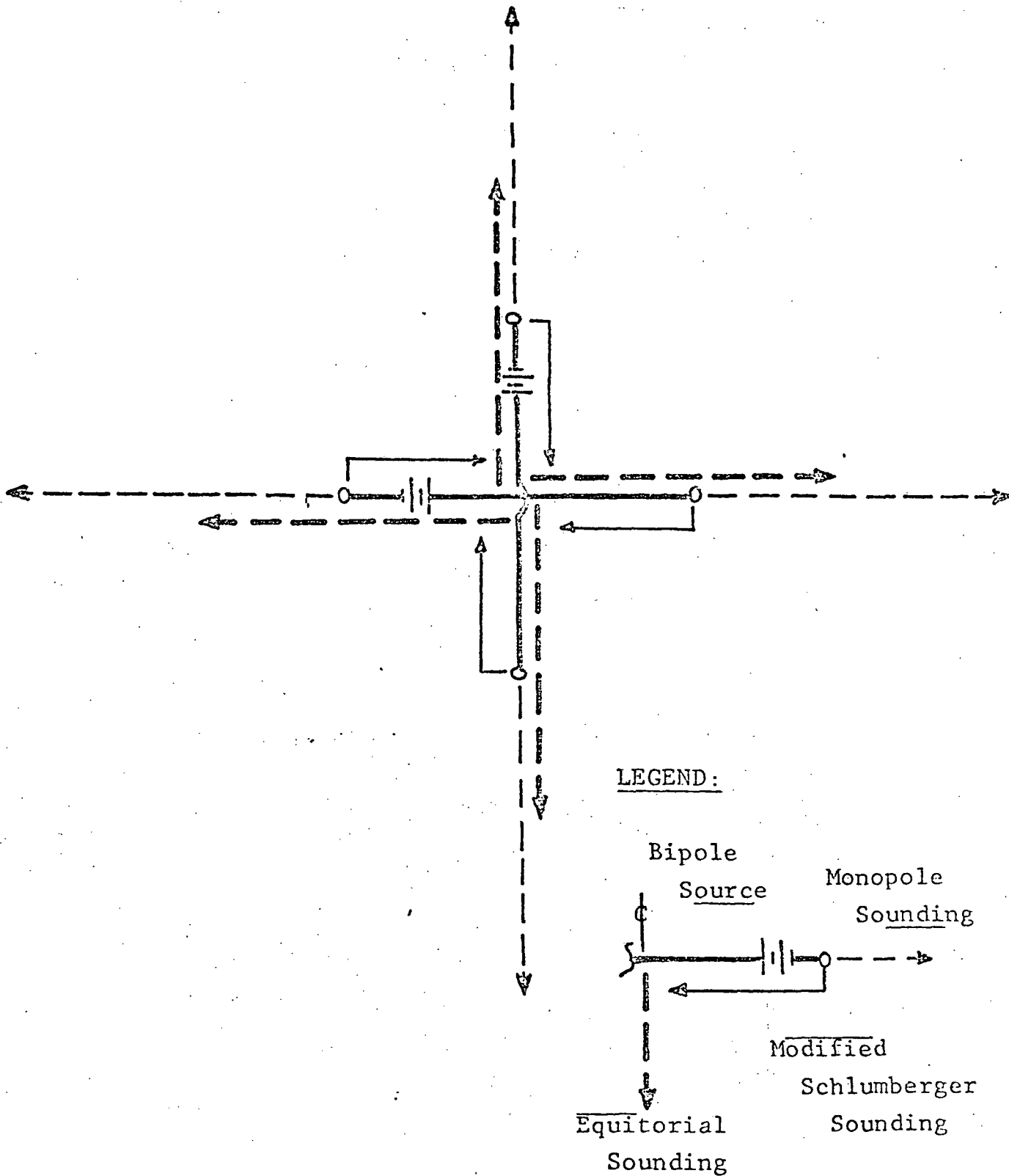


Figure 1. Cross Bipole Source--Modified Schlumberger, Monopole, and Equatorial Sounding Array Representation.

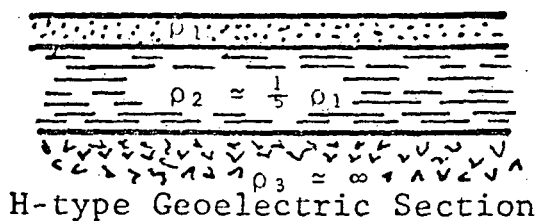
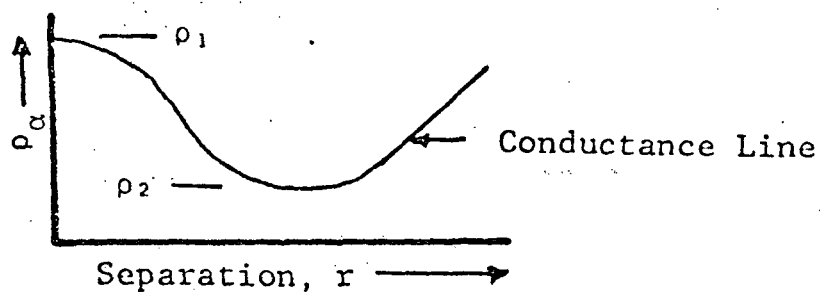


Figure 2. Typical 3-layer Geothermal Model and Sounding

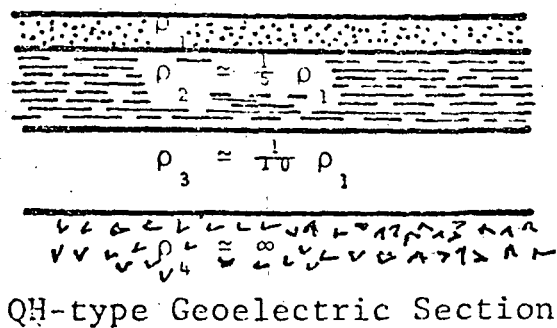
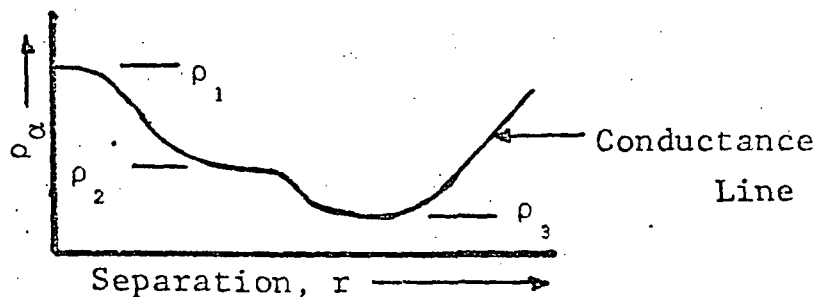
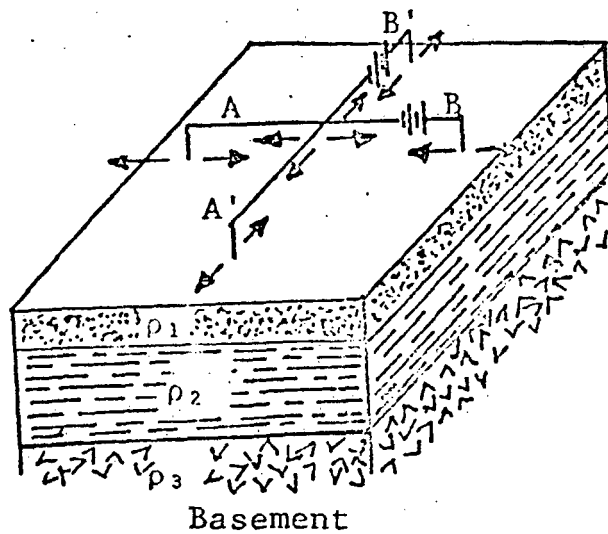
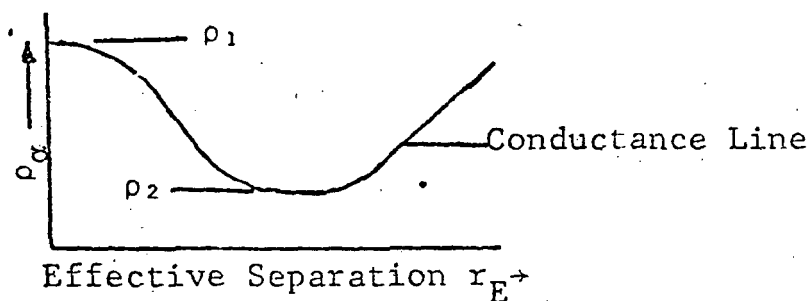


Figure 3. Typical 4-layer Geothermal Model and Sounding



$$\rho_1 > \rho_2 \ll \rho_3$$



Typical Sounding Curve for All
Electrical Resistivity Arrays:
Monopole,
Modified Schlumberger,
and Equatorial Arrays.

Figure 4. Typical Response Curves for a One-dimensional variation (vertical) in Electrical Resistivity

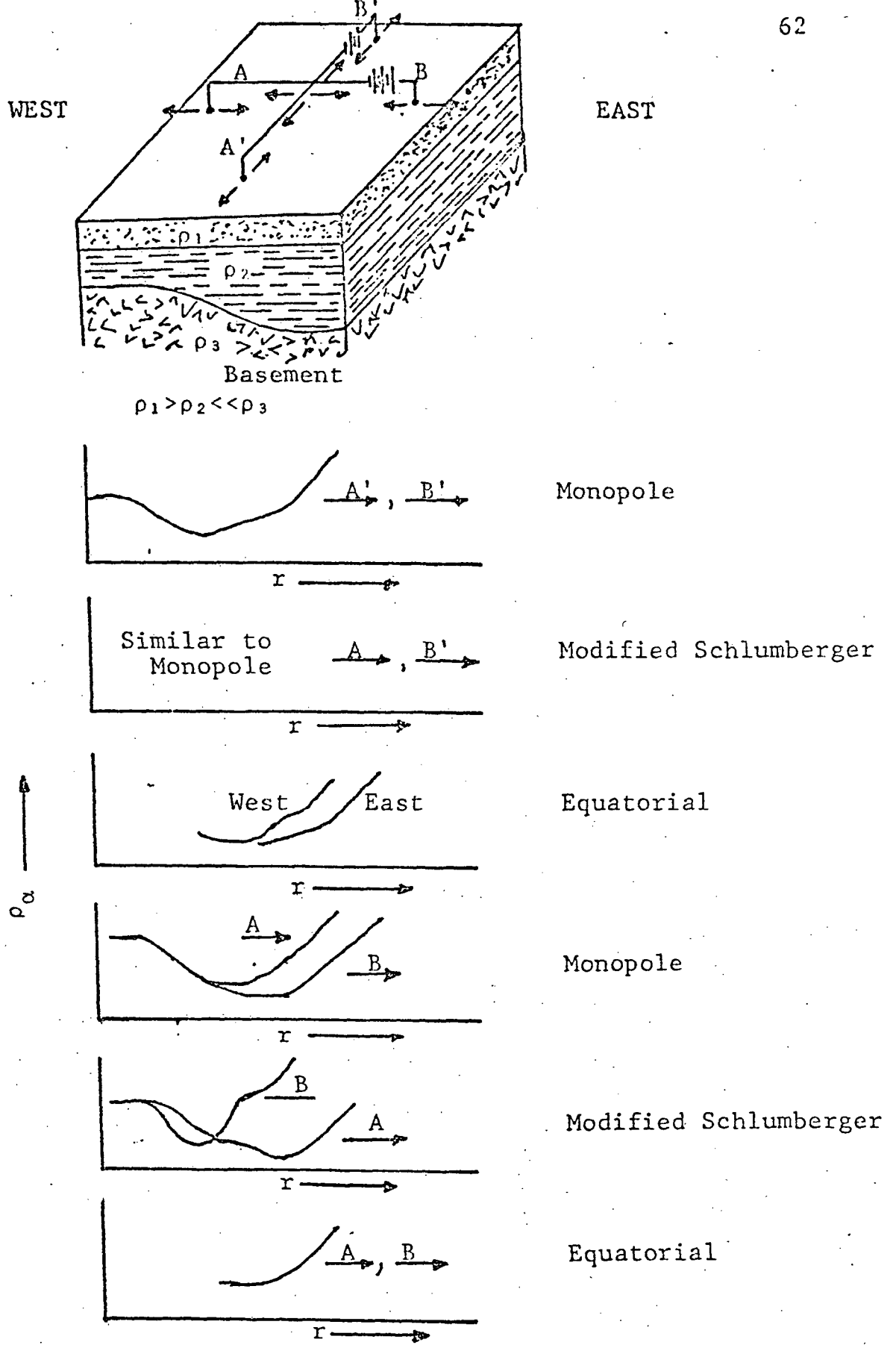
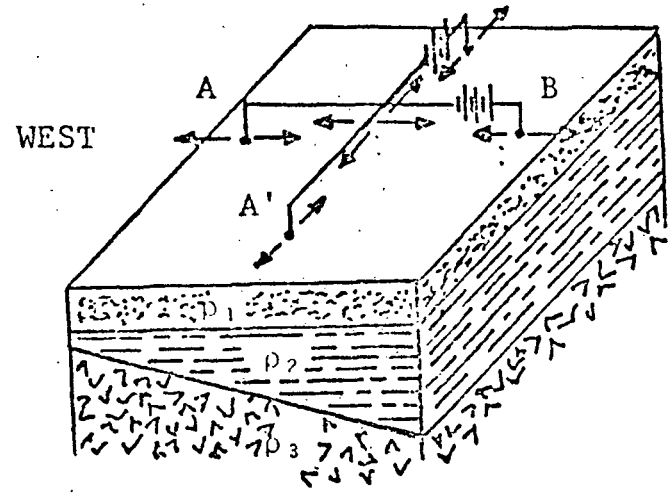


Figure 5. Typical Response Curves for a Basement Monocline



$\rho_1 > \rho_2 \ll \rho_3$

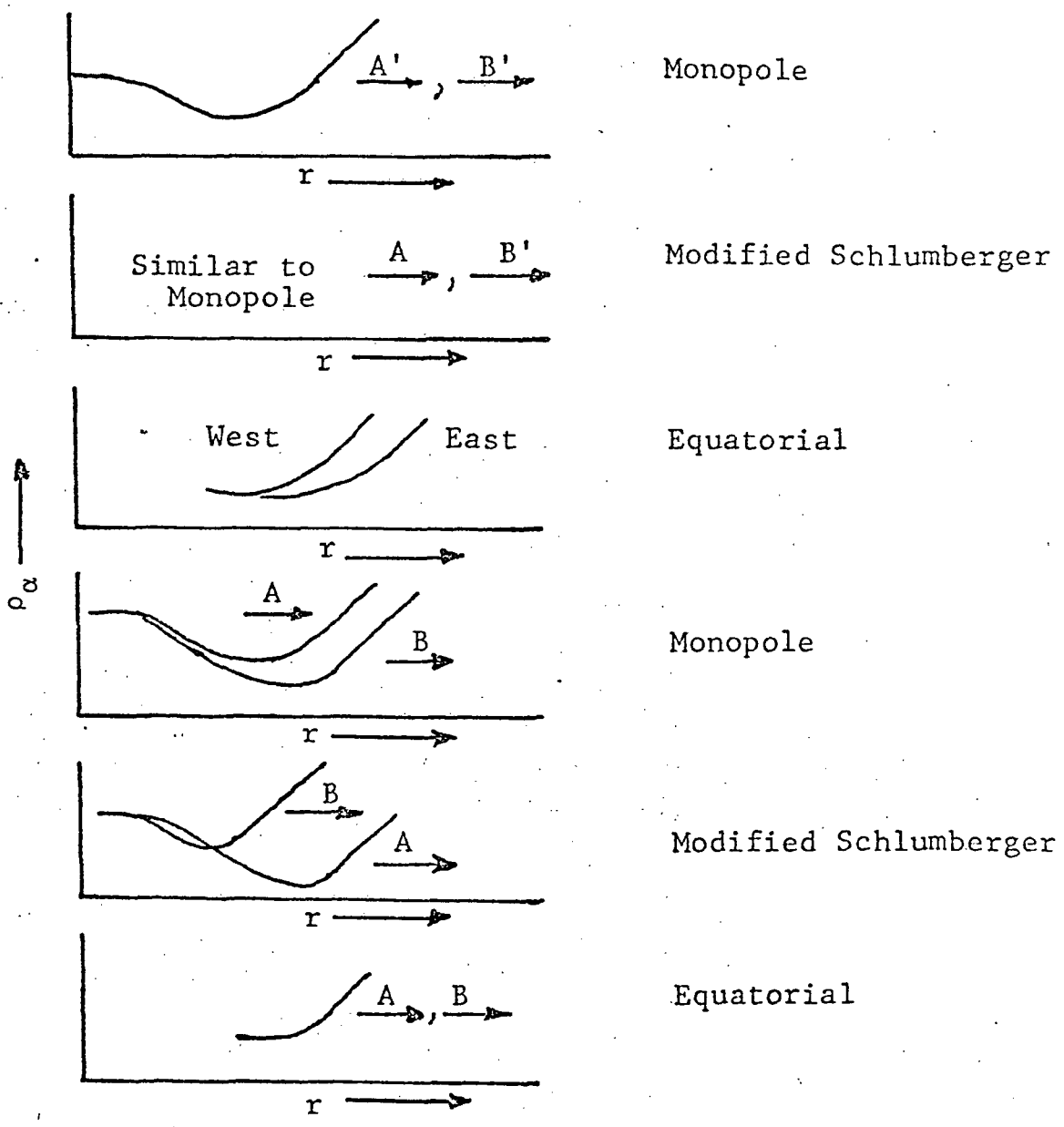


Figure 6. Typical Response Curves for a Dipping Basement Model

KEY TO SOUNDING ANNOTATION

C | R

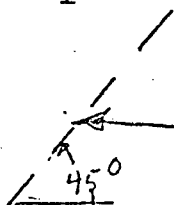
Conductive--Resistive Contrast

 ρ_i

Interpreted resistivity value for the ith layer.

 h_i

Interpreted thickness value for the ith layer



Apparent uniform conductance line

$h_i \cong x$ -depth Sounding did not penetrate into electrical basement.

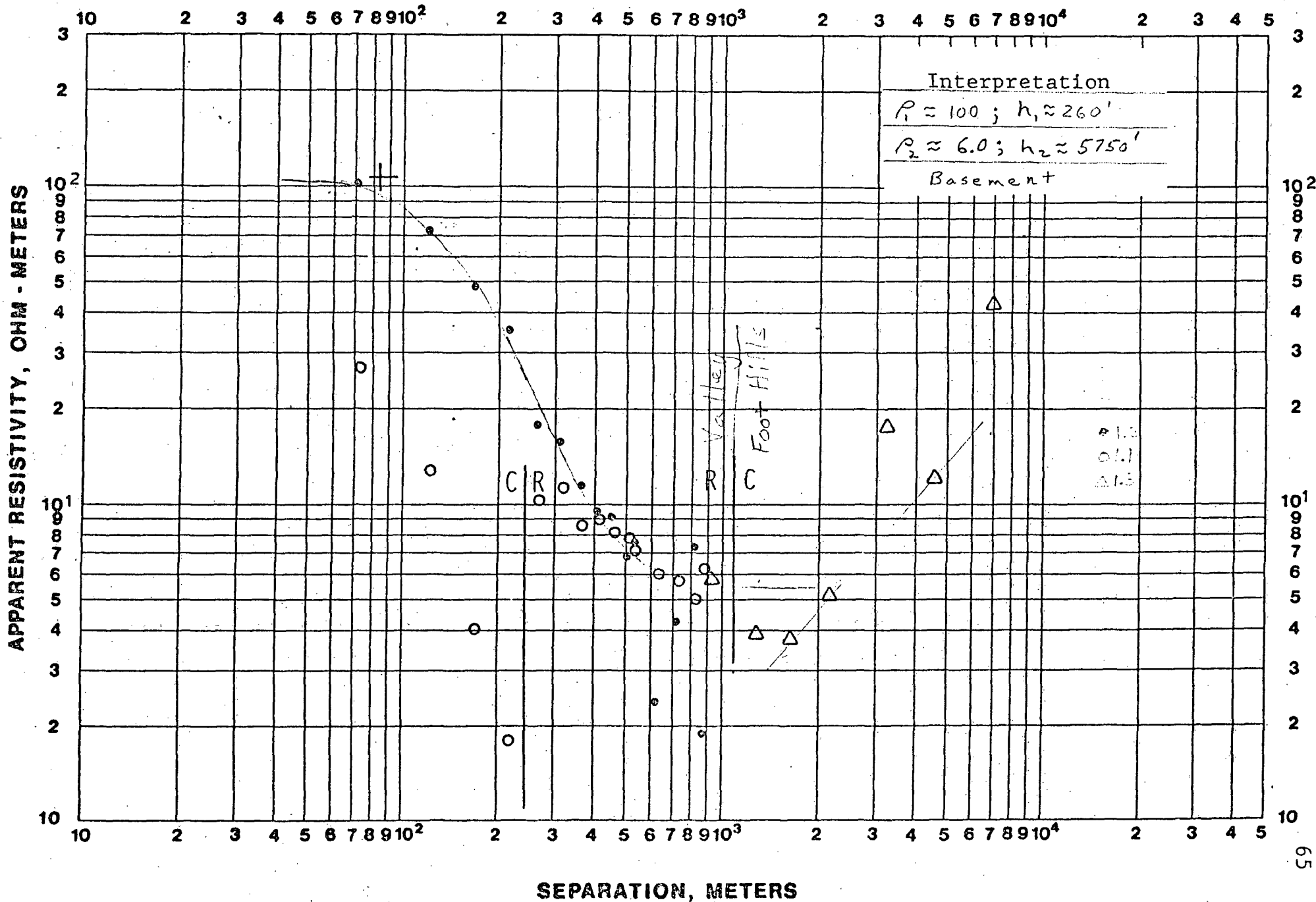


Figure V-1. Soundings 1.1, 1.2, and 1.3,
Combined Modified Schlumberger and Equatorial Soundings

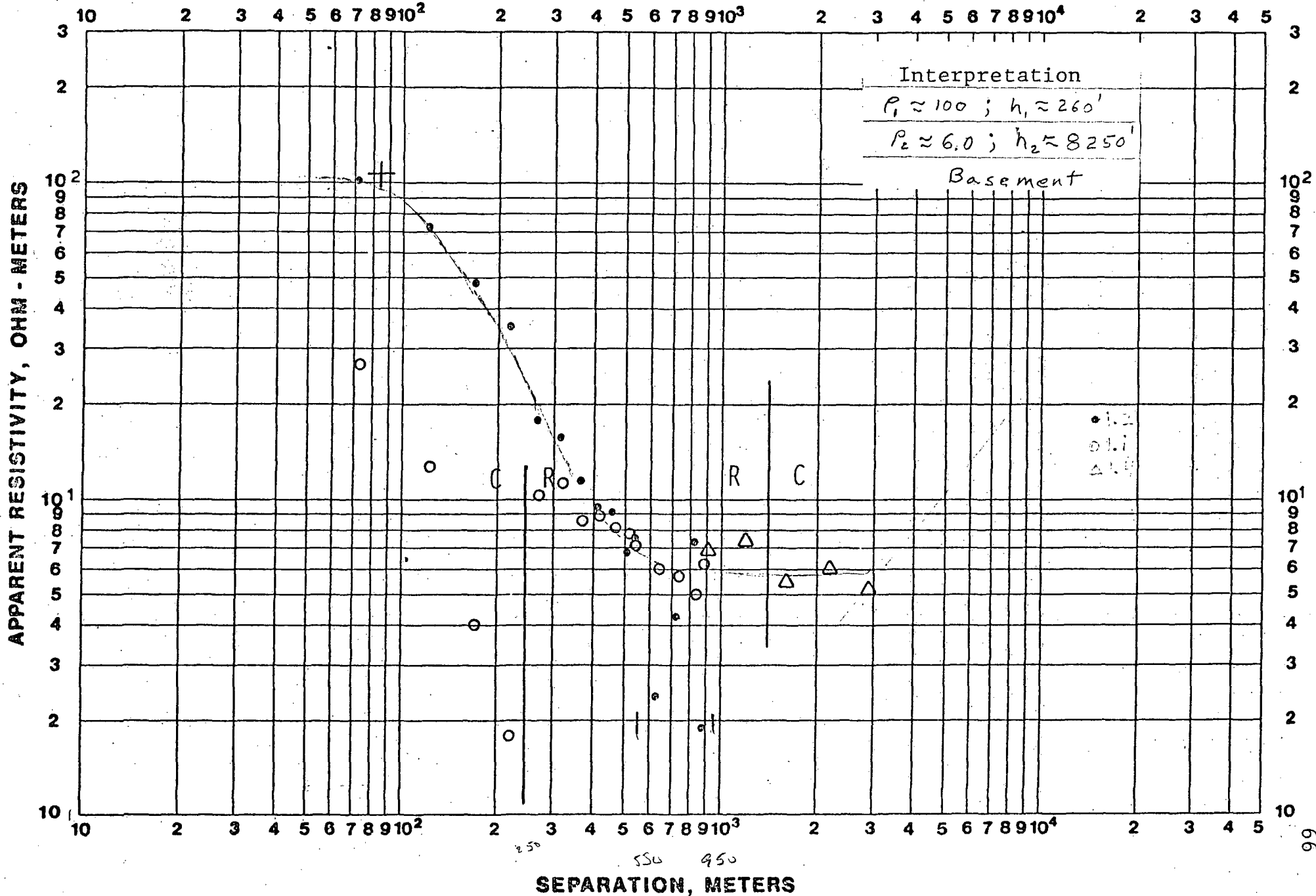


Figure V-2. Soundings 1.1, 1.2, and 1.4,
 Combined Modified Schlumberger and Equatorial Soundings

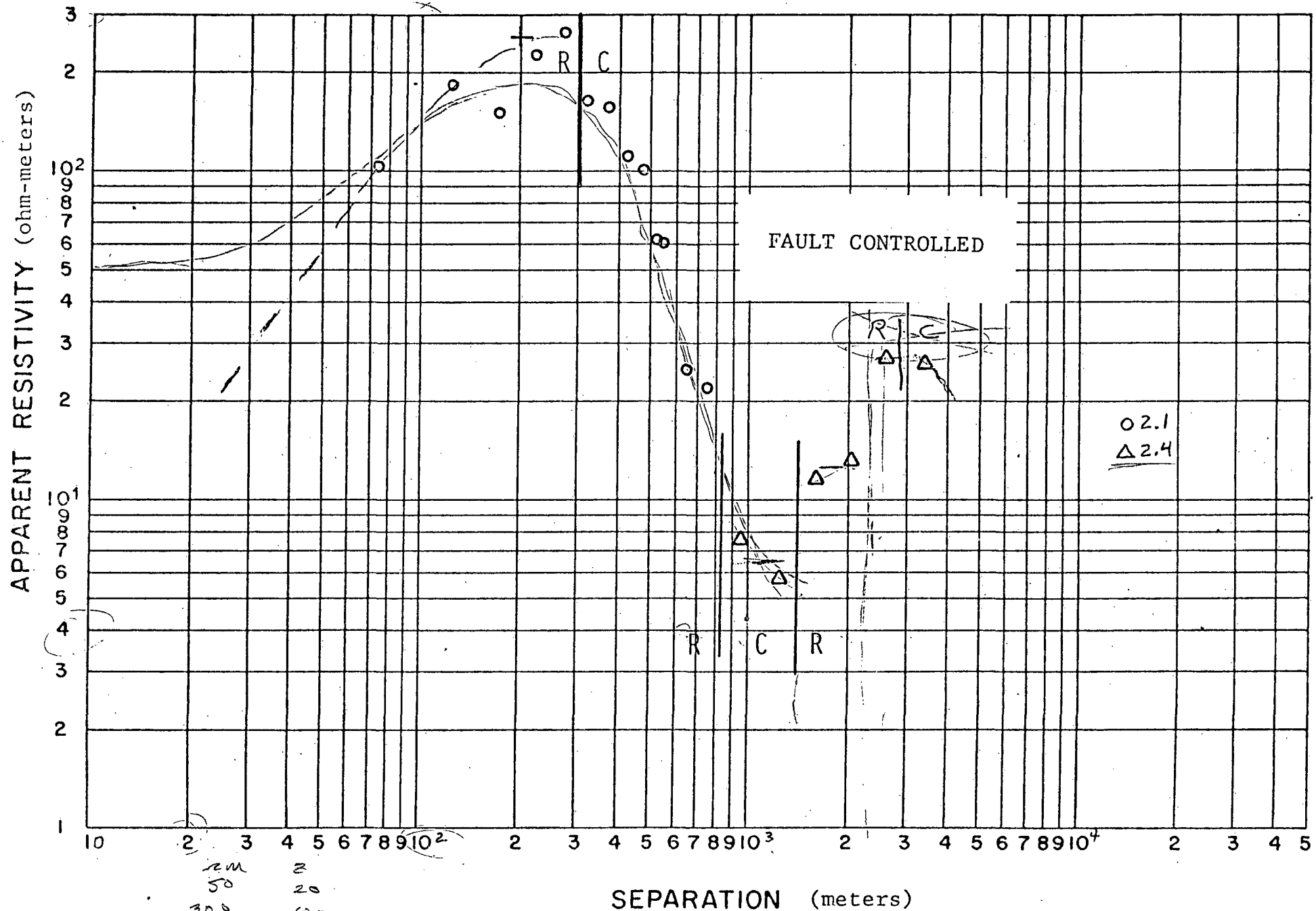


Figure V-3 . Soundings 2.1 and 2.4,
 Combined Modified Schlumberger and Equatorial Soundings

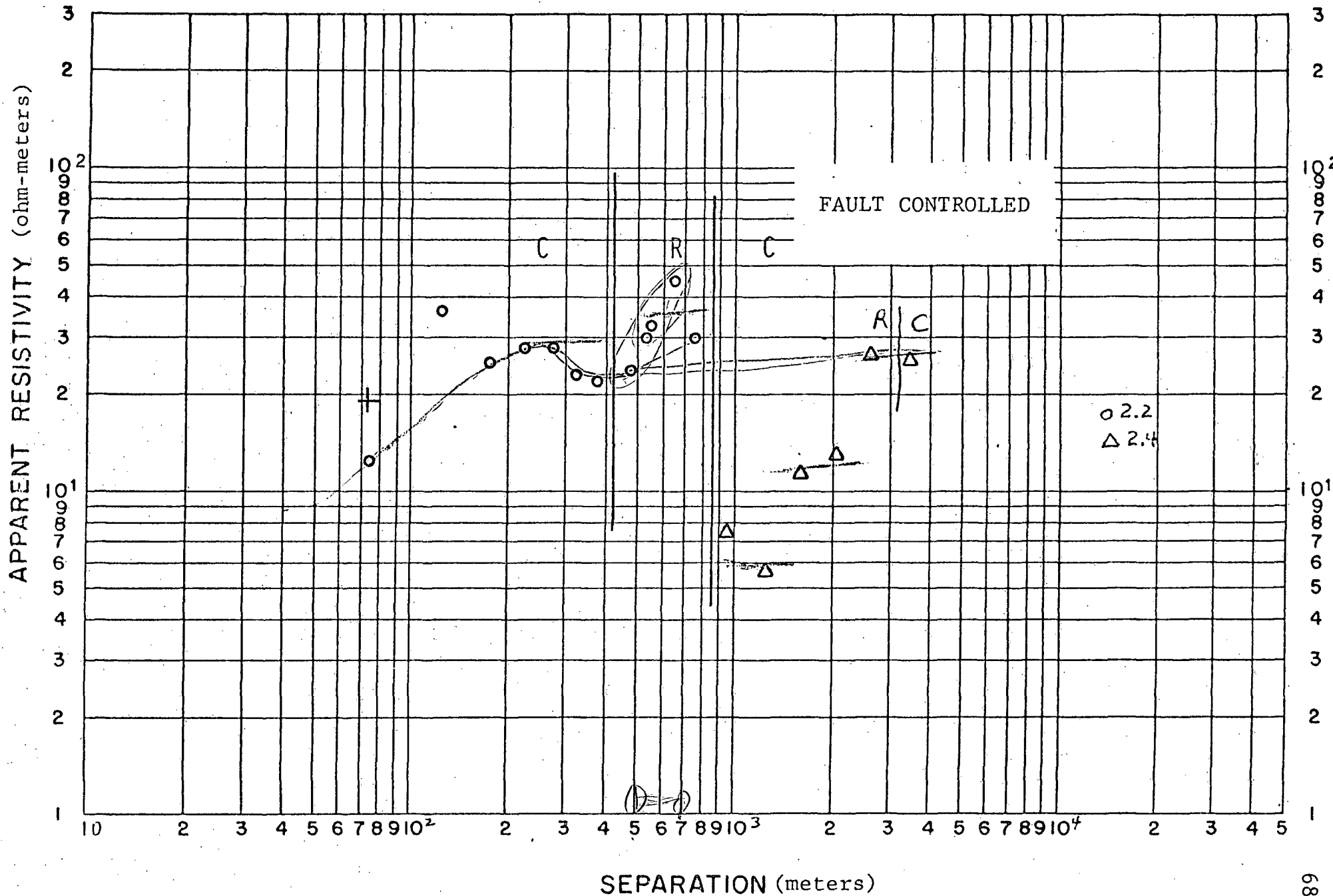


Figure V-4. Soundings 2.2 and 2.4,
 Combined Modified Schlumberger and Equatorial Soundings

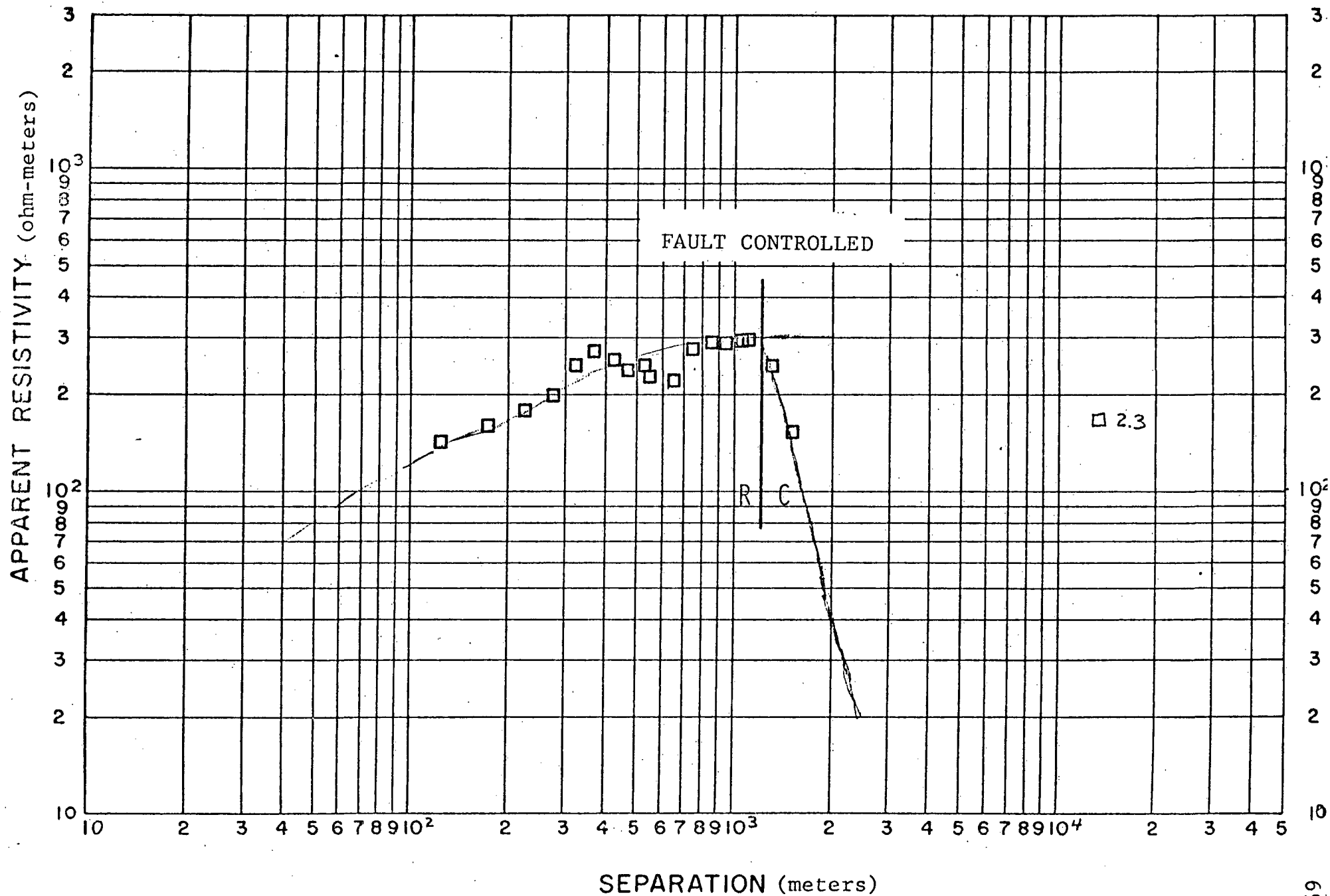


Figure V-5. Sounding 2.3
Monopole Sounding

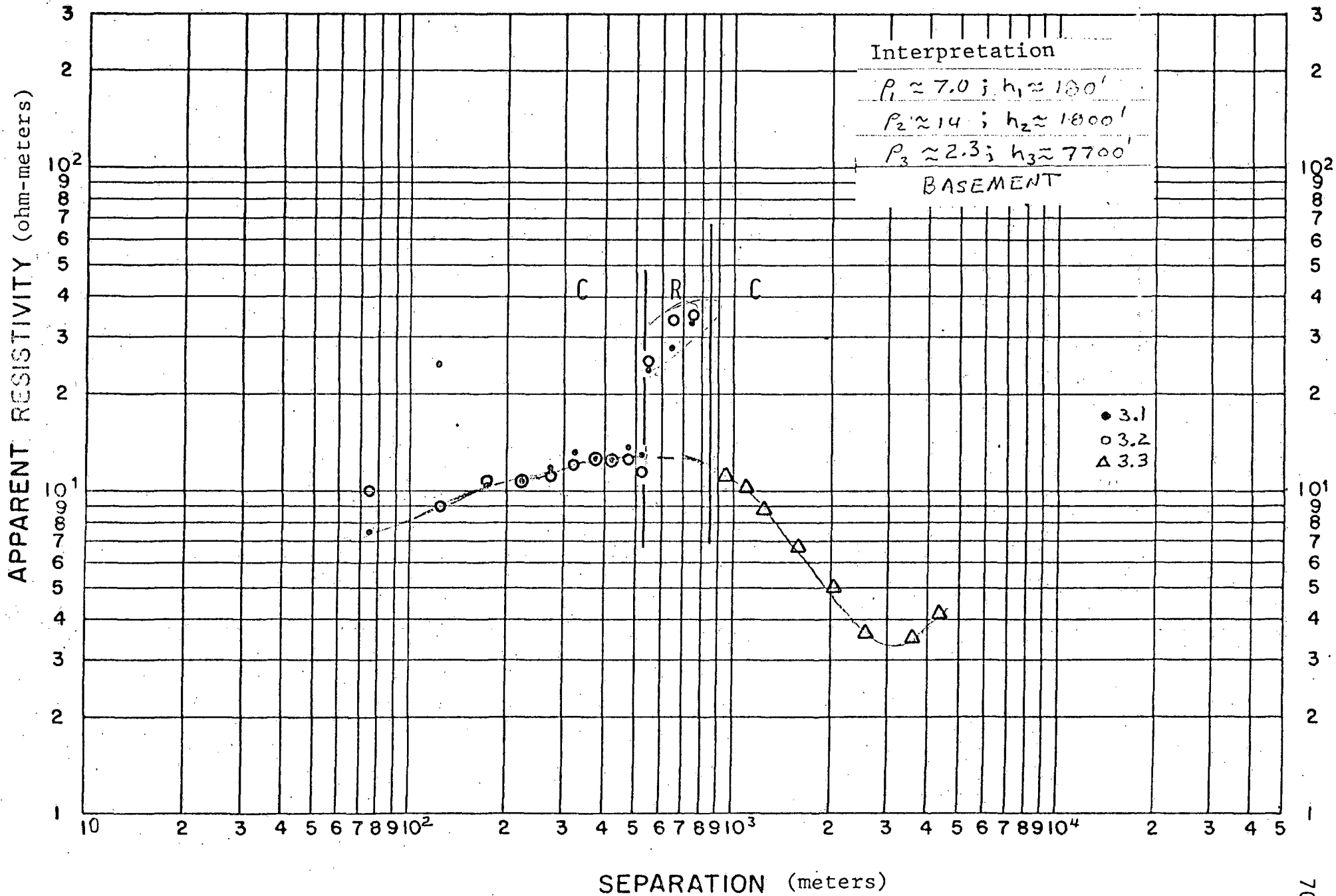


Figure V-6. Soundings 3.1, 3.2, and 3.3,
Combined Modified Schlumberger and Equatorial Soundings

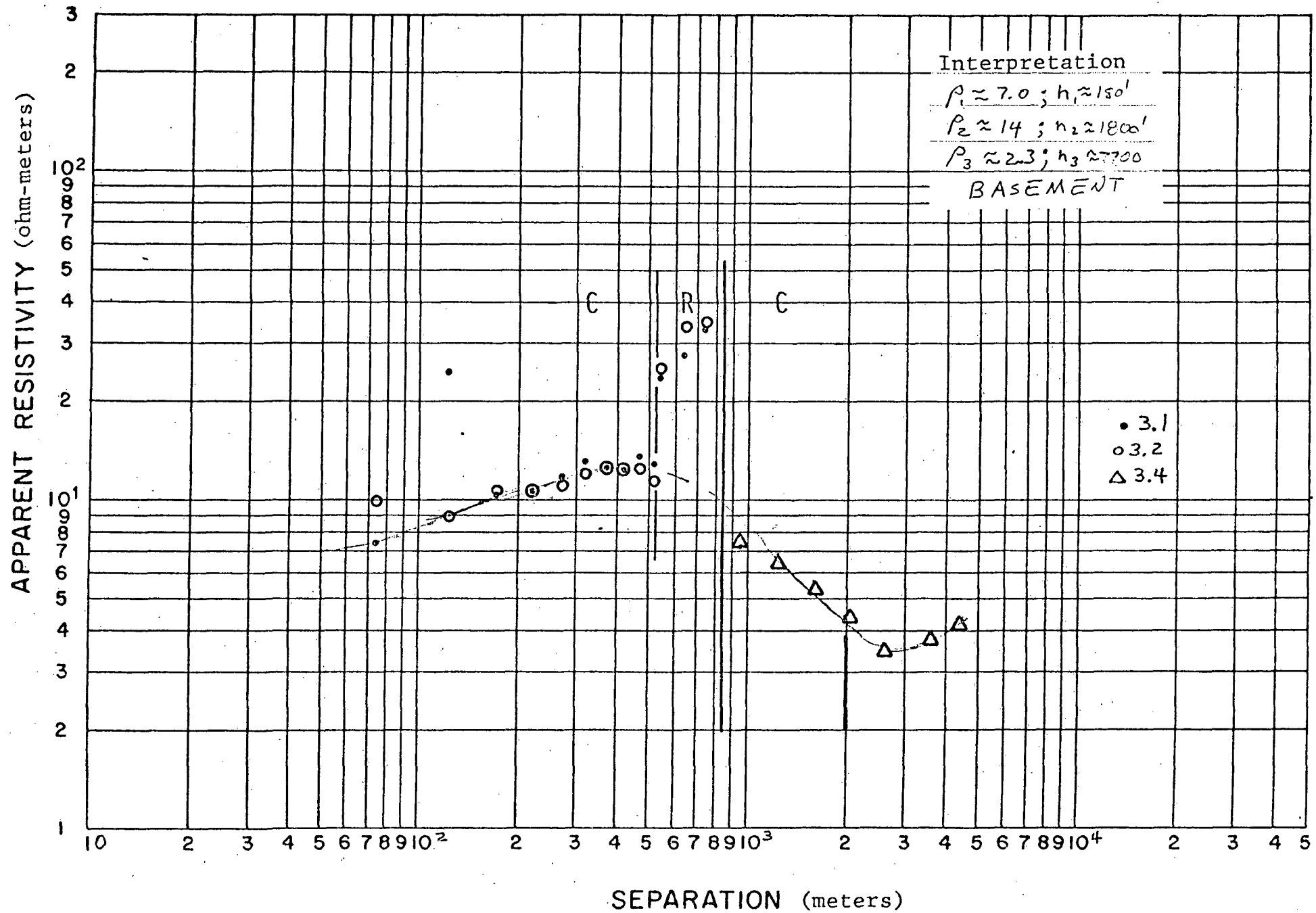


Figure V-7. Soundings 3.1, 3.2, and 3.4,
 Combined Modified Schlumberger and Equatorial Soundings

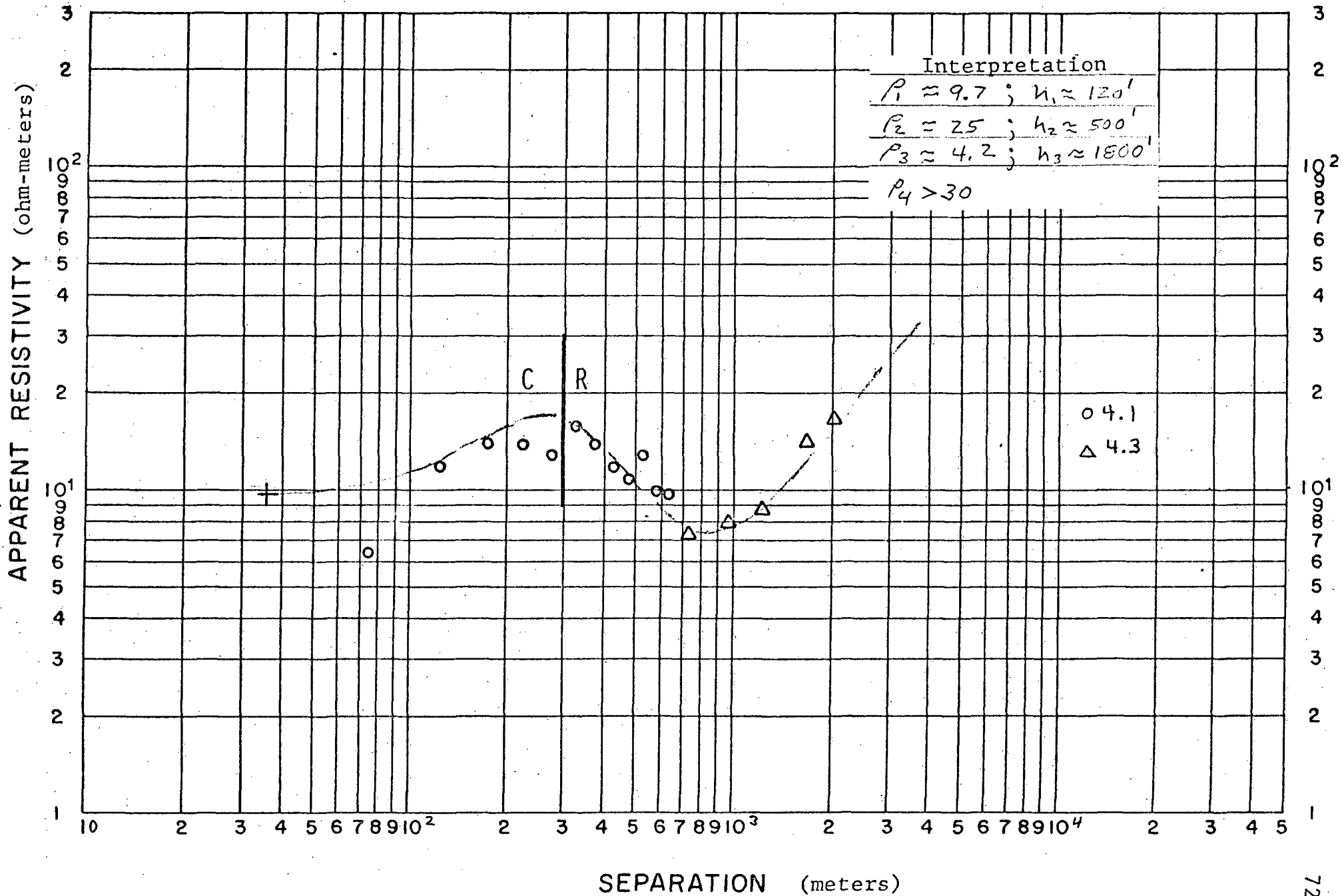


Figure V-8. Soundings 4.1 and 4.3;
 Combined Modified Schlumberger and Equatorial Soundings

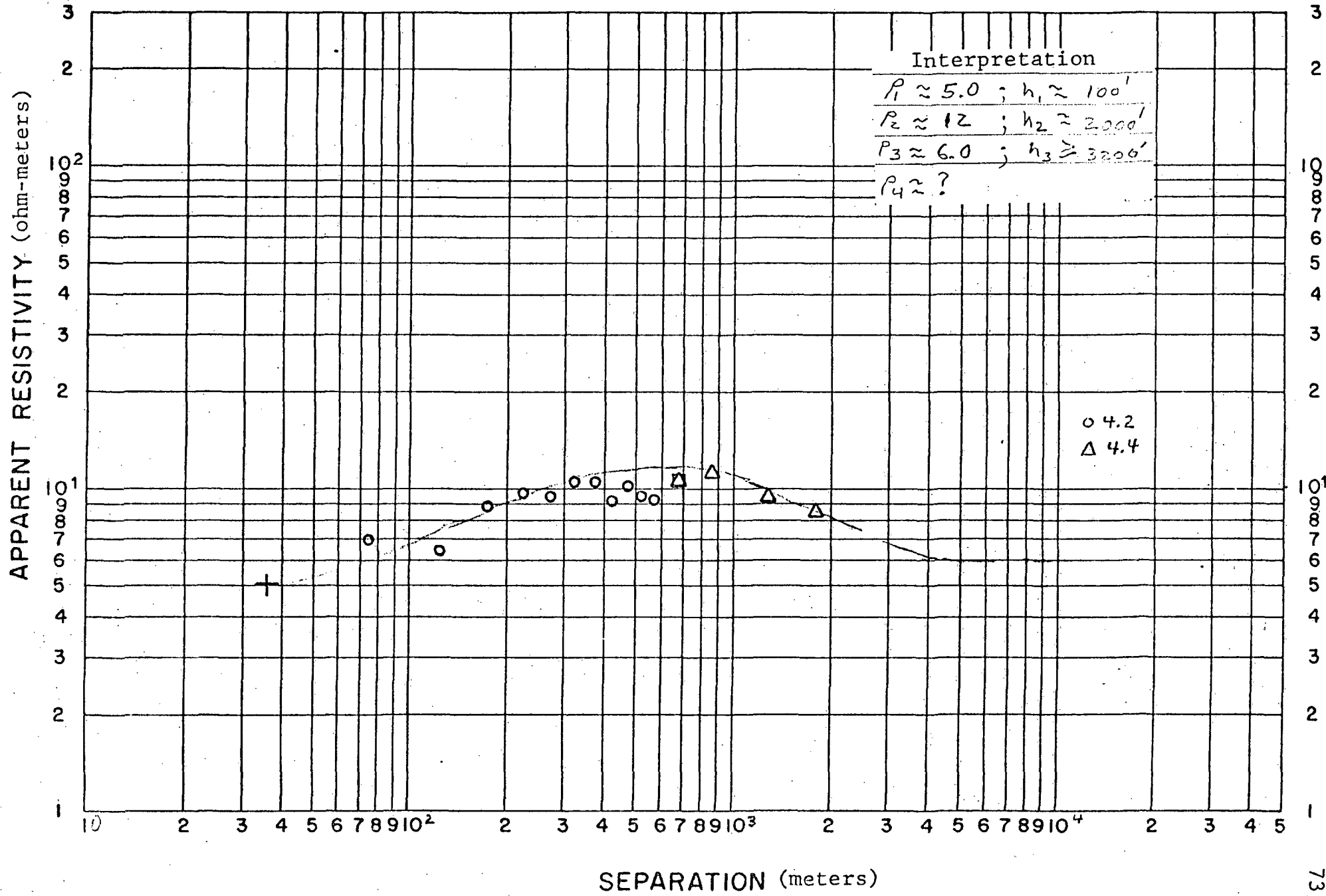


Figure V-9. Soundings 4.2 and 4.4,
Combined Modified Schlumberger and Equatorial Soundings

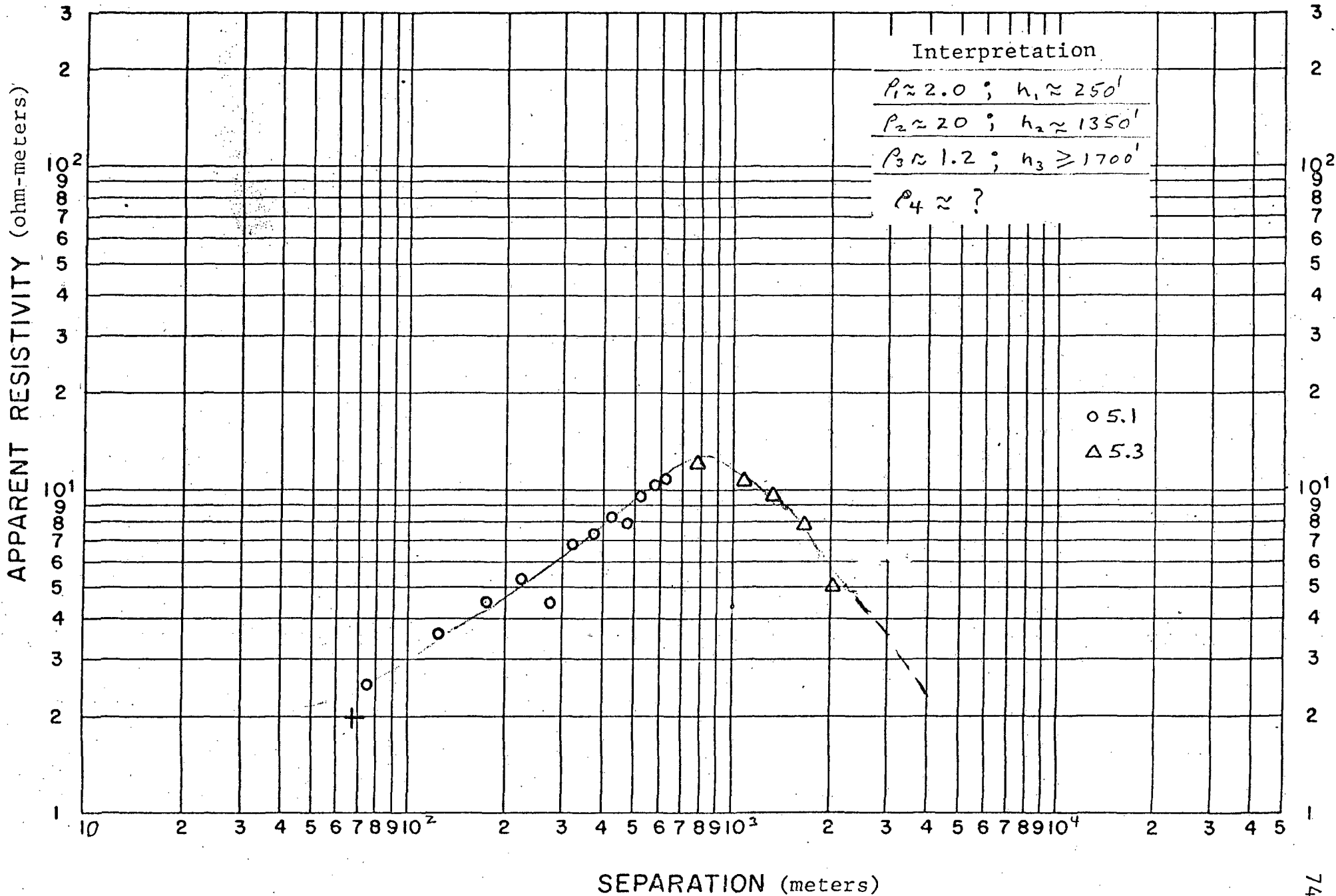


Figure V-10. Soundings 5.1 and 5.3,
Combined Modified Schlumberger and Equatorial Soundings

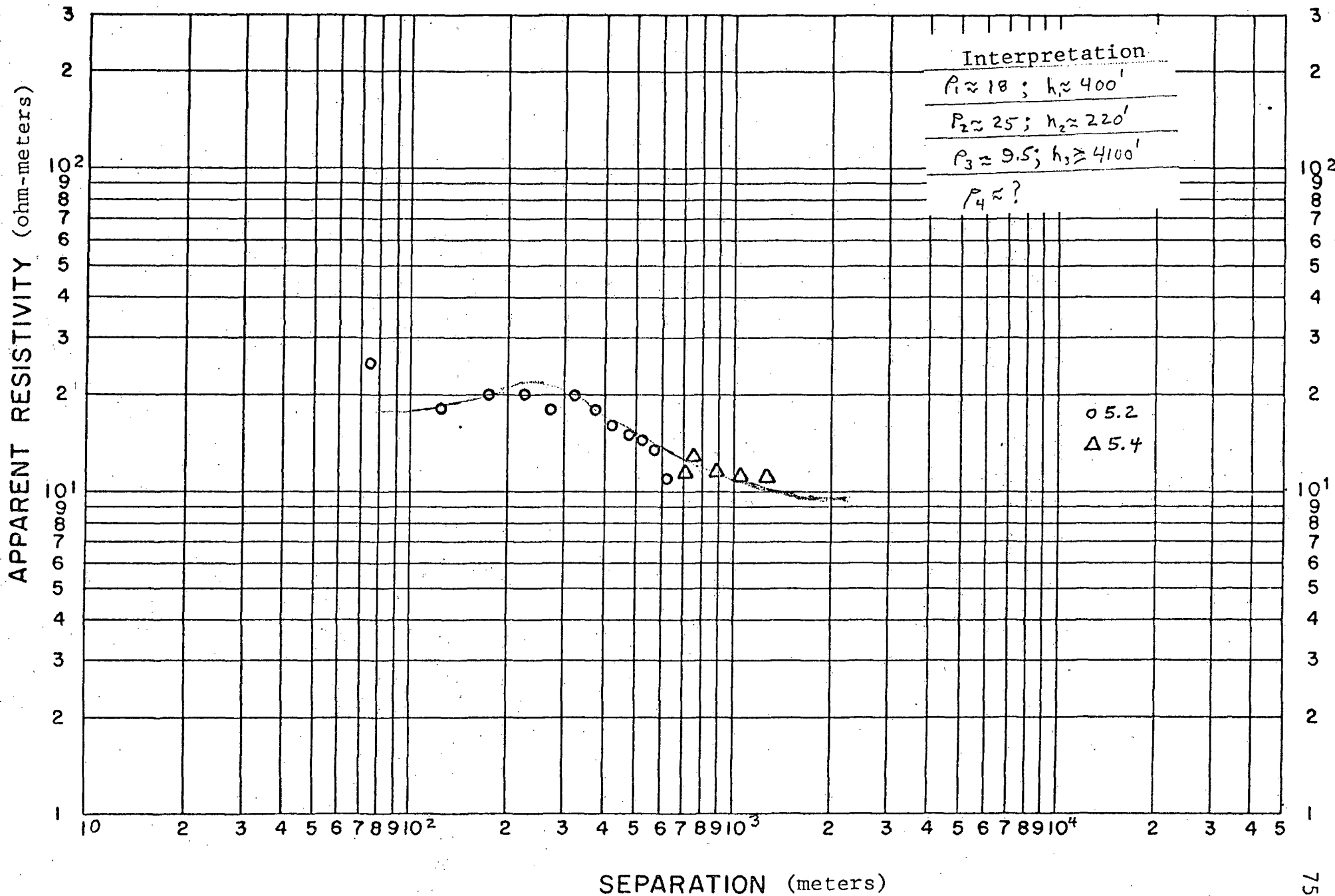


Figure V-11. Soundings 5.2 and 5.4,
Combined Modified Schlumberger and Equatorial Soundings

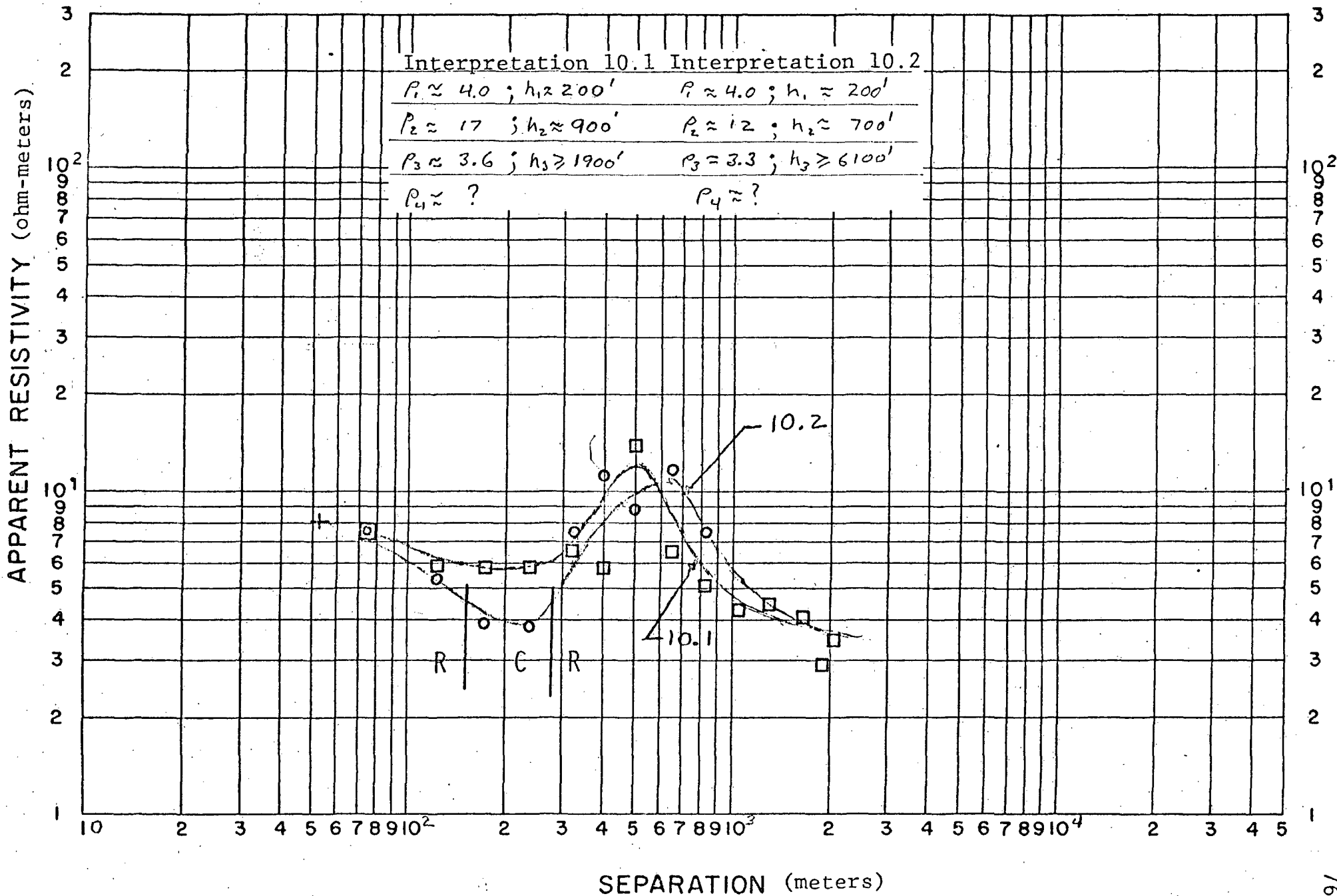


Figure V-12. Soundings 10.1 and 10.2,
Combined Modified Schlumberger and Monopole Soundings

APPENDIX VI

Parallel (dc) Electrical Resistivity Profiles

Contents:

Description

Tables of Apparent Resistivity

Description of the Method

The parallel electric field dipole receiver--bipole source method is a relatively unknown galvanic resistivity technique. We do not know of it being described in the literature, either as a general survey method nor as a geothermal prospect survey method. The layout of the bipole source and the multiple receivers is shown in the figure below.

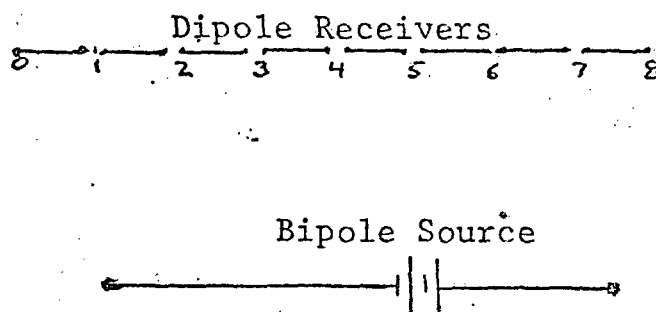


Figure 1. Layout of the parallel dipole receiver--bipole source.

The objectives of these parallel profile measurements are multi-fold. They are:

- a. To discover the lateral limits of geothermal zones at depth.
- b. To discover fault-like expressions which may contain geothermal fluids.

and

- c. To discover anomalously conductive (low resistivity value) areas that are continuous over economic geometry considerations.

To achieve the above objectives, the separation between the bipole source and the line of the dipole receivers is optimized to provide penetration depth to or into features of interest. The parallel dipole measurements approximate equatorial measurements of the equatorial dipole array. Therefore, for an H-type geoelectric section, penetration for source-receiver separations less than the depth to basement will approximate the source-

receiver separation. For source-receiver separations greater than the depth to basement, the parallel dipole method may be used to profile the variations in conductance along the profile. The interpretation of the results of the parallel electric field dipole receiver--bipole source measurements is guided by the interpretations described in Appendix V.

A consideration of the angle between a line connecting the receiver to the source and the direction of the source must be considered. The result, similar to those of a parallel dipole receiver array, will occur at an angle approximately equal to one radian. The electric field approximates zero and the geometric factor, K , approximates infinity for measurements over a uniform or one-dimensional (vertically changing) earth. For the dipole receiver--bipole source array, such a condition will occur when the receiver orientation is perpendicular to the general current flow in the earth.

TABLE VI-1

Parrallel Electric (dc) Field
Apparent Resistivity Values

PROFILE 8.2		PROFILE 8.3	
STATION NUMBER	APPARENT RESISTIVITY (ohm-meter)	STATION NUMBER	APPARENT RESISTIVITY (ohm-meter)
1	13	1	6.4
2	12	2	6.0
3	16	3	5.8
4	15	4	6.4
5	11	5	7.9
6	16	6	9.0
7	17	7	7.9
8	17	8	8.7
		9	8.7

TABLE VI-2
 Parrallel Electric (dc) Field
 Apparent Resistivity Values

PROFILE 9.1		PROFILE 9.2		PROFILE 9.3	
STATION NUMBER	APPARENT RESISTIVITY (ohm-meter)	STATION NUMBER	APPARENT RESISTIVITY (ohm-meter)	STATION NUMBER	APPARENT RESISTIVITY (ohm-meter)
1	4.9	1	69	1	1.7
2	2.8	3	44	2	2.0
3	3.9	4	24	3	4.1
4	3.2	5	14	4	13
5	3.2	6	15	5	7.3
6	3.4	7	6.7	6	7.9
7	4.0	8	6.6	7	7.7
8	3.7	9	5.2	8	7.2
9	3.7	10	7.6	9	7.0
10	3.9	11	3.8	10	8.6
11	4.0	12	5.6	11	8.5
12	8.9	13	4.8	12	9.4
13	21	14	6.8	13	11
14	34	15	6.6	14	9.6
15	20	16	7.3	15	10
16	6.6	17	7.8	16	11
		18	5.9		
		19	4.6		
		NO VALUE STATION 2			

TABLE VI-3
 Parrellel Electric (dc) Field
 Apparent Resistivity Values

PROFILE 9.4		PROFILE 9.5	
STATION NUMBER	APPARENT RESISTIVITY (ohm-meter)	STATION NUMBER	APPARENT RESISTIVITY (ohm-meter)
1	10	1	7.1
2	8.2	2	5.8
3	6.2	3	8.1
4	7.1	4	11
5	8.0	5	N.V.
6	11	6	N.V.
		7	21
		8	20
		9	9.5
		10	N.V.
		11	6.1
		12	4.1
		13	4.1
		14	4.0
		15	3.8
		16	3.6
		17	3.4
		18	3.6
		N.V. - NO VALUE	

APPENDIX VII

Time-Domain Electromagnetic Soundings

E_p (parallel) & H_z (vertical) Components

Contents:

Discussion and Description

Data Acquisition

Interpretation Curves for the Colado Hot Springs Prospect

TABLE VI-4

Parallel Electric (dc) Field
Apparent Resistivity Values

PROFILE 10.1		PROFILE 10.2		PROFILE 10.3	
STATION NUMBER	APPARENT RESISTIVITY (ohm-meter)	STATION NUMBER	APPARENT RESISTIVITY (ohm-meter)	STATION NUMBER	APPARENT RESISTIVITY (ohm-meter)
1	3.7	1	0.6	1	11
2	6.0	2	2.1	2	15
3	13	3	1.1	3	27
4	22	4	7.0	4	7.1
5	29	5	3.8	5	5.5
6	1.0	6	3.9	6	6.1
7	2.4	7	3.5	7	14
8	4.8	8	2.1	8	3.4
9	5.3	9	2.7	9	3.9
10	4.4	10	5.7	10	4.9
11	0.8	11	3.4	11	4.1
12	4.3	12	3.1	12	4.3
13	3.8	13	3.1	13	4.7
14	3.0	14	3.8	14	4.7
15	3.7	15	7.1	15	4.1
16	3.8	16	HIGHLY SKEWED	16	4.1
17	2.7	17	" "		
18	0.6	18	16		

TABLE VI-5
 Parrallel Electric (dc) Field
 Apparent Resistivity Values

PROFILE 11.1		PROFILE 11.2		PROFILE 11.3	
STATION NUMBER	APPARENT RESISTIVITY (ohm-meter)	STATION NUMBER	APPARENT RESISTIVITY (ohm-meter)	STATION NUMBER	APPARENT RESISTIVITY (ohm-meter)
1	9.5	1	5.2	1	1.7
2	1.6	2	2.6	2	1.9
3	0.7	3	1.2	3	1.3
4	1.0	4	3.0	4	3.2
5	1.3	5	4.2	5	3.6
6	1.1	6	7.5	6	4.4
7	1.0			7	4.7
8	1.6			8	3.8
9	1.5			9	3.5
10	2.4			10	9.6
11	2.6				
12	2.0				

Discussion and Description
Controlled Source EM Methods

For some years, electromagnetic controlled source, vertical magnetic field receiver soundings have been used in geothermal exploration in the United States and other parts of the world. The U.S.S.R. and Eastern Block Countries' literature describes their use in various geophysical surveys, particularly for surveying geologic sections having thick resistive sections in them.

Much less widely known and discussed in the free-world are the horizontal electric field EM soundings from grounded dipole or grounded bipole sources. There are numerous articles written in the Soviet and Eastern Block Countries' literature, but, the only interest to date in the United States seems to come out of studies at the Colorado School of Mines (CSM) and the USGS. There has been reported success in the use of the "Electroflex Technique" (a rather primitive approach to EM soundings) in surveying carbonate sections (reef problems, etc.) where the parameter of control is resistivity.

Published works by G. V. Keller (Chairman of the Geophysics Department), Pritchard and other graduate students at CSM show that the grounded source--electric field receiver soundings will provide interpretative data for resolution of:

1. Vertical anisotropy of layers within the geologic section, and
2. The thickness and resistivity of resistive screening layers

(screen dc electrical resistivity soundings from penetrating to depth and are virtually undetectable by magnetic receiver soundings, MT soundings, and all magnetic source soundings).

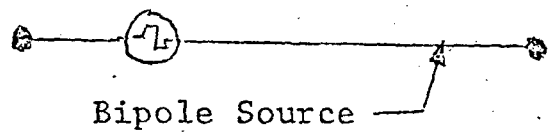
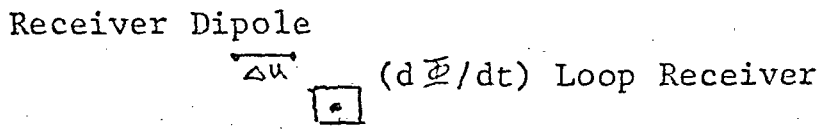
Knowledge of screening layers and vertical anisotropy are very important in making correct depth interpretation in survey investigations of geothermal areas. Further, we believe that resolution of vertical anisotropy will become an important parameter in geothermal investigations as drilling tests qualify the results in areas of large anisotropy versus no anisotropy.

Electrodyne Data Acquisition

The source-receiver layout is shown in the figure below. Electrodyne's receiver system is comprised of a parallel electric field dipole and a multiturn vertical $d\phi/dt$ receiver. The signal is preconditioned by a filter-amplifier system and recorded on analogue tape. The tape recorder used a four channel Hp recorder.

The total transient response and an "early time" amplitude clipped response is recorded for each component. The source signal input into the ground is square-waves of 12.8 seconds period and ^{10³}2.0 seconds period to give an equivalent frequency domain band of 0.08 Hz to 32.0 Hz.

0.5



Typical Electrodyne EM Sounding Layout

Electrodyne Data Interpretation

Electrodyne performs a preliminary partial curve matching interpretation of the sounding curves. The assumption made is that all data corresponds to two frequency domain responses, plane-wave and static field responses. The incorporation of the quasistatic response is incorporated when the inversion modeling is performed in the computer inversion interpretation process. The inversion interpretation is not performed if the preliminary partial curve matching indicates that the sounding is two or three dimensionally controlled.

Interpretation Considerations

Electrodyne is in the preliminary stages of developing the full interpretation capability of the combined E_p and H_z EM soundings. At this time, a pseudo-anisotropy is determined by taking the ratio of the E_p resistivity value of a layer to the H_z resistivity of a layer. The E_p soundings are used to interpret the layer thickness. The H_z soundings are used to interpret the true resistivity of the conductive layers of interest.

$$\frac{\rho_{E_p}}{\rho_{H_z}} = \lambda$$

$$H_z \rightarrow \rho$$

Electrodyne Data Reduction

Electrodyne uses a wave analyser to transform the total transient response signal from a square-wave input to the frequency domain. This done in a manner similar to the AMT-MT data reduction, i. e., a number of visually inspected time windows are transformed and these are stacked to give the best average amplitude spectra. The system response is removed and the data are ready for frequency domain interpretation. Electrodyne does not transform back to the time domain for interpretation.

To date signal to noise relationships have been high enough that we have not had to bring up additional resolution from the stacking of the clipped amplitude transient recording.

square wave signal
 fourier transform (2)
 to freq. domain
 magnitude of signal in
 freq domain → sounding
 P/F

KEY TO SOUNDING ANNOTATION

The apparent resistivity on the sounding curves is derived by the plane-wave formula

FAULT CONTROLLED --Two or three dimensional control on the sounding

 E_p Soundings

ρ_i ---ith layer resistivity value

h_i ---ith layer thickness

S_R --- Residual conductance --- determined by taking the difference between the (dc) total conductance and the E_p total conductance

 H_z Soundings

ρ_i ---ith layer resistivity value

h_i ---ith layer thickness

λ_i --- $\rho_{i_{E_p}} / \rho_{i_{H_z}}$

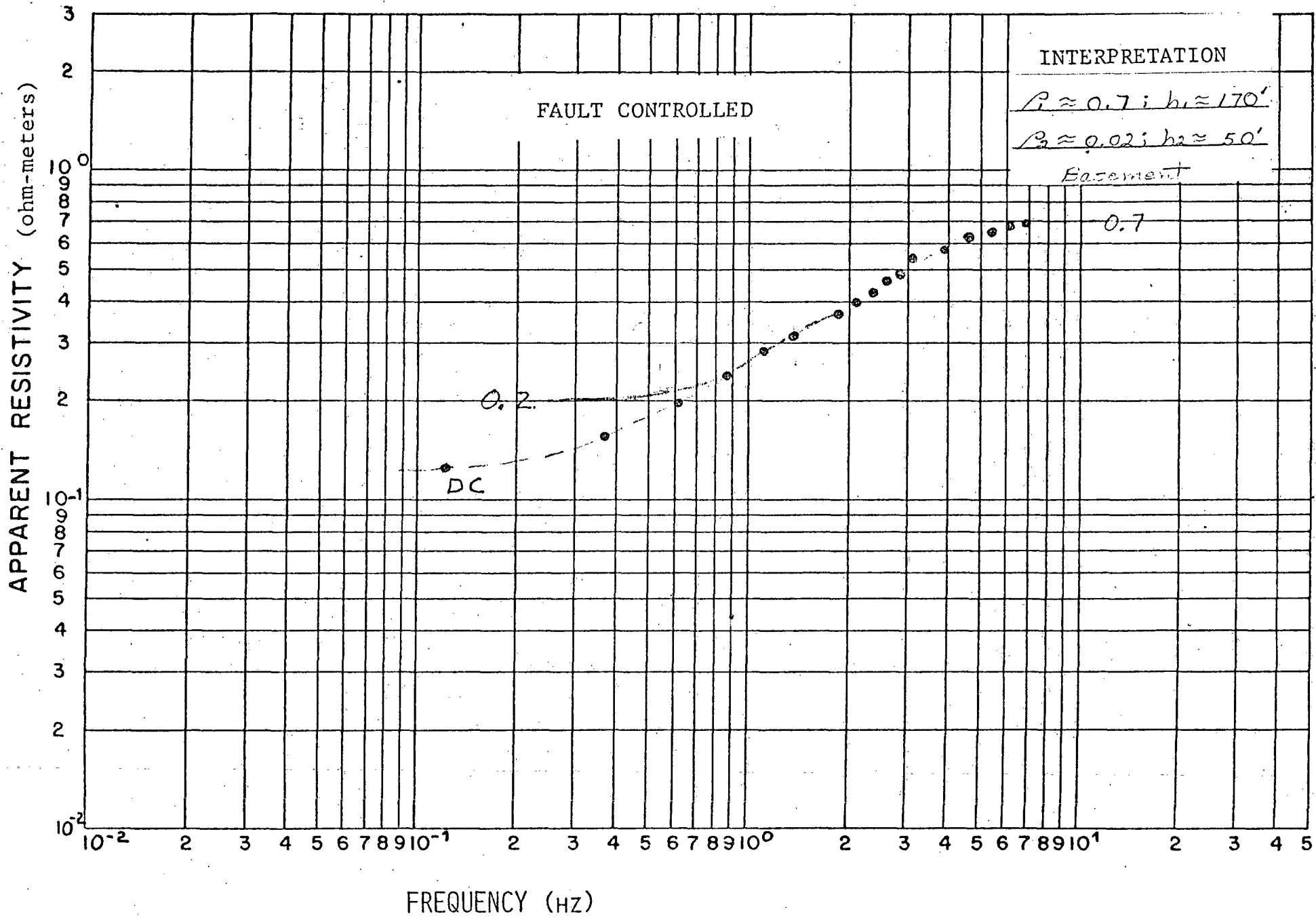


Figure VII-1. TDEM Ep Sounding 3.02.

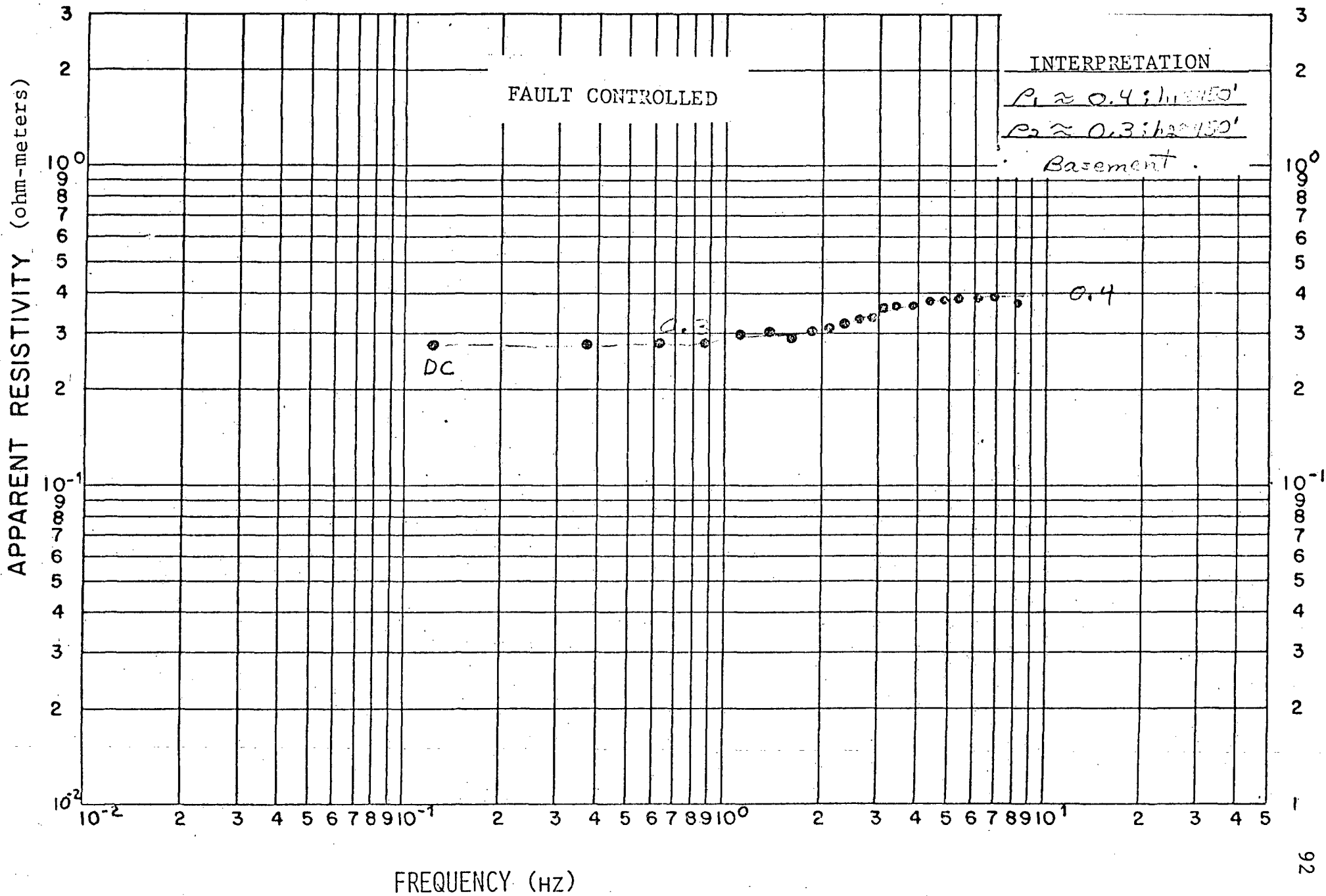


Figure VII-2. TDEM Ep Sounding 6.01.

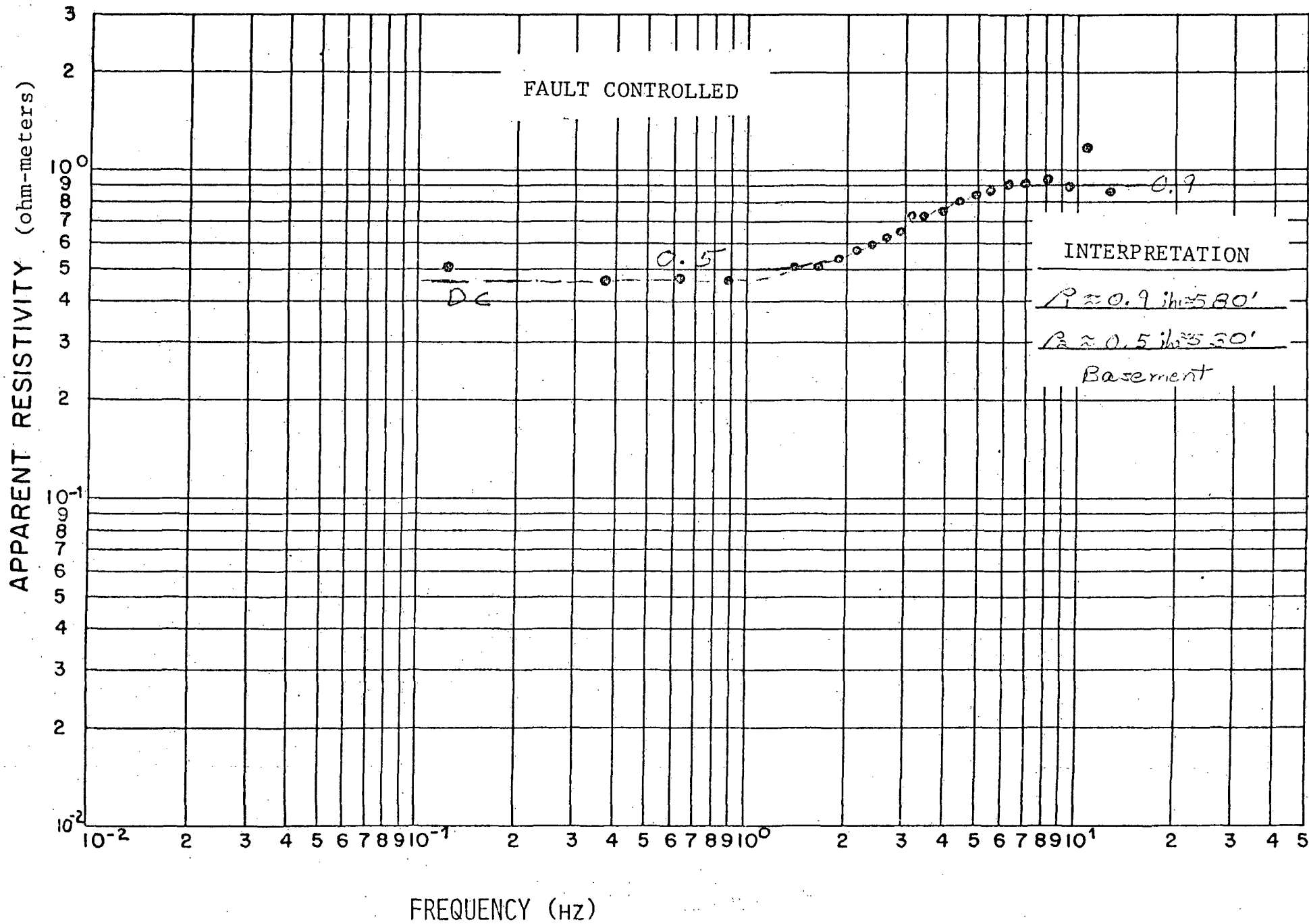


Figure VII-3. TDEM Ep Sounding 6.02.

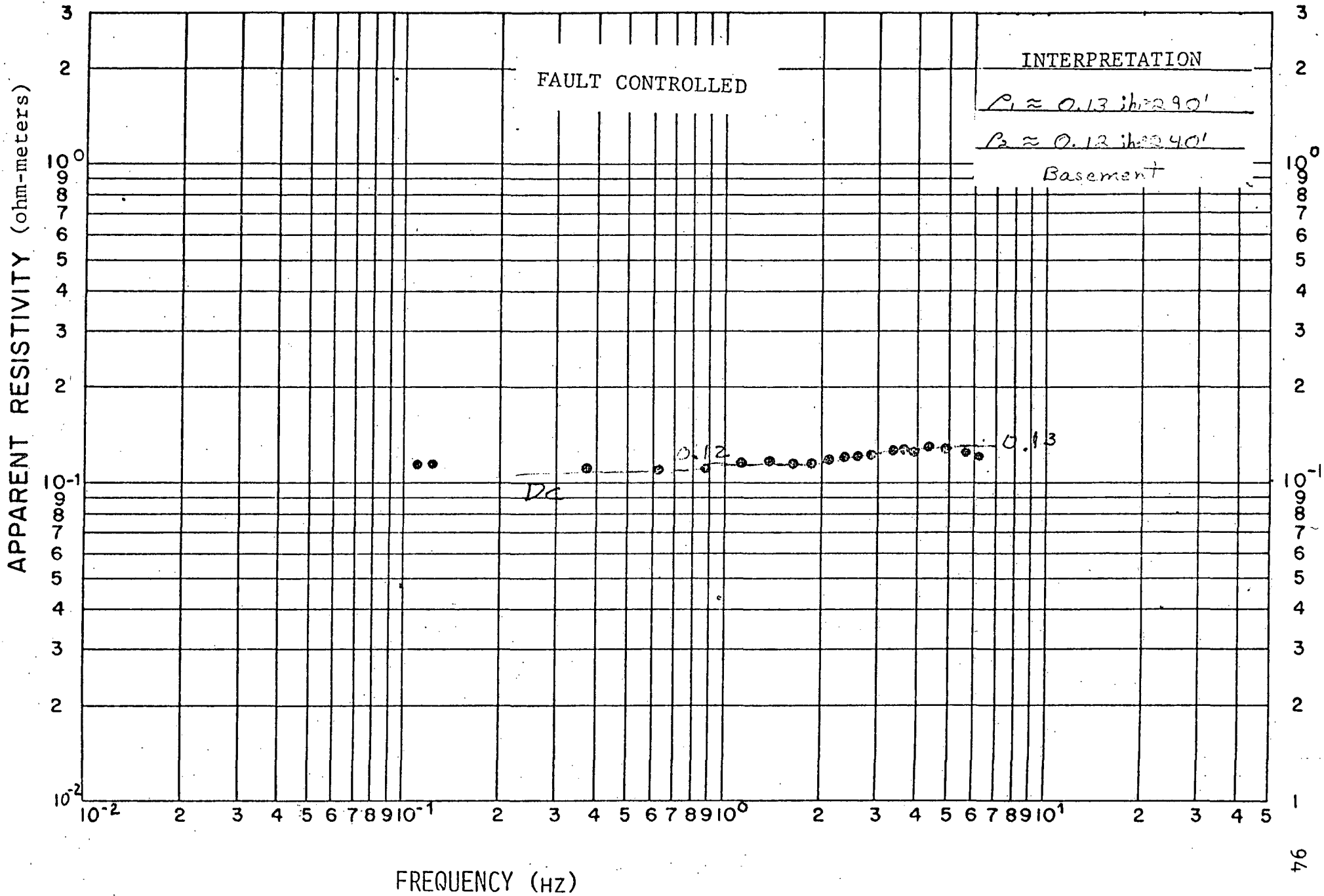


Figure VII-4. TDEM Ep Sounding 6.03.

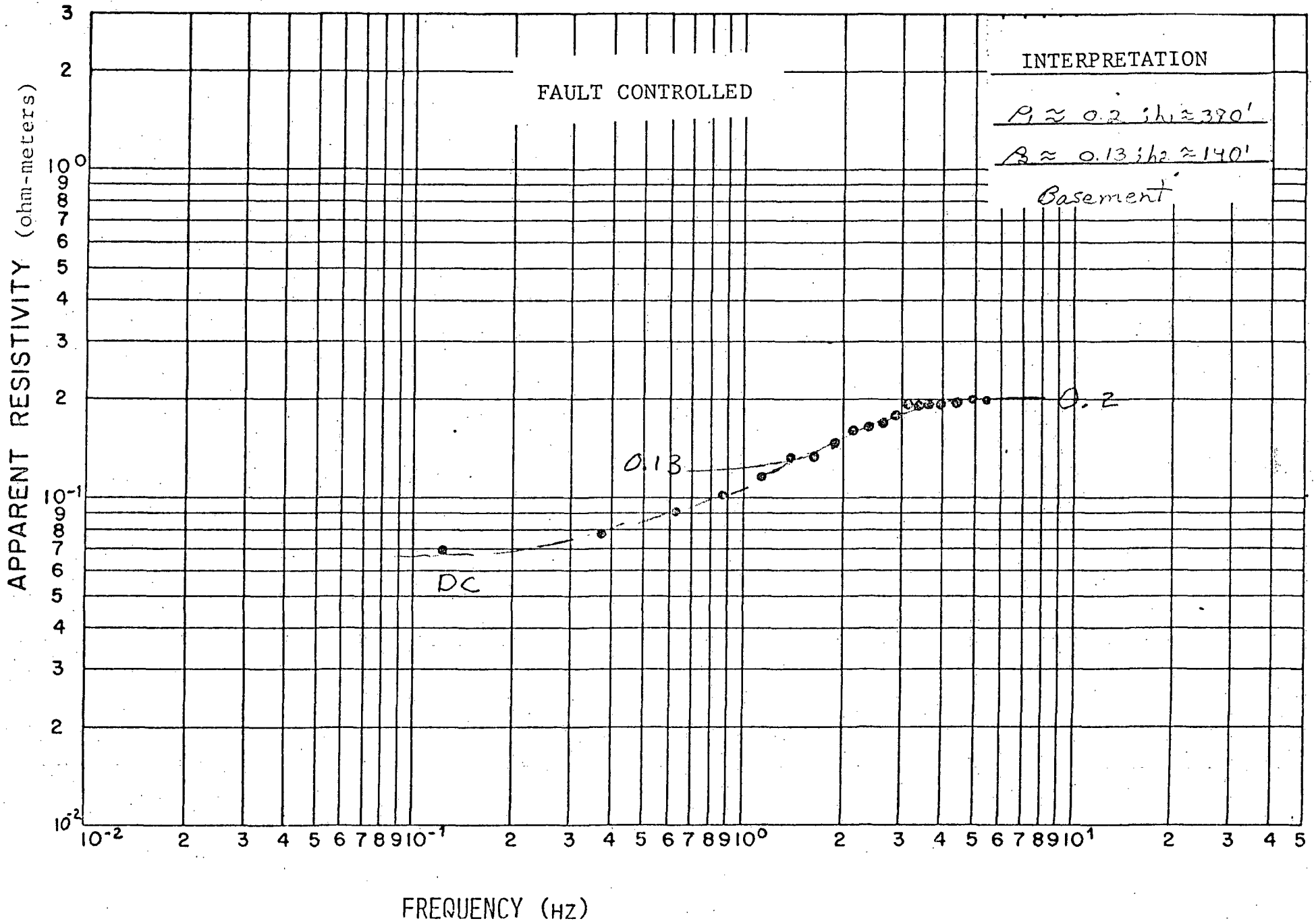


Figure VII-5. TDEM Ep Sounding 6.04.

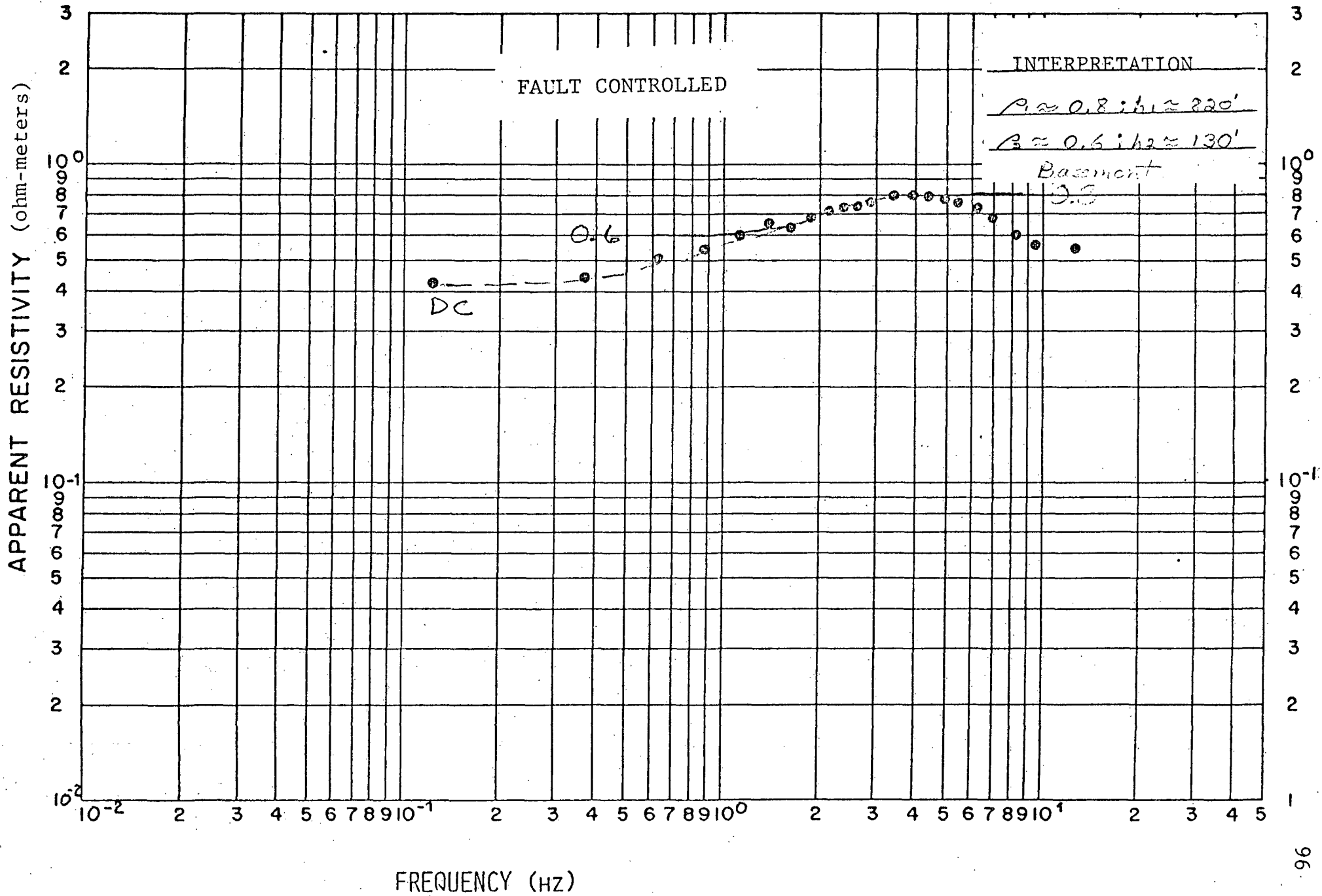


Figure VII-6. TDEM Ep Sounding 6.05.

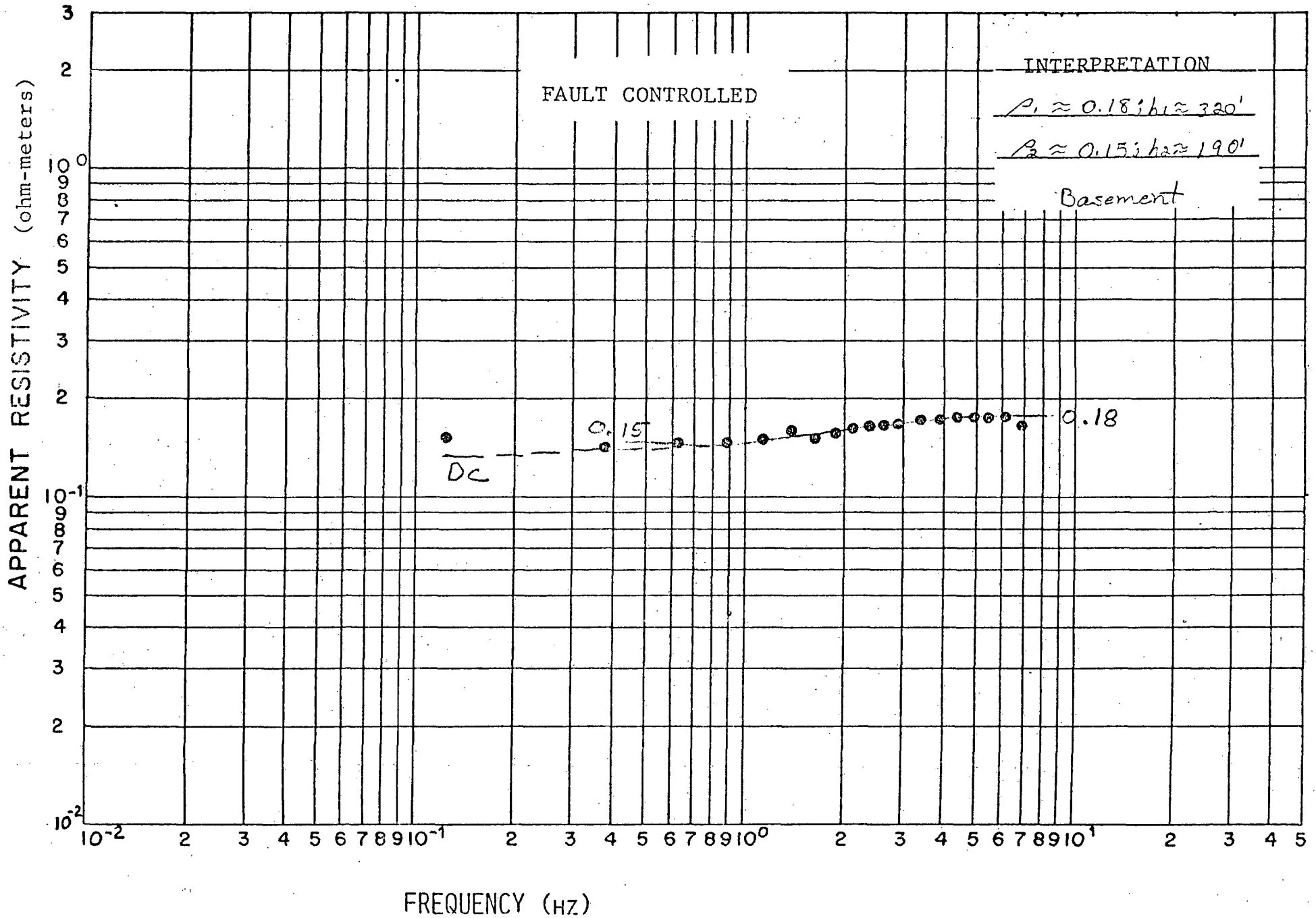


Figure VII-7. TDEM Ep Sounding 7.01.

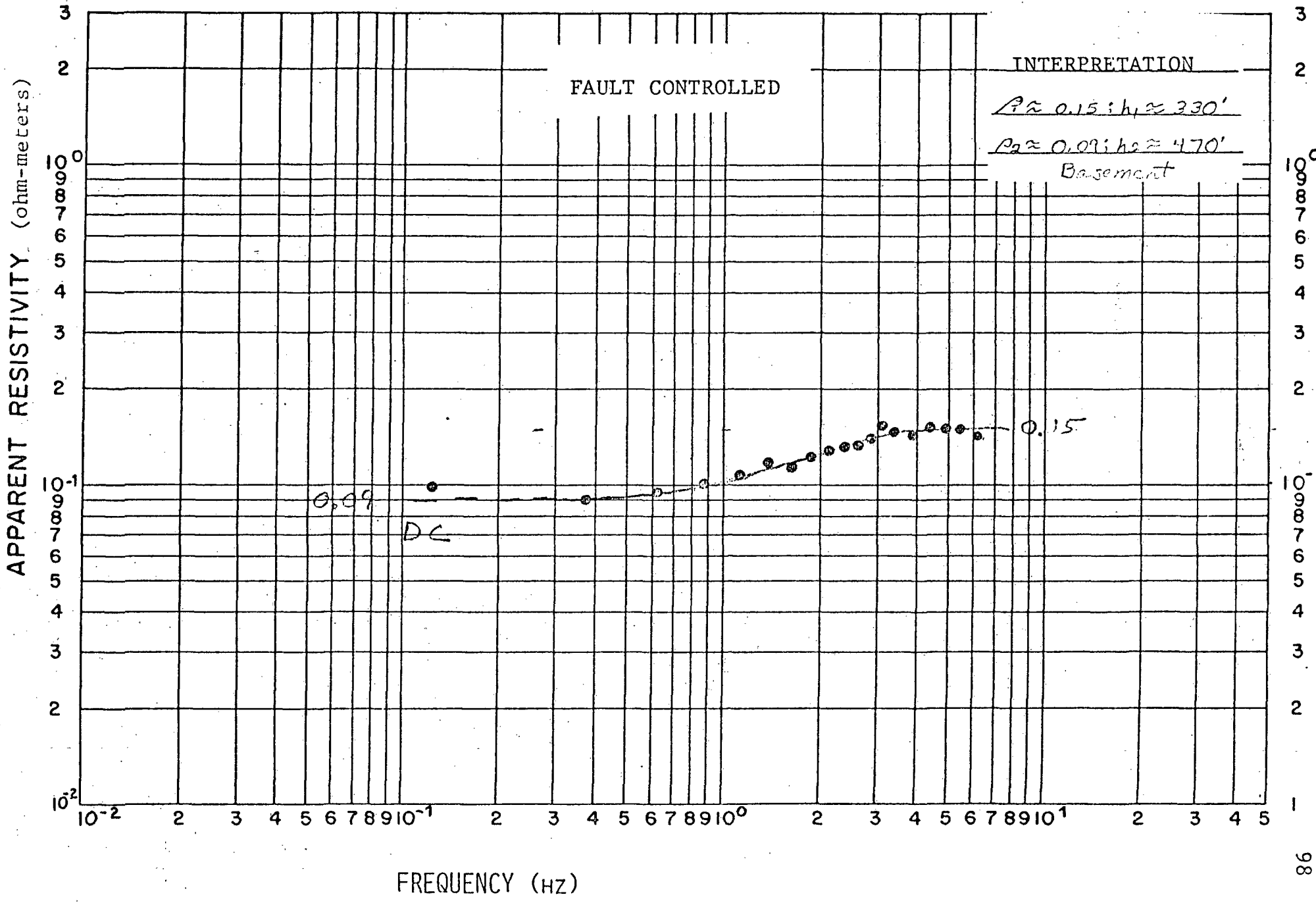


Figure VII-8. TDEM Ep Sounding 7.02.

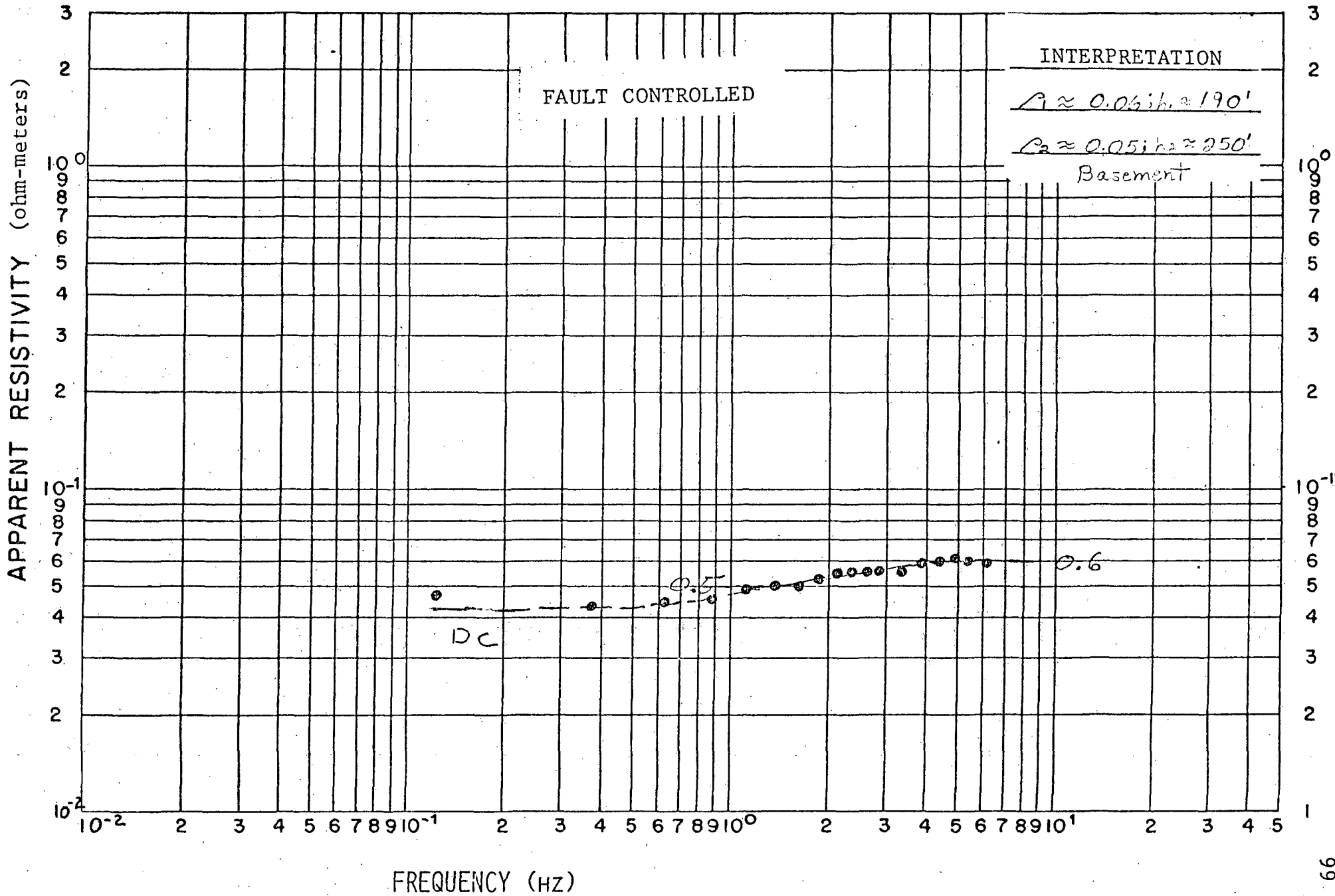


Figure VII-9. TDEM Ep Sounding 7.03

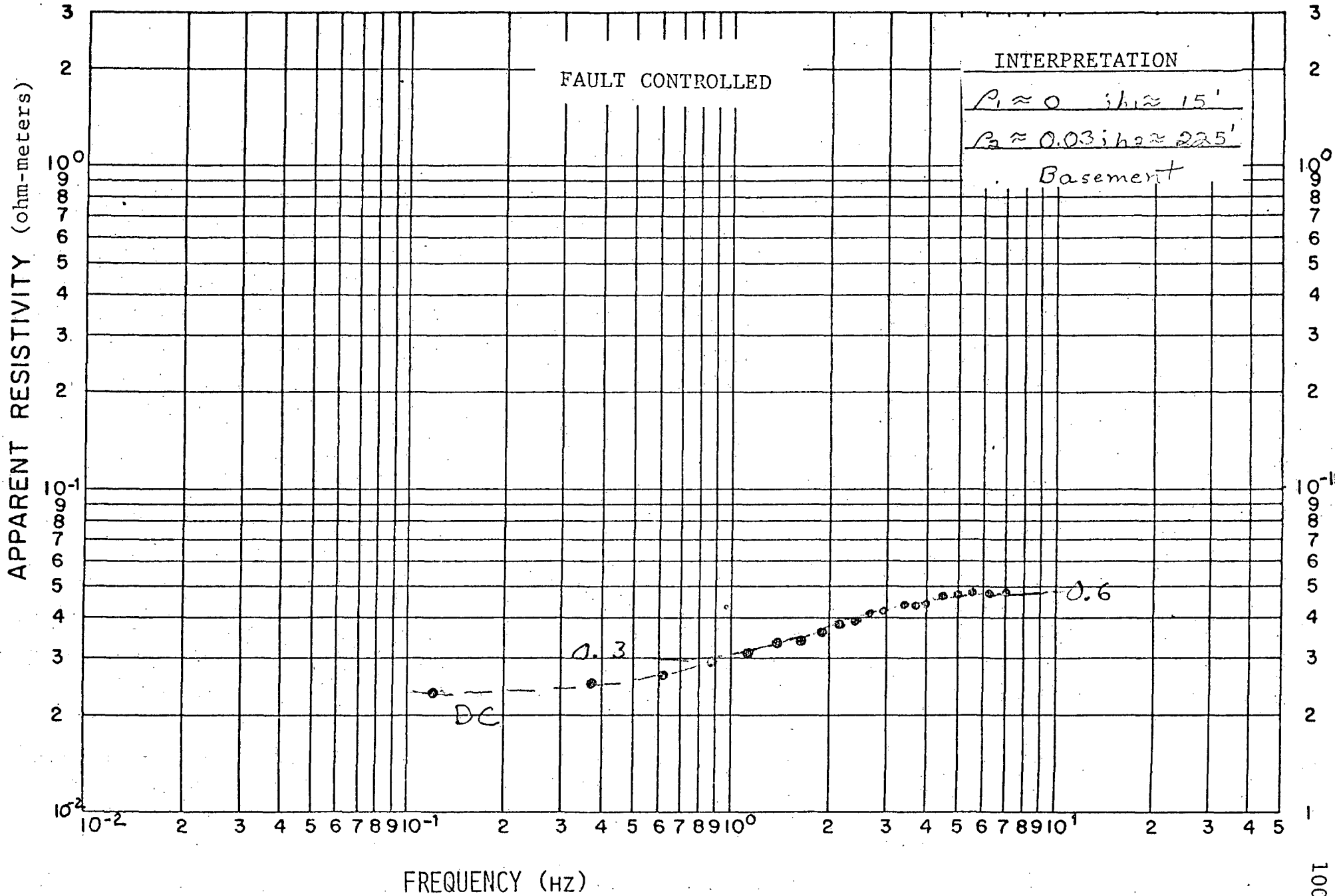


Figure VII-10. TDEM Ep Sounding 7.04

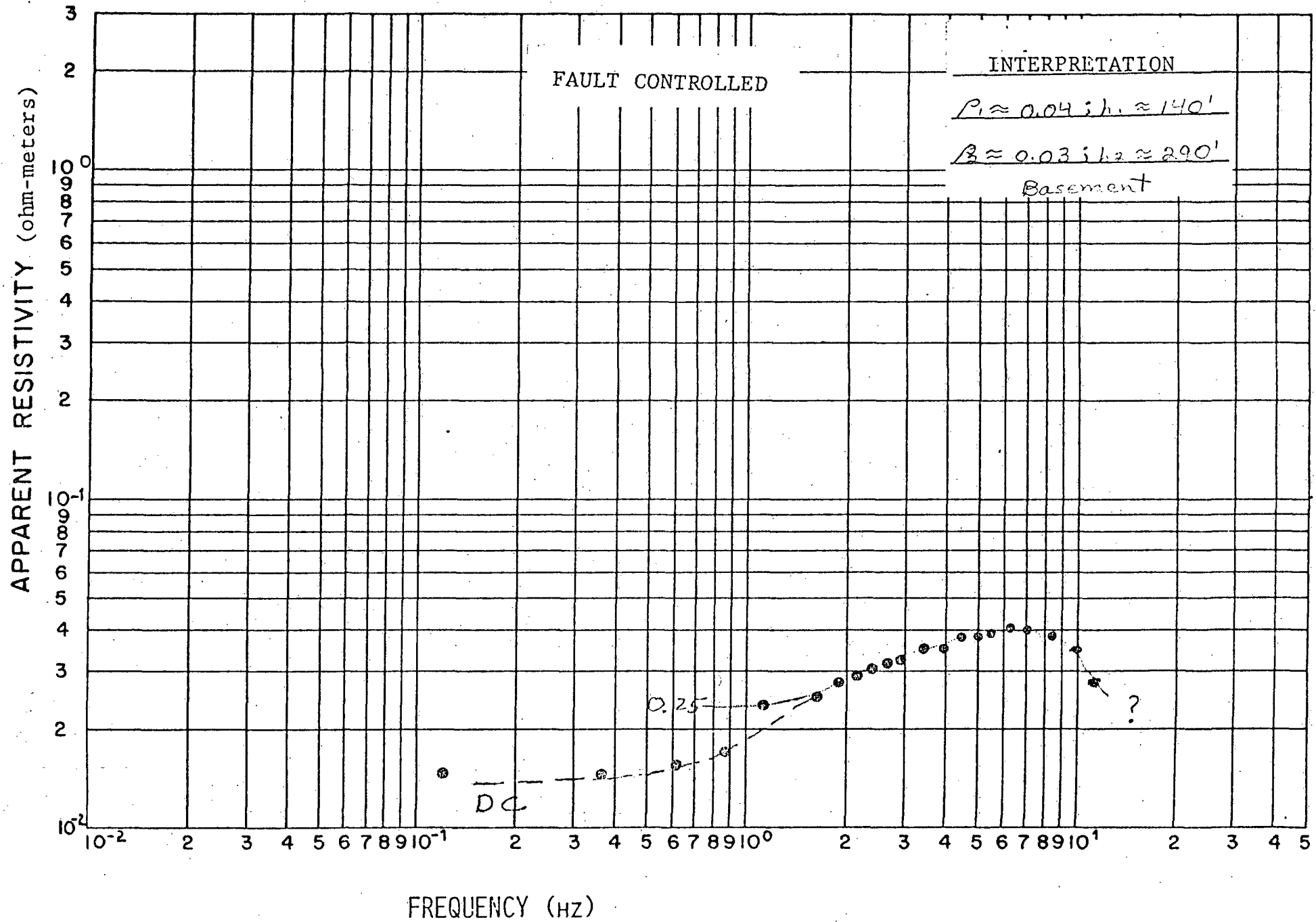


Figure VII-11. TDEM Ep Sounding 7.05

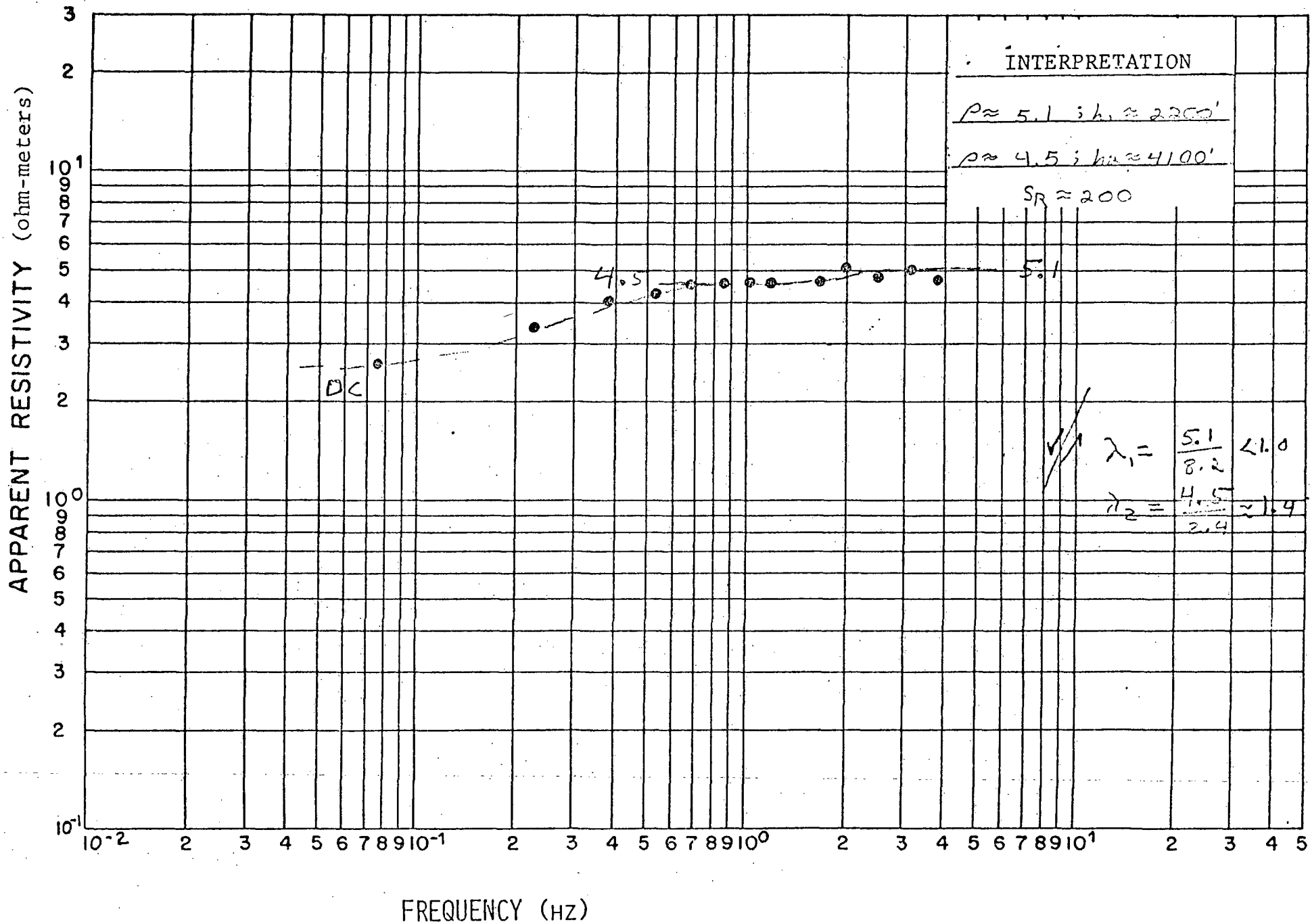


Figure VII-12. TDEM Ep Sounding 8.02

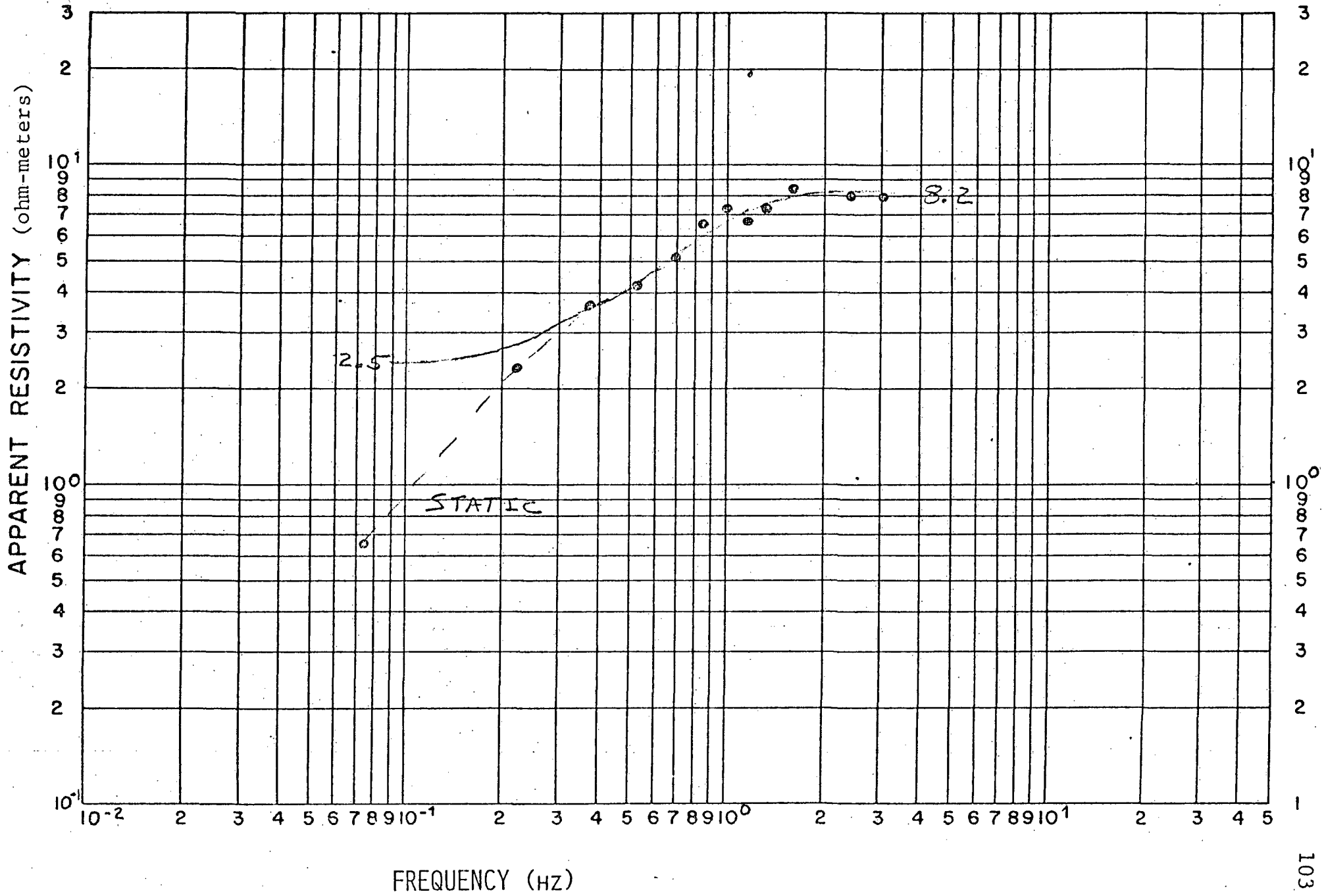


Figure VII-13. TDEM Hz Sounding 8.02

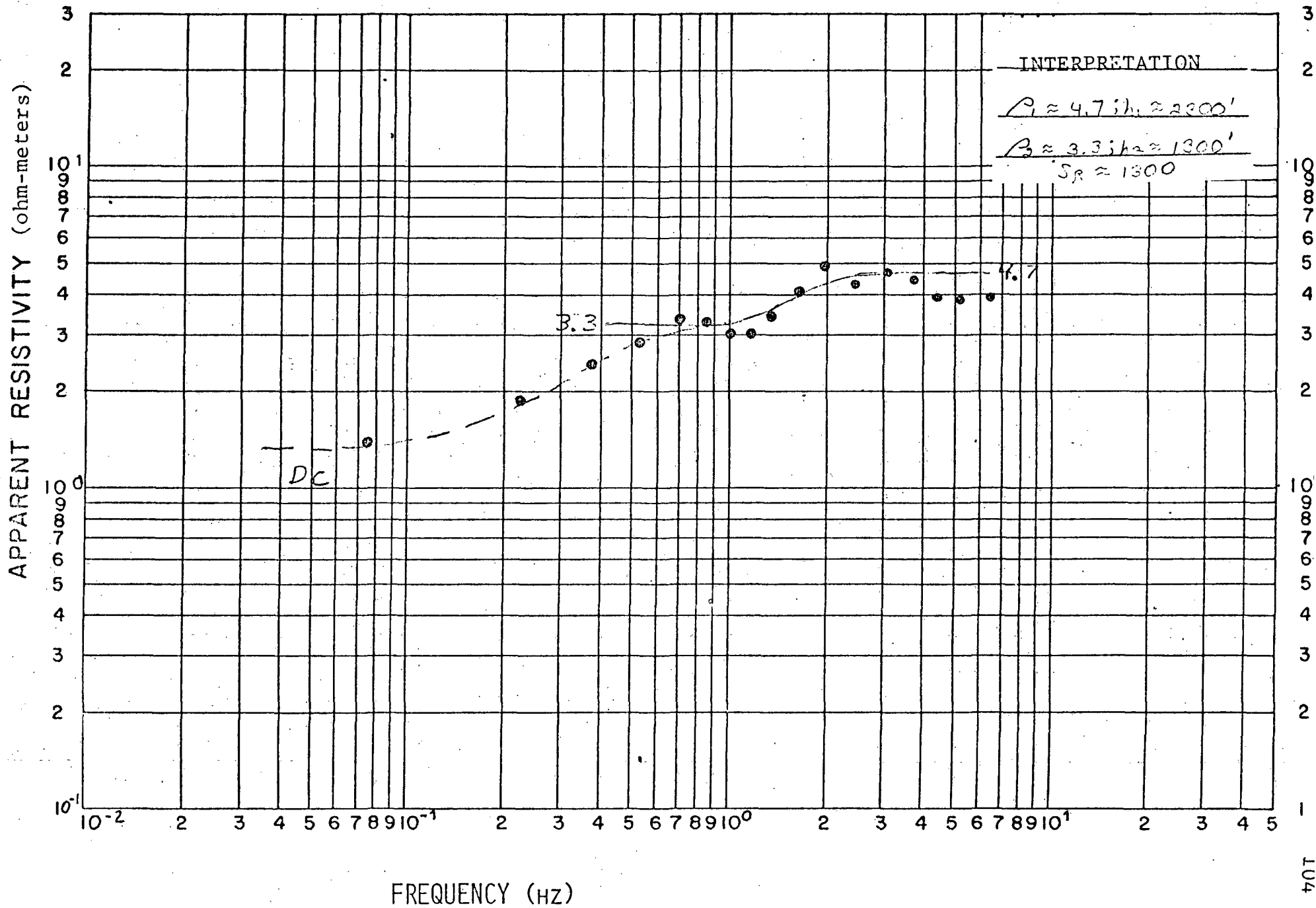


Figure VII-14. TDEM Ep Sounding 8.03

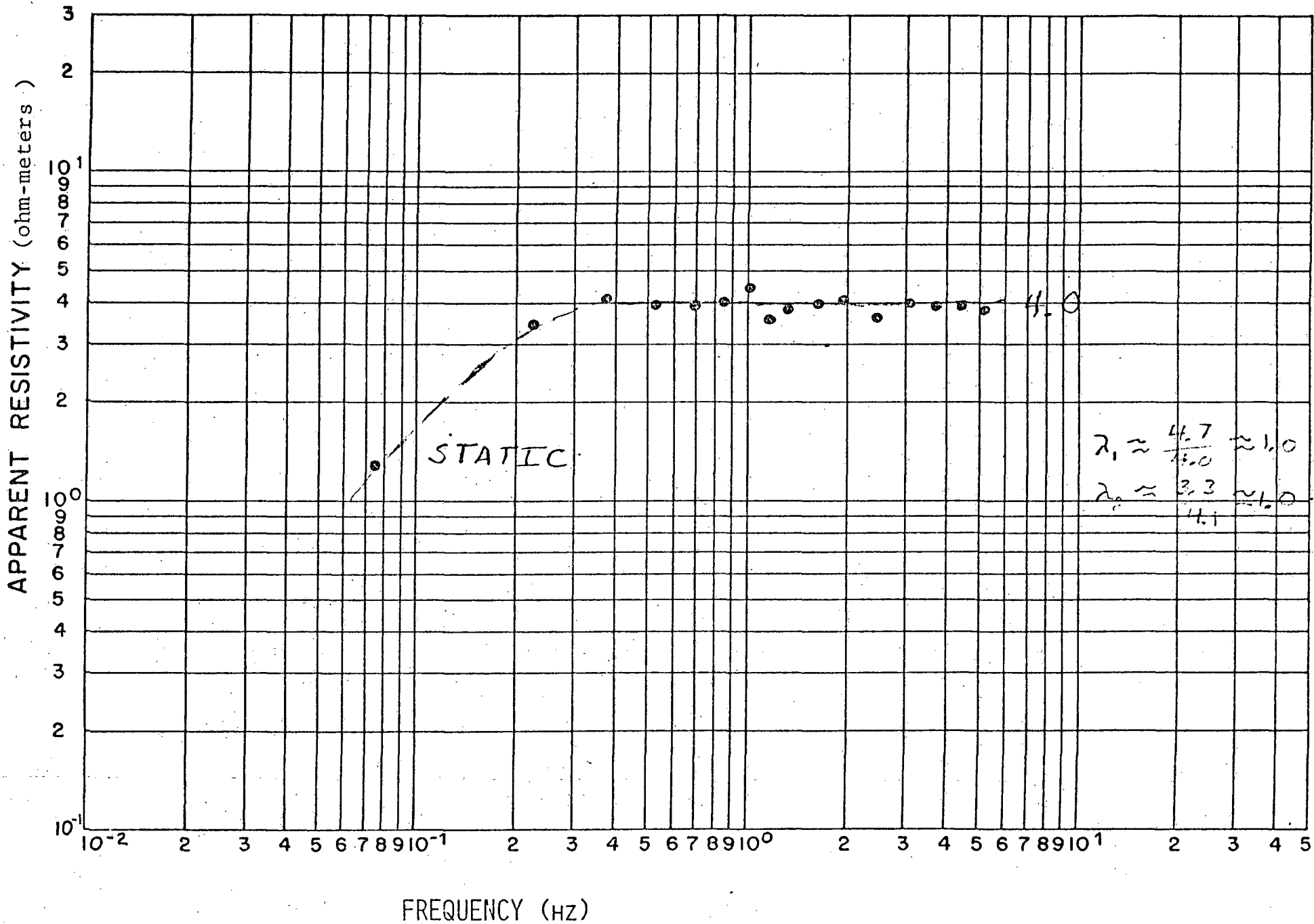


Figure VII-15.

TDEM Hz Sounding 8.03

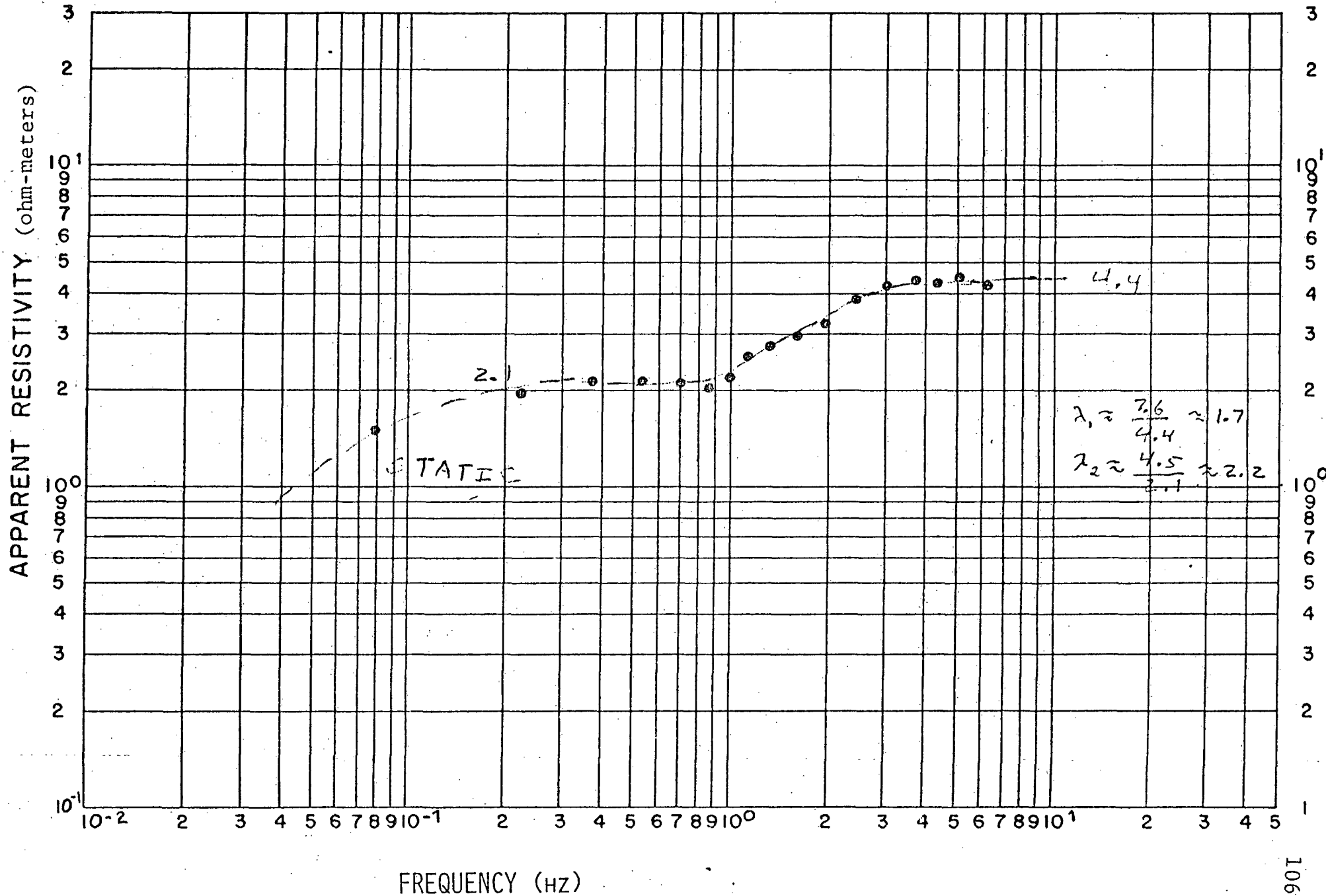


Figure VII-16. TDEM Hz Sounding 9.01

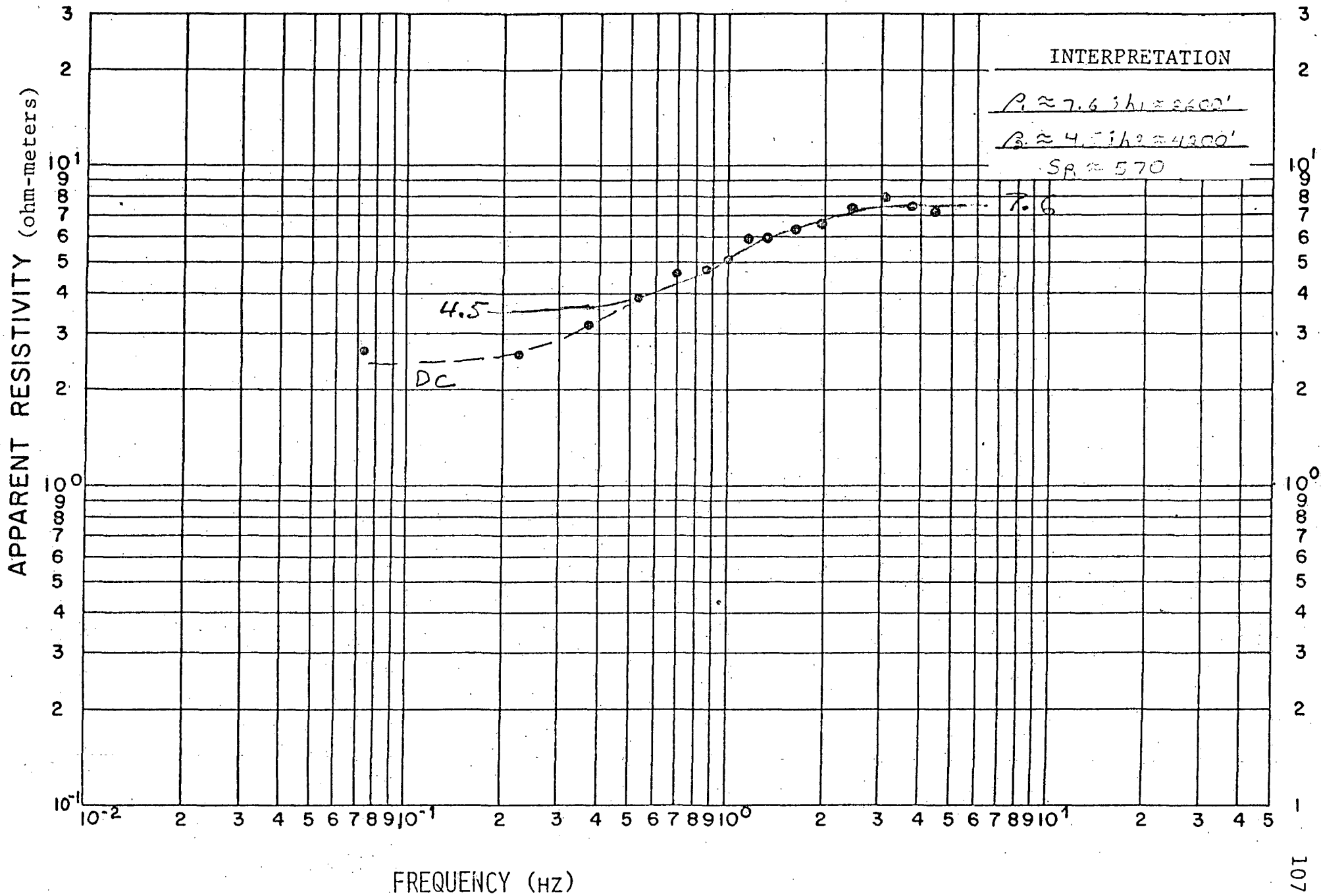


Figure VII-17. TDEM Ep Sounding 9.01

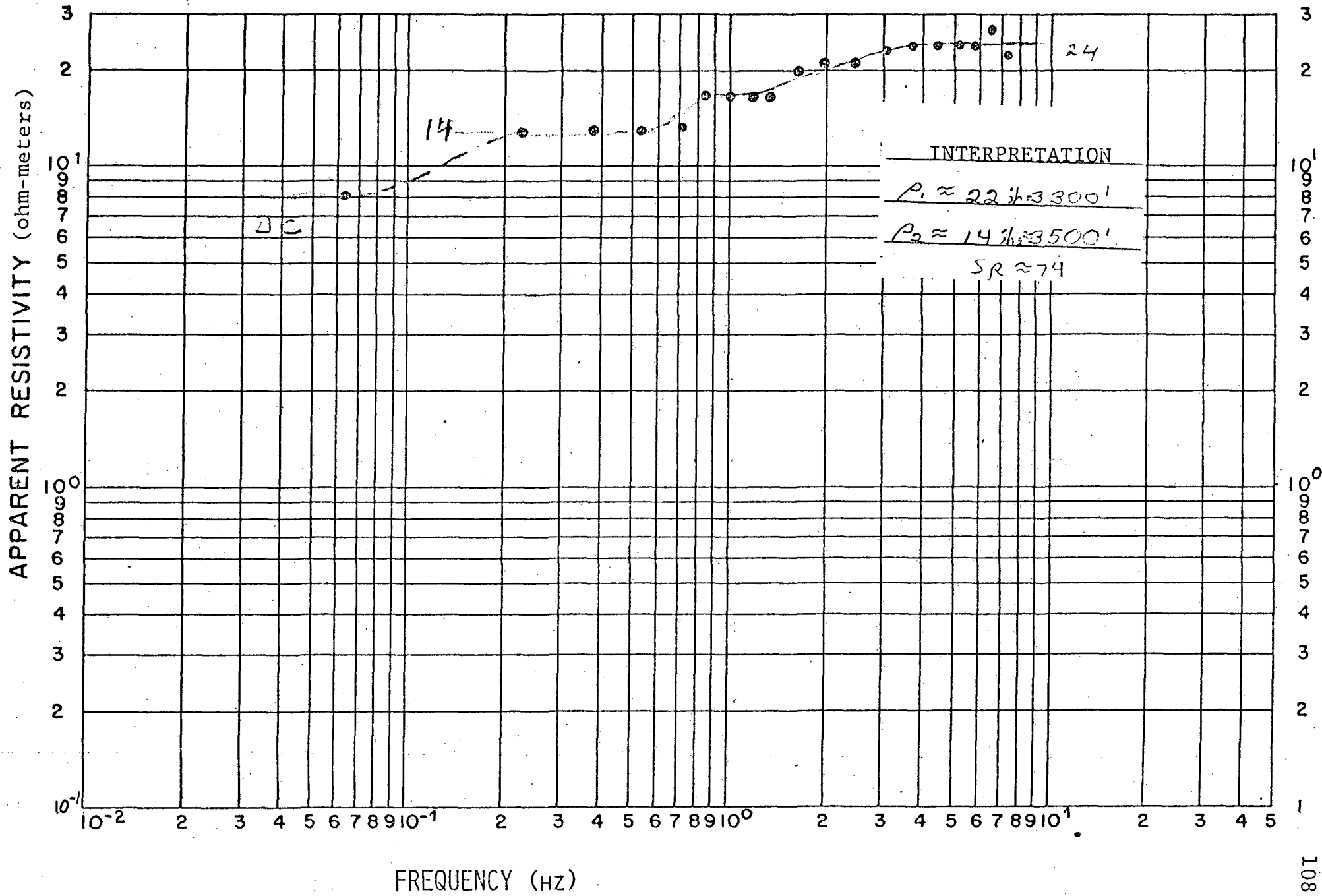


Figure VII-18. TDEM Ep Sounding 9.02

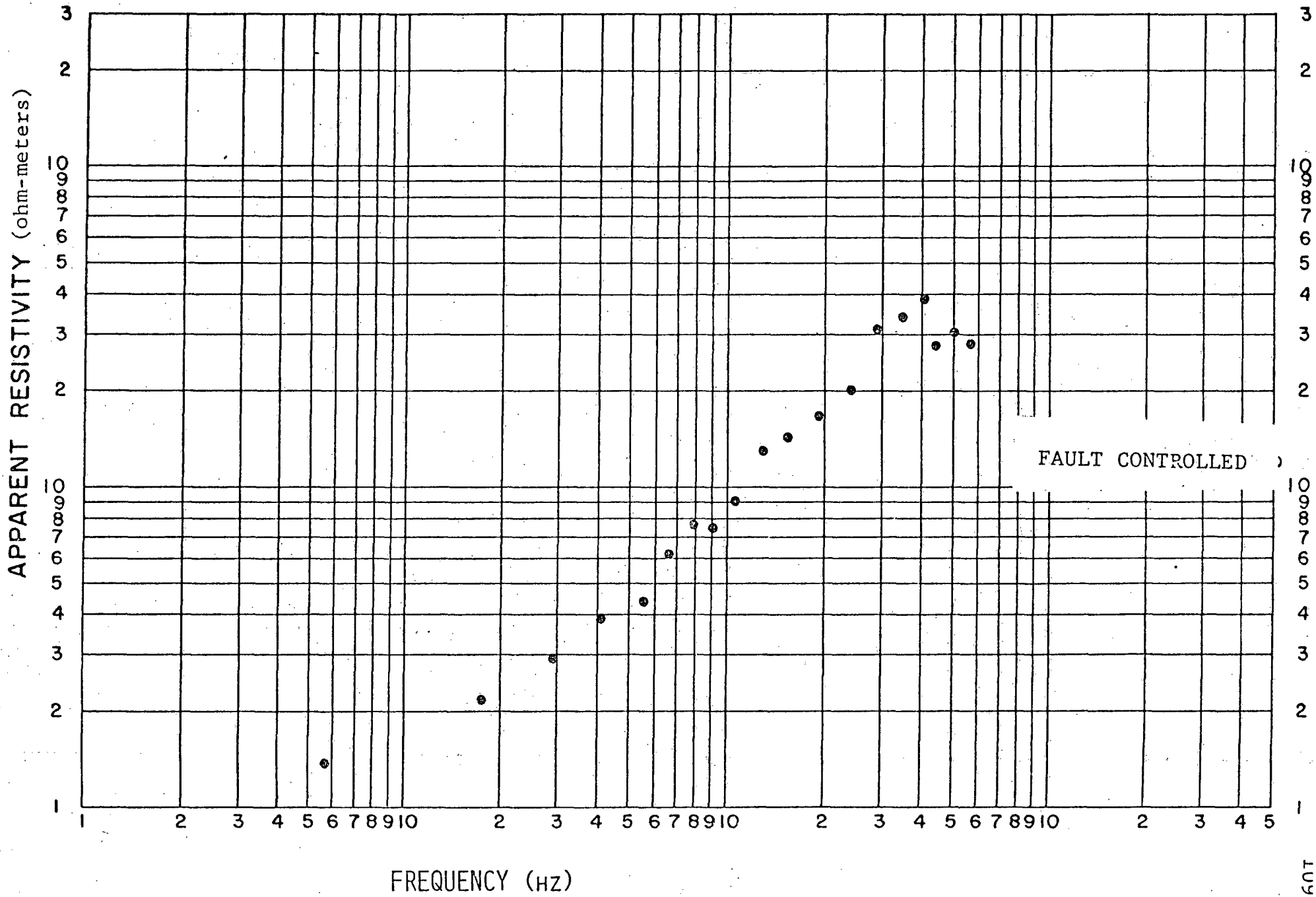


Figure VII-19. TDEM Hz Sounding 9.02

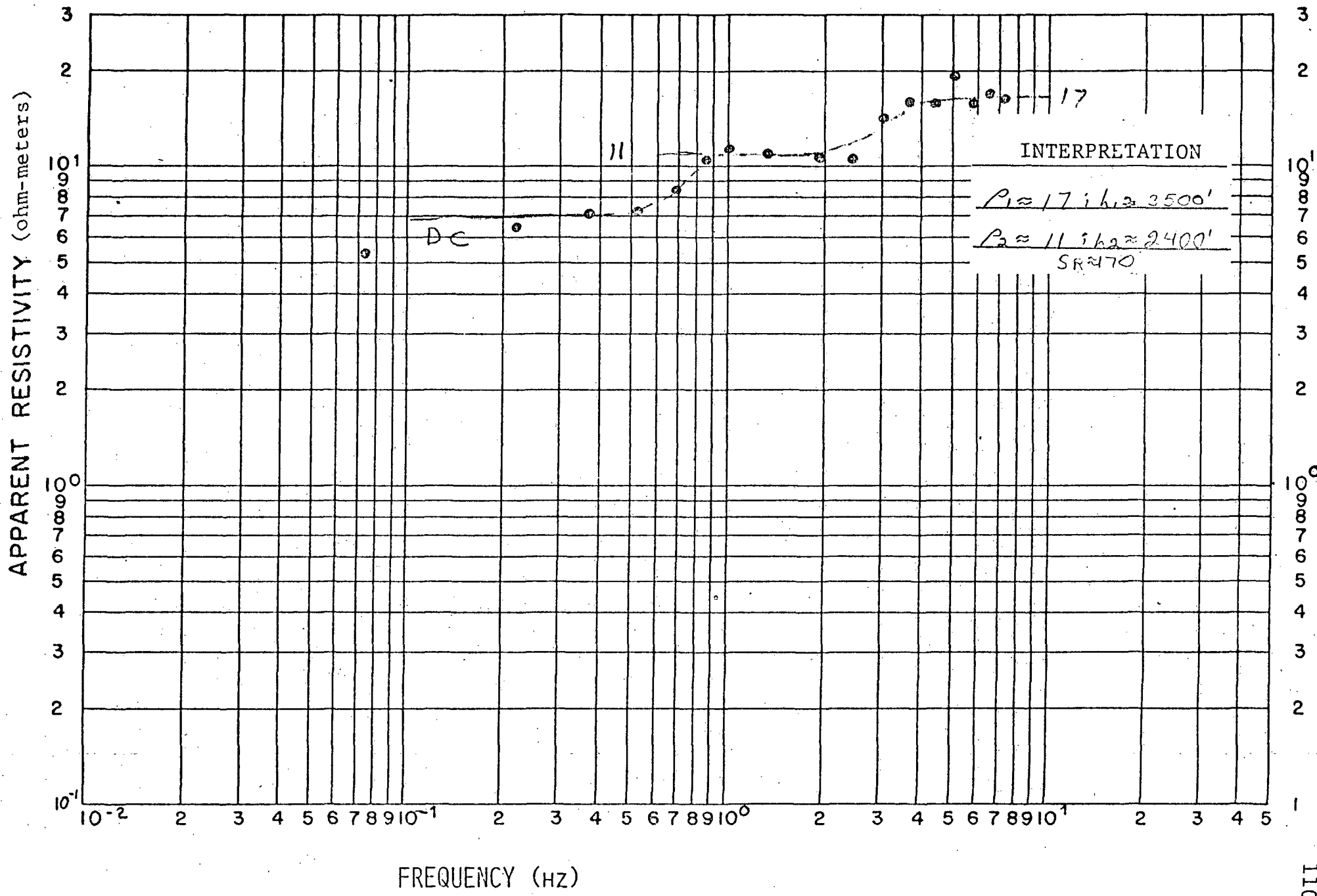


Figure VII-20. TDEM Ep Sounding 10.01

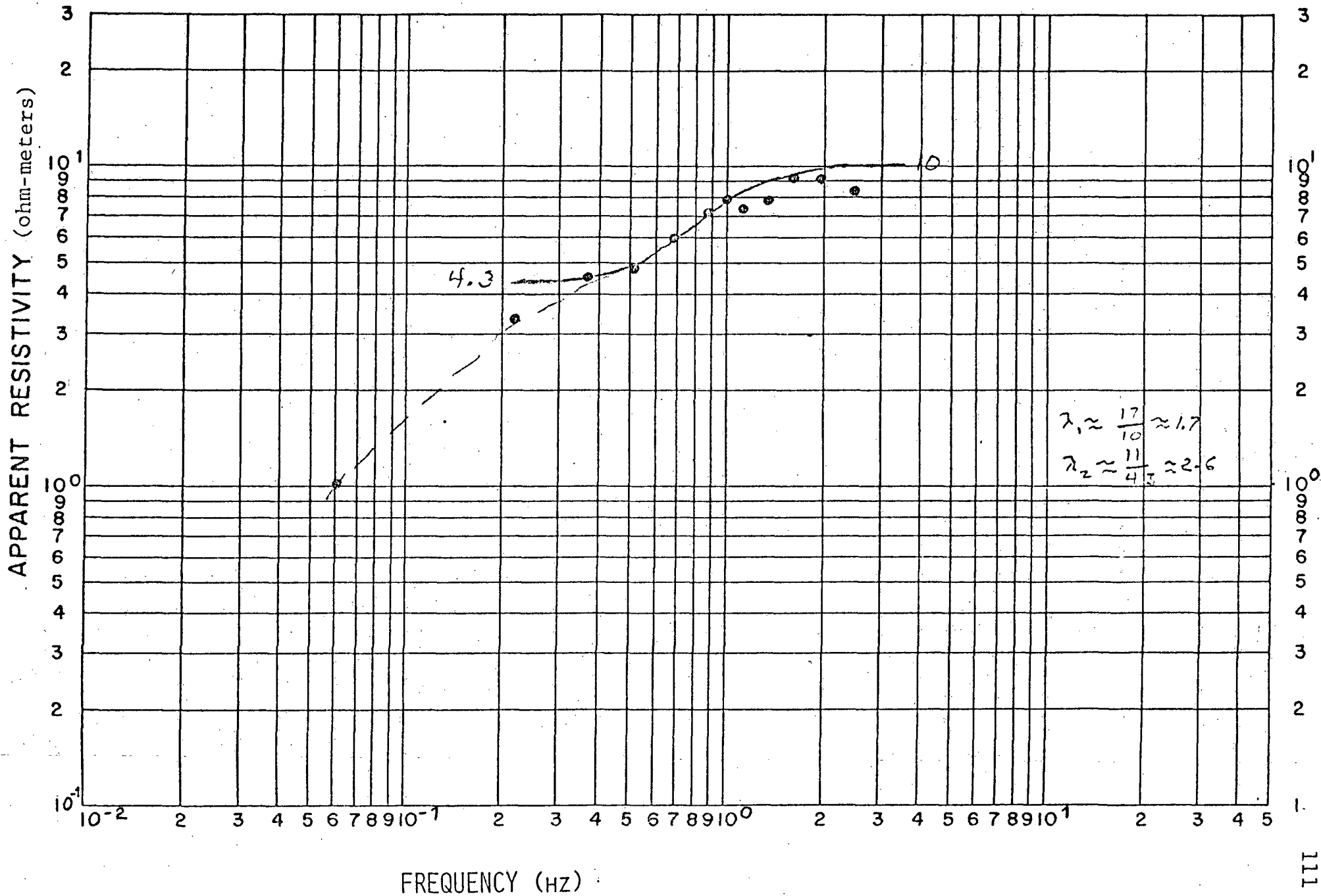


Figure VII-21. TDEM Hz Sounding 10.01

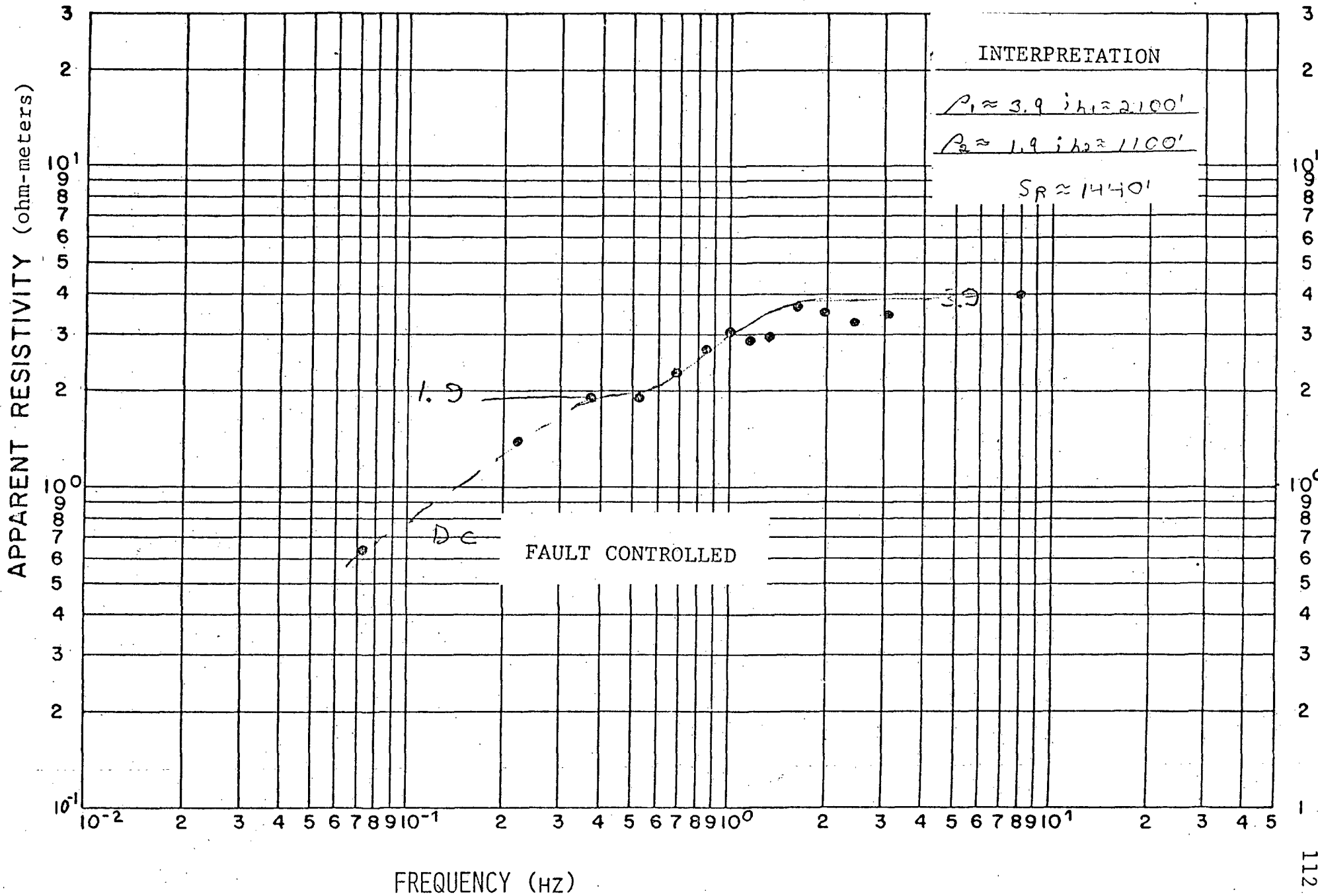


Figure VII-22. TDEM Ep Sounding 11.01

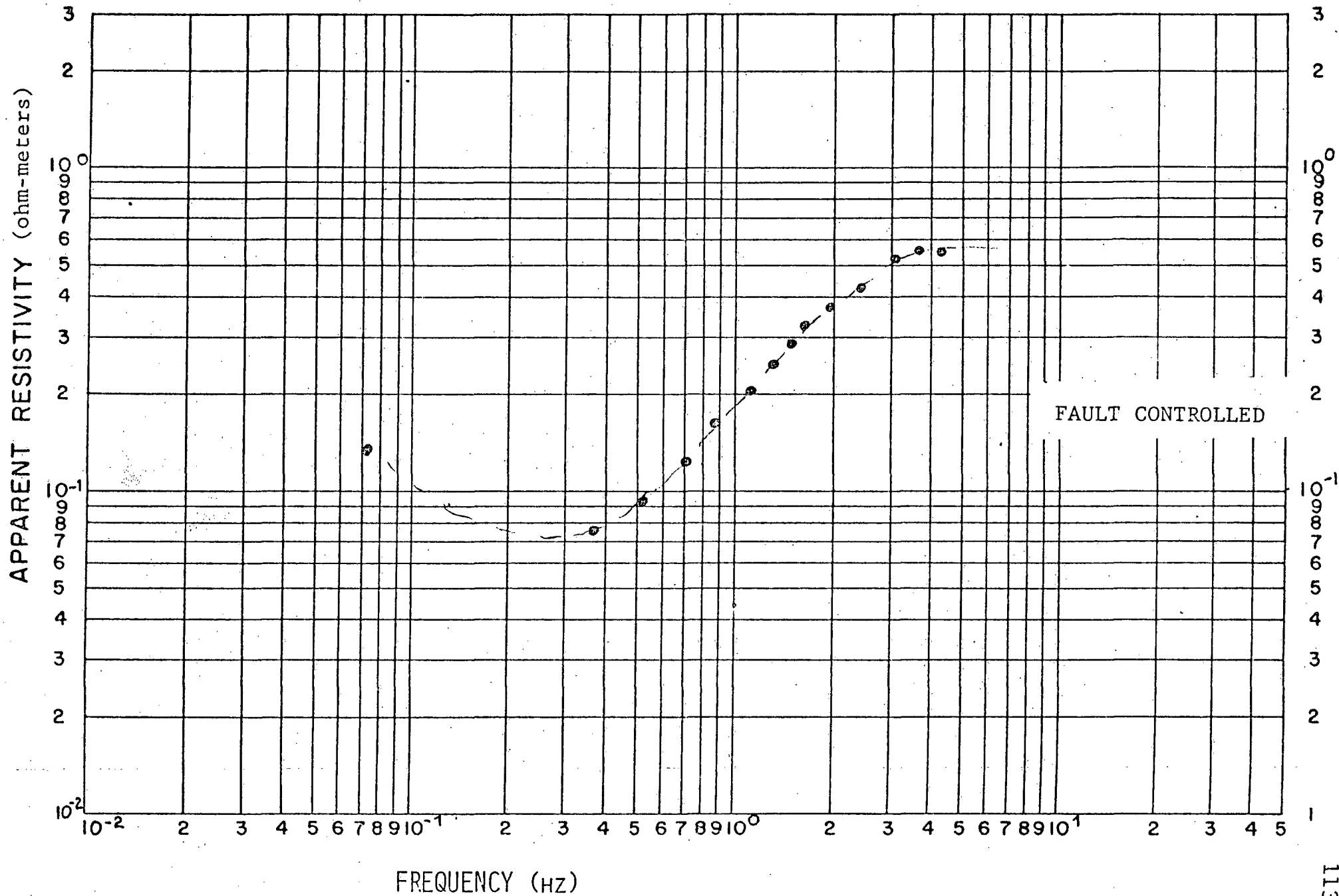


Figure VII-23. TDEM Hz Sounding 11.01

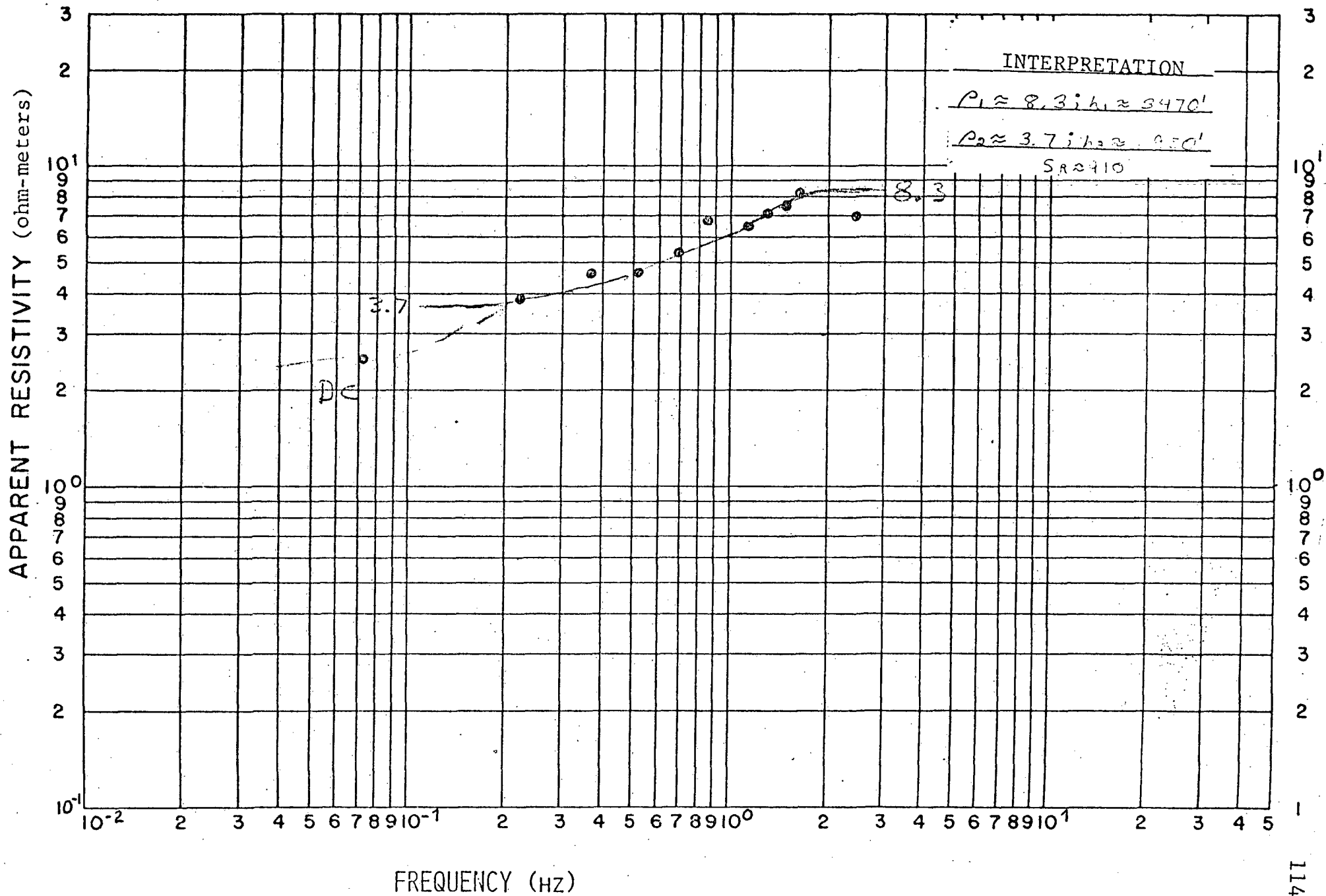


Figure VII-24. TDEM Ep Sounding 11.02

APPARENT RESISTIVITY (ohm-meters)

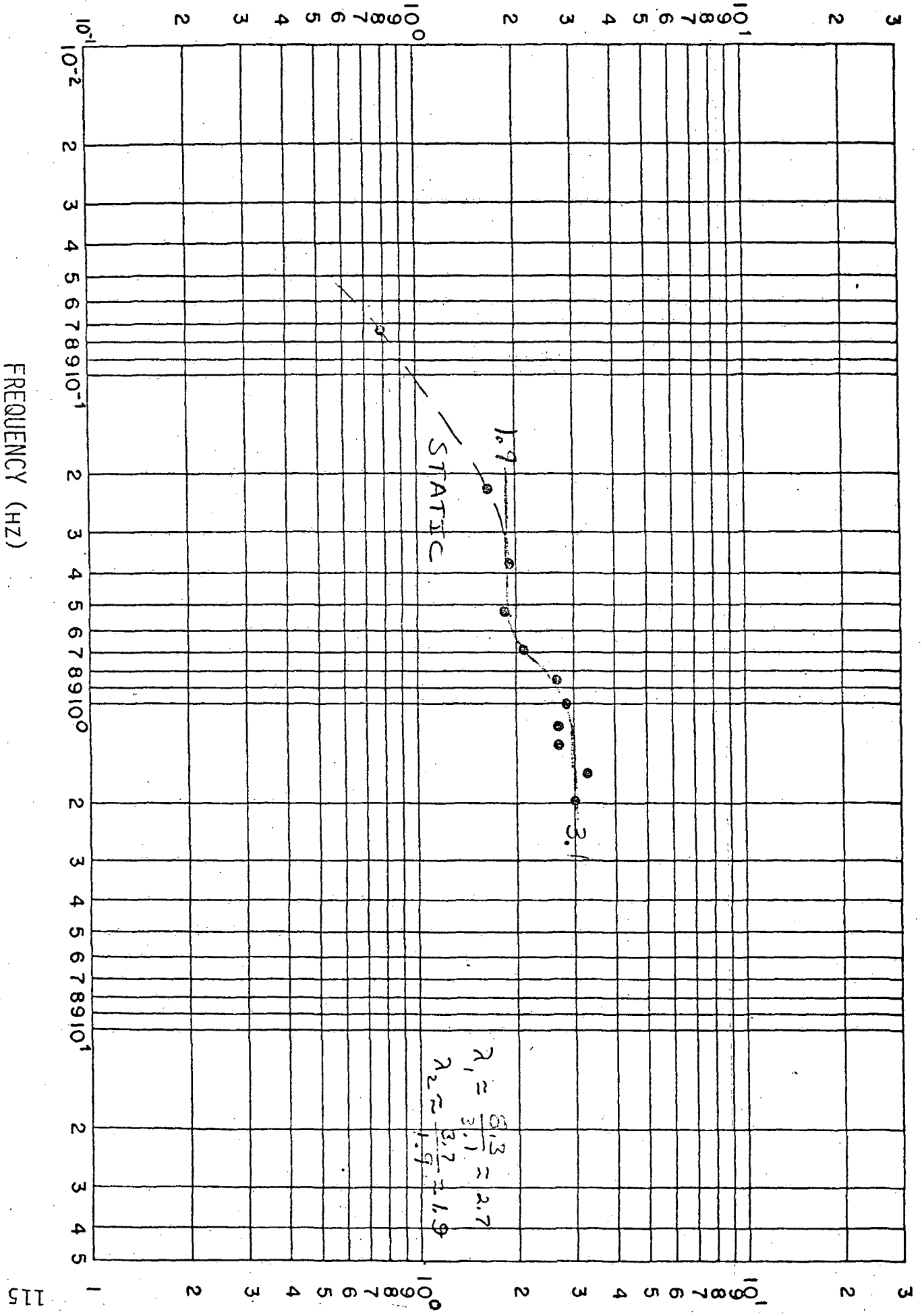


Figure VII-25. TDEM Hz Sounding 11.02

APPARENT RESISTIVITY (ohm-meters)

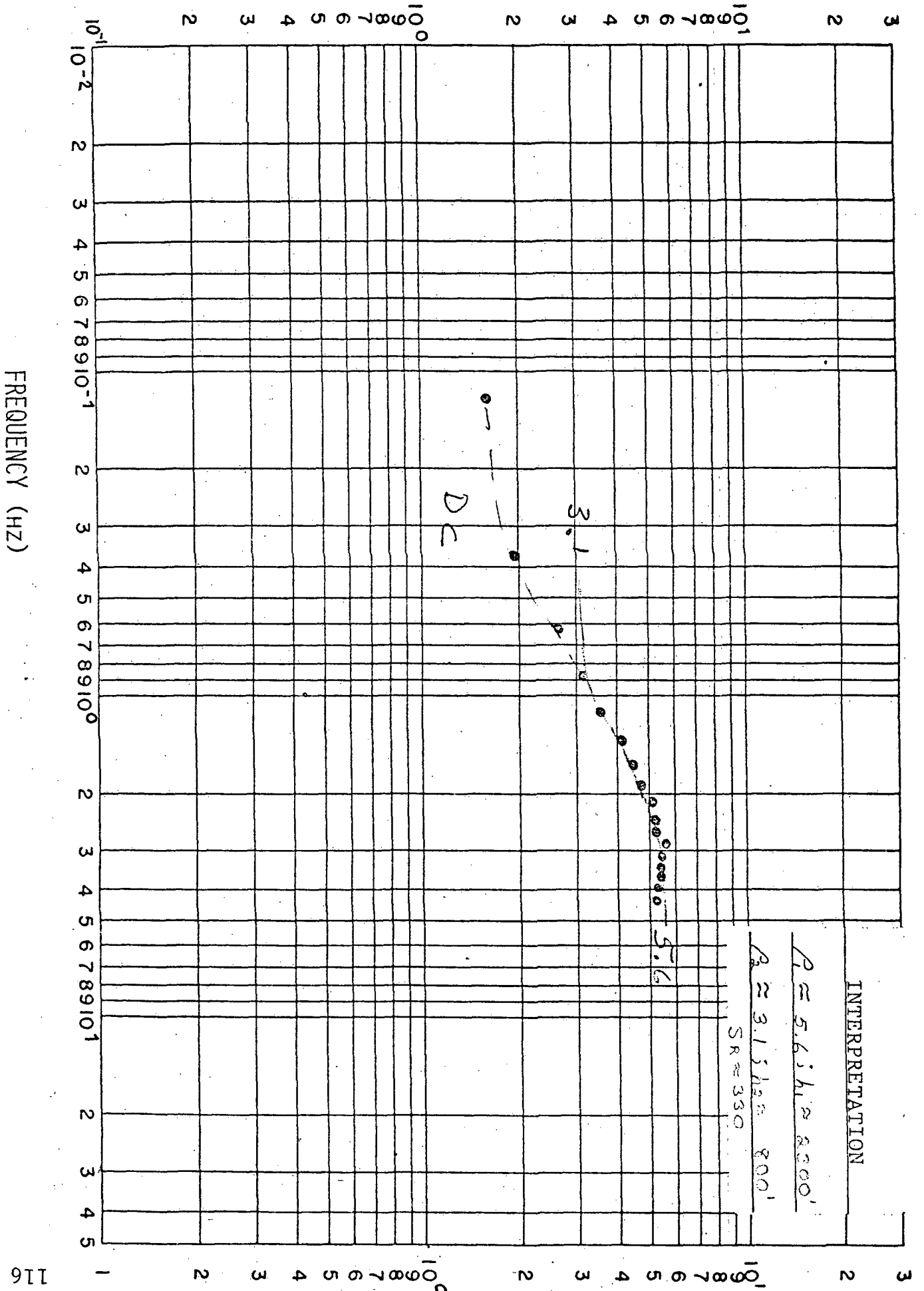


Figure VII-26. TDEM Ep Sounding 12.01

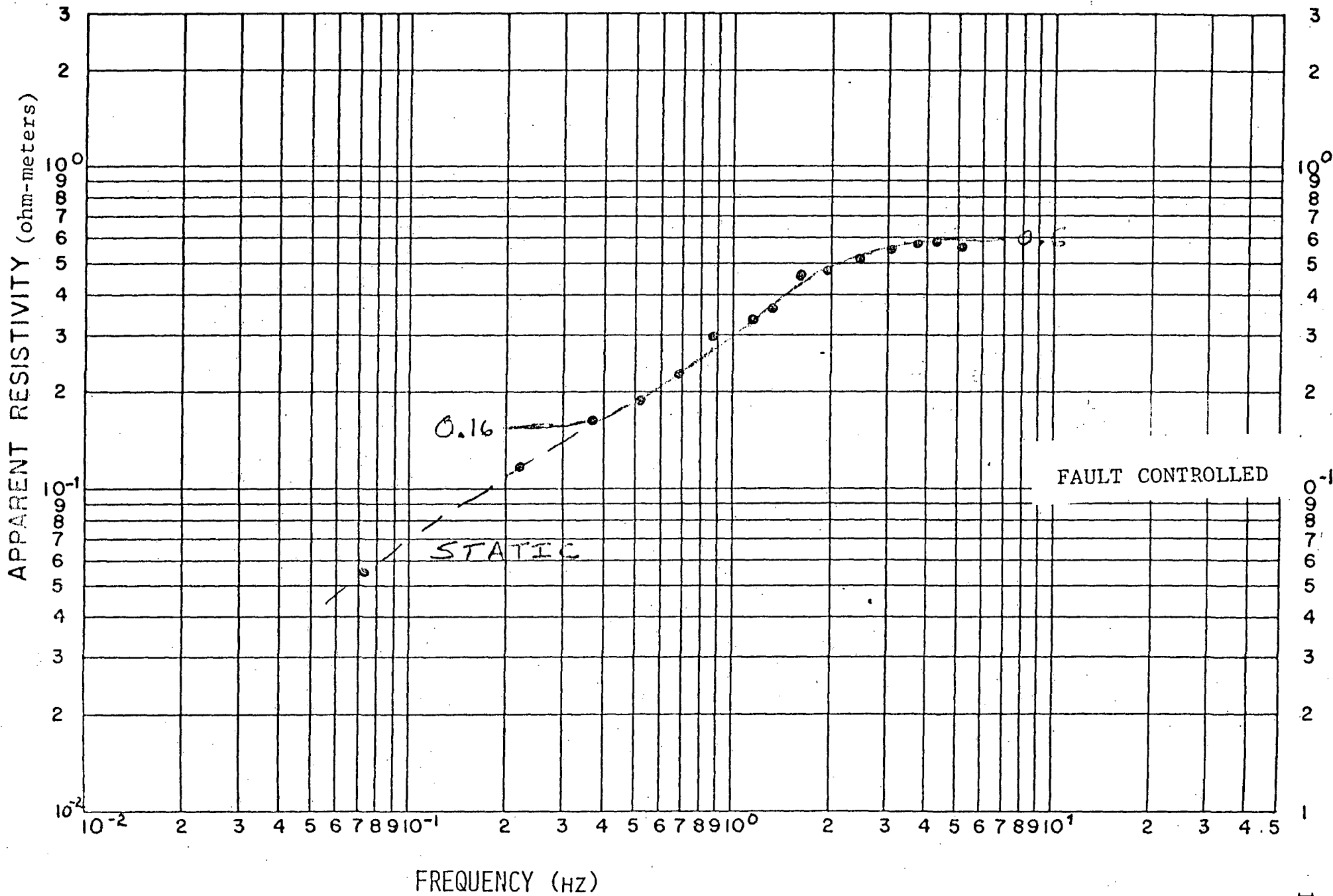


Figure VII-27. TDEM Hz Sounding 12.01

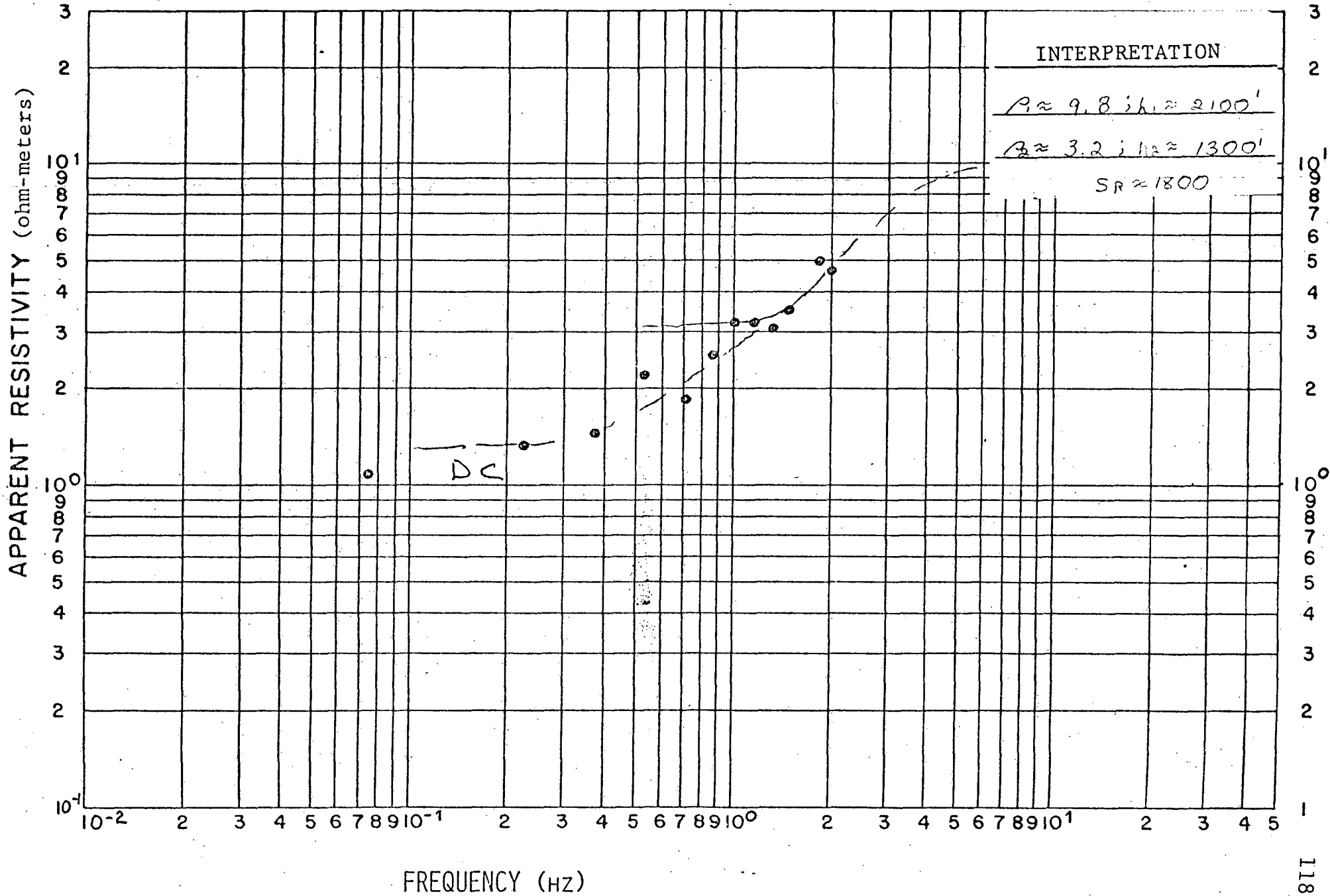


Figure VII-28. TDEM Ep Sounding 12.02

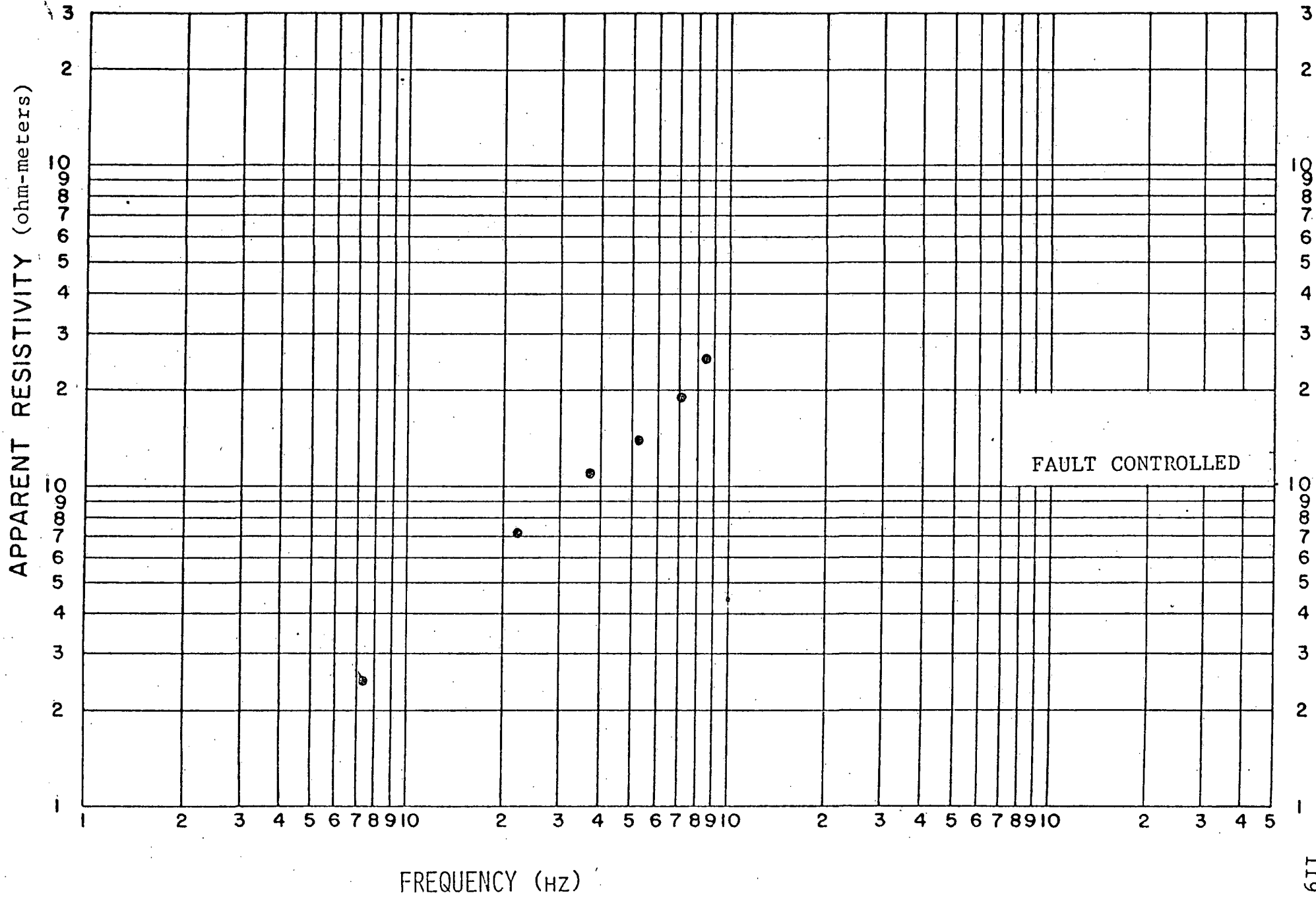


Figure VII-29. TDEM Hz Sounding 12.02

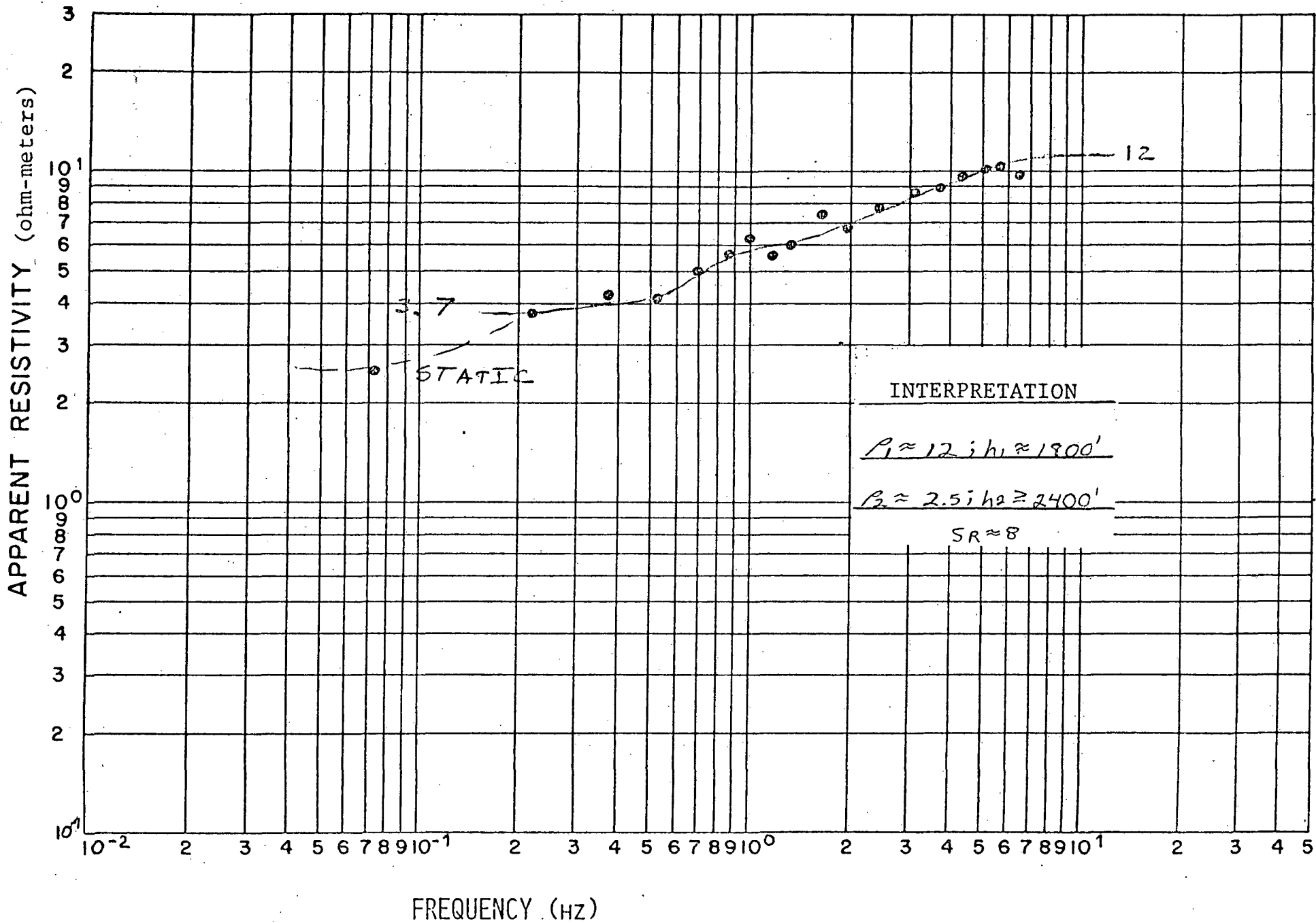


Figure VII-30. TDEM Ep Sounding 12.03

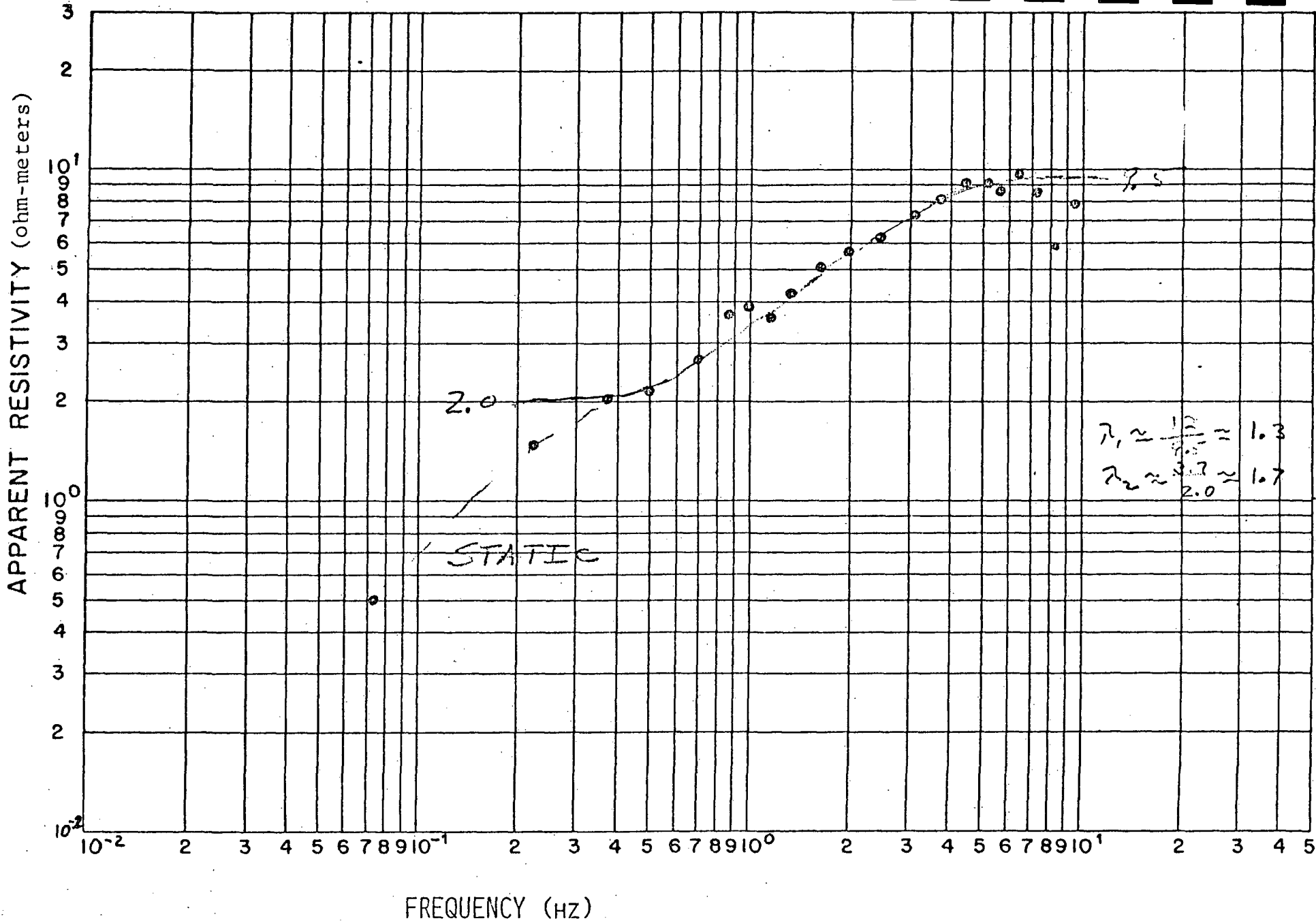


Figure VII-31. TDEM Hz Sounding 12.03

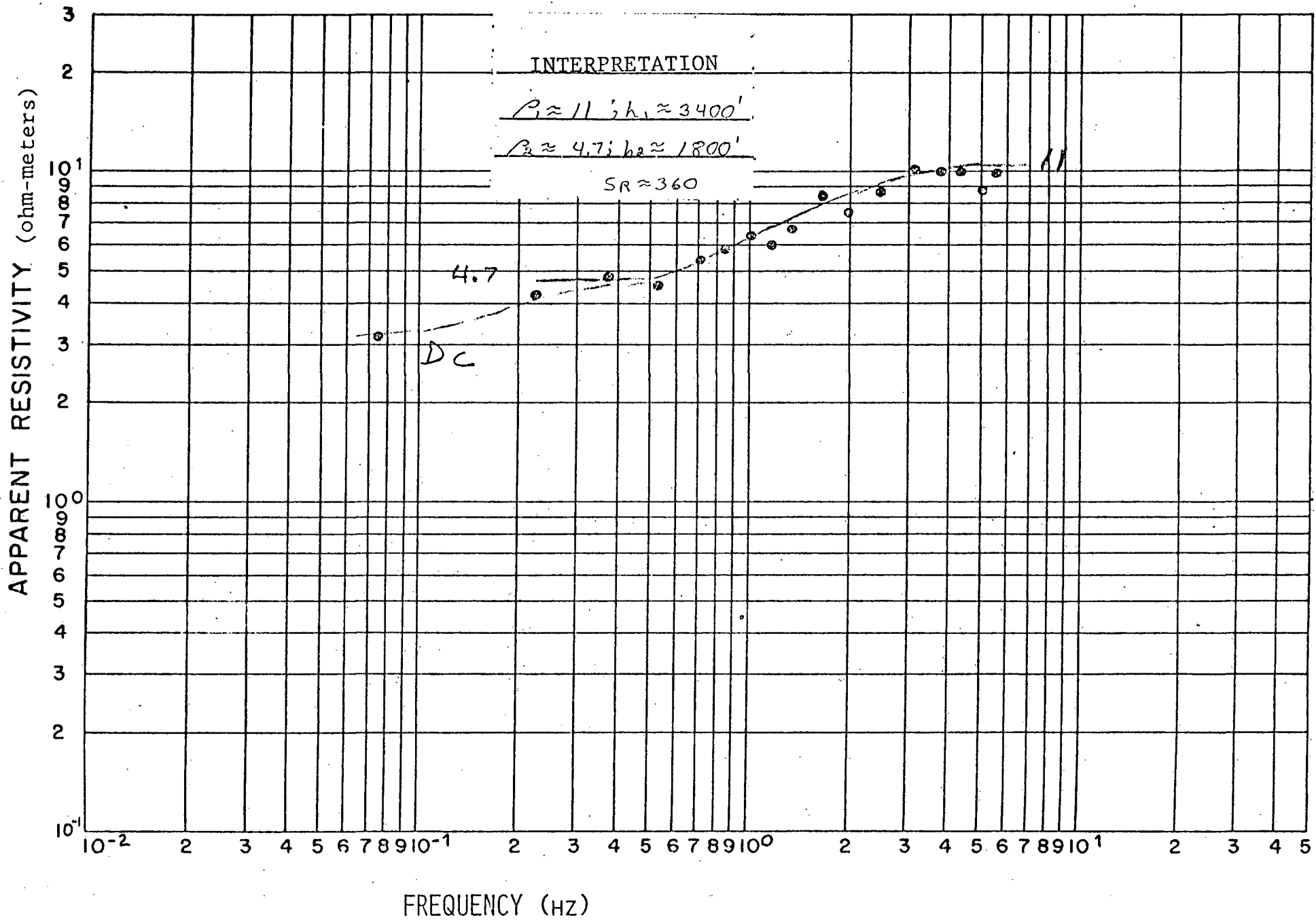


Figure VII-32. TDEM Ep Sounding 12.04

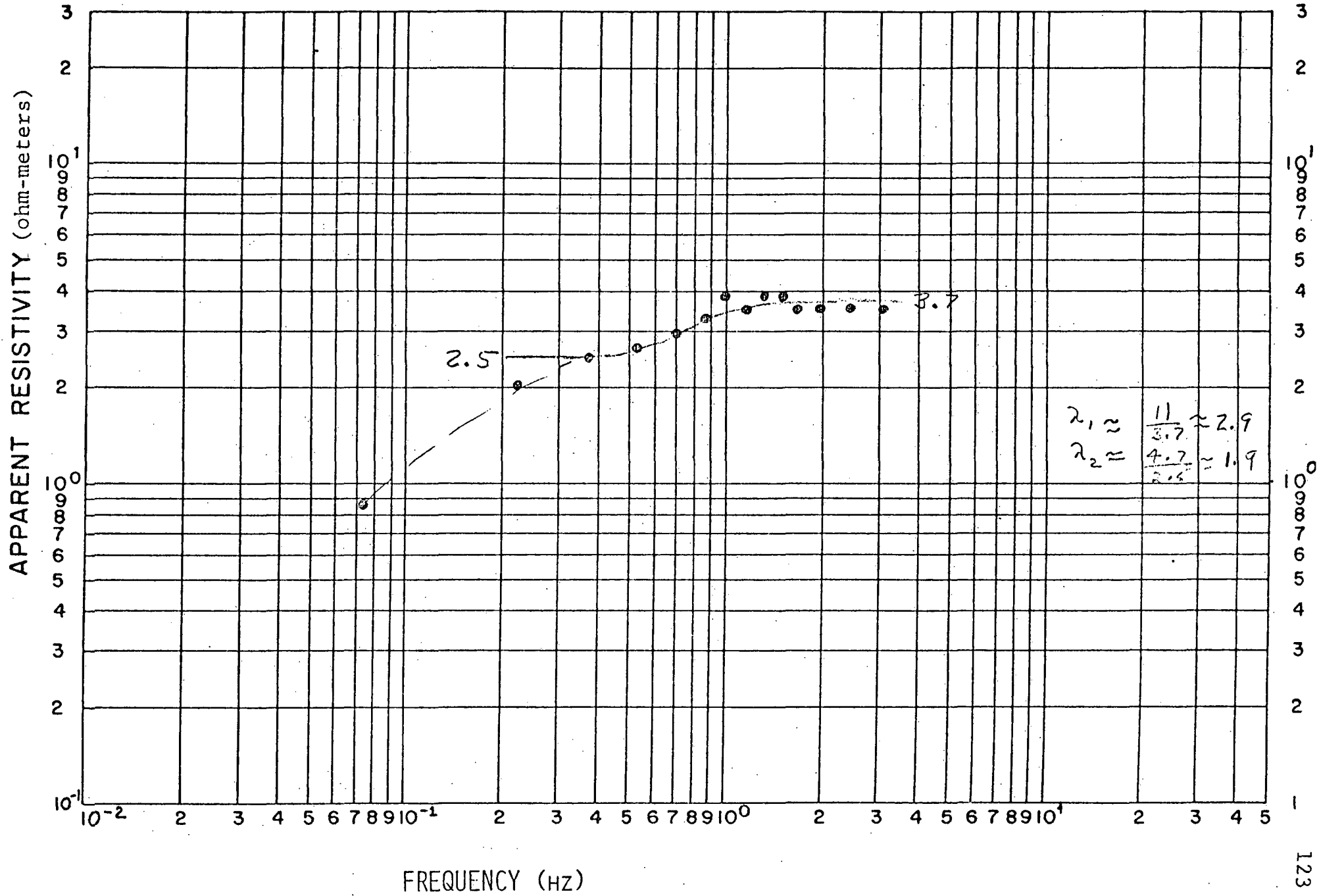


Figure VII-33. TDEM Hz Sounding 12.04